

Roles of TMP21 in Alzheimer's Disease

by

Xiaojie Zhang

B. Medicine, Xiangya Medical School, Central South University, 2008

M. Medicine, The Xiangya Second Hospital, Central South University, 2011

A THESIS SUBMITTED IN PARTIAL FULFILLMENT OF
THE REQUIREMENTS FOR THE DEGREE OF

DOCTOR OF PHILOSOPHY

in

THE FACULTY OF GRADUATE AND POSTDOCTORAL STUDIES
(Neuroscience)

THE UNIVERSITY OF BRITISH COLUMBIA
(Vancouver)

September 2014

© Xiaojie Zhang, 2014

Abstract

Deposition of amyloid β protein ($A\beta$) to form neuritic plaques in the brain is the unique pathological feature of Alzheimer's disease (AD). $A\beta$ is derived from the cleavages of amyloid β precursor protein (APP) by β -secretase at Asp-1 site and by γ -secretase. Beta-site APP cleaving enzyme 1 (BACE1) is the β -secretase. It mainly cleaves APP within the $A\beta$ region at the Glu-11 site to generate truncated $A\beta$ species. Twenty-one kilodalton transmembrane trafficking protein, TMP21 (also named TMED10, p23) is a vesicular trafficking protein and a member of p24 family proteins. TMP21 mediates protein endoplasmic reticulum (ER)/Golgi transport and selectively guides the glycosylphosphatidylinositol-anchored proteins into lipid rafts. It is also essential for forming Golgi structural organization. Recent studies show that the downregulation of TMP21 increases $A\beta$ generation by affecting APP trafficking and selectively modulating γ -cleavage on APP. However, the precise roles of TMP21 in AD pathogenesis remain unknown.

In this thesis, we reported the discovery of a novel AD-associated single nucleotide polymorphism (SNP) in the intron 4 of *Tmp21*. This SNP significantly increases TMP21 transcript splicing efficiency *in vitro*, resulting in upregulation of TMP21 gene expression. Furthermore, we found that overexpression of TMP21 shifts APP processing from the non-amyloidogenic to the amyloidogenic pathway by specifically increasing the BACE1 activity at Asp-1 site. Downregulation of TMP21 also facilitates amyloidogenic cleavage. The interaction between TMP21 and BACE1 is essential for BACE1's ER export, and TMP21 enhances APP/BACE1 co-residency and might guide both APP and immature BACE1 in lipid rafts-like structures.

In summary, this study defined the roles of TMP21 in AD pathogenesis. It demonstrated for the first time the genetic association between TMP21 and AD. The study also found that TMP21 facilitates APP amyloidogenic processing by modulating BACE1 maturation and trafficking, leading to increased BACE1 cleavage at Asp-1 site to generate $A\beta$. Therefore, interrupting the

interaction between TMP21 and BACE1 to reduce A β production could be potential strategy to develop drugs for treating AD.

Preface

Chapter 1

A large portion of section 1.1 and section 1.2 has been originally published. (**Zhang, X.**, Song, W. (2013). The role of APP and BACE1 trafficking in APP processing and amyloid- β generation. *Alzheimer's Research & Therapy* 5, 46.). I was the first-author and wrote the first draft. Dr. Yili Wu helped in drawing the schematic figures and Dr. Philip Ly provided critical comments.

Chapter 2

Material covered in this chapter had been submitted for publication. I wrote the first manuscript and was the co-first author with a collaborator from China, Dr. Kun Xia. Dr. Yili Wu provided the assistance in figures organization and text revision.

For this work, I performed the experiments and data analysis in detections of TMP21 expression at protein, mRNA and the pre-mRNA levels, as well as luciferase assays in HEK293 cells; Dr. Yili Wu performed these experiments and data analysis in SH-SY5Y cells. In the experiment of screening *Tmp21* SNPs, the co-first author, Dr. Kun Xia preformed sequencing and analyses of *Tmp21* exonic regions excluding the 5' UTR and 3' UTR, and the flanking intronic regions in 261 sporadic AD patients and 236 controls. Dr. Fang Cai provided technical support in sequencing and plasmids construction.

Chapter 3

Data showed in this chapter had been submitted for publication. I wrote the first manuscript and was the co-first author with Dr. Zhe Wang and Dr. Kelley Bromley-Brits.

For this work, the HTM stable cell line was established by Dr. Kelley Bromley-Brits. Figure 3.6 A Dr. Zhe Wang preformed the coimmunoprecipitation. Dr. Jeffrey LeDue provided technical assistance in confocal images and time-lapse images recoding. Plasmid TMP21-GFP was cloned

by Kelley Bromley-Brits; plasmid BACE1-Dsred was from Dr. Weihui Zhou; expression plasmids BACE1-myc D93A and BACE1-myc D93/289A were constructed by Dr. Zhe Wang. All procedures with mice were in accordance with guidelines established by the Canadian Council on Animal Care and approved by the University of British Columbia Animal Care Committee (Protocols A05-1888, A10-0040, and A06-0007).

Chapter 4

Data showed in this chapter has been submitted for publication. I wrote the first draft of the manuscript and was the co-first author with Dr. Zhe Wang and Dr. Kelley Bromley-Brits.

For this work, expression plasmids GFP-TMP21, GFP-TMP134, TMP178myc, BACE1313, BACE1313C and BACE1kkklk were constructed by Dr. Zhe Wang. Plasmid TMP21 with no tag was from Kelley Bromley-Brits.

Table of Contents

Abstract	ii
Preface	iv
Table of Contents	vi
List of Tables	xi
List of Figures	xii
List of Abbreviations	xiv
Acknowledgements	xvii
Dedication	xix
Chapter 1: General Introduction	1
1.1 Alzheimer's disease pathogenesis.....	1
1.1.1 An overview of Alzheimer's disease	1
1.1.2 Genetic factors predisposing to Alzheimer's disease	1
1.1.3 The amyloid hypothesis of Alzheimer's disease	2
1.1.4 APP amyloidogenic and non-amyloidogenic processing	3
1.2 APP and BACE1 trafficking in pathogenesis of Alzheimer's disease	6
1.2.1 The intracellular localization of APP and BACE1.	6
1.2.2 Subcellular localizations for A β generation.....	6
1.2.3 Co-residency of APP and BACE1 increases A β production	10
1.2.4 BACE1 cleaves APP at two sites.....	12
1.2.5 Lipid rafts---platform for APP amyloidogenic processing	13
1.3 Transmembrane emp24 domain-containing protein (TMED) /P24 family proteins	16
1.4 Transmembrane protein TMP21	17
1.4.1 TMP21 facilitates protein transport between ER and Golgi.....	18
1.4.2 TMP21 contributes to the organization of Golgi apparatus.....	20
1.4.3 The roles of TMP21 in ER quality control and unfolded protein response (UPR)...	21

1.4.4	TMP21 facilitates the ER export of GPI-anchored proteins and guides them into lipid rafts	22
1.5	TMP21 and Alzheimer’s disease	23
1.6	Overall goals of this research.....	25
1.6.1	Genetic analysis of <i>Tmp21</i> SNPs in AD patients.....	26
1.6.2	Explore the role of TMP21 in APP processing.....	26
1.6.3	Investigate the effect of TMP21 in BACE1 maturation and trafficking.....	26
Chapter 2: A Novel AD-associated SNP in <i>Tmp21</i> Increases TMP21 Expression by Potentiating the Splicing Efficiency		28
2.1	Introduction.....	28
2.2	Methods.....	29
2.2.1	Subjects.....	29
2.2.2	SNP detection.....	29
2.2.3	Plasmids constructions.....	30
2.2.4	Cell culture, transfection and drug treatments.....	31
2.2.5	Immunoblotting.....	31
2.2.6	Semi-quantitative RT-PCR.....	32
2.2.7	Luciferase assay.....	32
2.2.8	Statistical analysis.....	33
2.3	Results.....	33
2.3.1	Identification of a novel AD-associated SNP in intron4 of TMP21	33
2.3.2	rs12435391 had no effect on <i>Tmp21</i> splicing site recognition	35
2.3.3	rs12435391 increased <i>Tmp21</i> expression	37
2.3.4	rs12435391 increased <i>Tmp21</i> pre-mRNA splicing efficiency.....	38
2.3.5	rs12435391 had no effect on <i>Tmp21</i> transcription	41
2.4	Discussion.....	42
2.5	Conclusion	46
Chapter 3: The Dysregulated TMP21 Facilitates APP Amyloidogenic Processing.....		47

3.1	Introduction.....	47
3.2	Methods.....	48
3.2.1	Plasmids constructions.....	48
3.2.2	Cell culture and transfections.....	48
3.2.3	Immunoblotting.....	49
3.2.4	A β 40 enzyme linked-immunosorbent assay (ELISA).....	49
3.2.5	Coimmunoprecipitation.....	50
3.2.6	Subcellular fractionation.....	50
3.2.7	Immunocytochemistry.....	51
3.2.8	Confocal imaging and time-lapse live cell image analysis.....	51
3.2.9	SiRNA knockdown.....	51
3.2.10	Mice breeding.....	52
3.2.11	Genotyping.....	52
3.2.12	Neuritic plaque staining.....	53
3.3	Results.....	54
3.3.1	Upregulation of TMP21 shifted the APP processing from non-amyloidogenic to amyloidogenic pathway.....	54
3.3.2	Knockdown of TMP21 also preferentially enhanced C99 generation.....	56
3.3.3	Disruption of TMP21 facilitated plaque formation in AD transgenic mice.....	58
3.3.4	TMP21 accumulated immature BACE1 and interacted with immature BACE1.....	61
3.3.5	Overexpression of TMP21 altered trafficking of BACE1 and its subcellular distribution.....	64
3.4	Discussion.....	66
3.5	Conclusion.....	68
	Chapter 4: TMP21 Affects BACE1 Maturation and Trafficking.....	69
4.1	Introduction.....	69
4.2	Methods.....	69
4.2.1	Plasmids constructions.....	69

4.2.2	Cell culture and transfections.....	70
4.2.3	Immunoblotting.....	71
4.2.4	Coimmunoprecipitation.	72
4.2.5	Immunocytochemistry.	72
4.2.6	Pharmacological treatment.....	73
4.2.7	Lipid raft isolation.....	73
4.3	Results.....	73
4.3.1	Multiple binding sites between TMP21 and BACE1	73
4.3.2	The interaction between TMP21 and BACE1 accumulated the immature BACE1 .	77
4.3.3	TMP21 delayed the ER export of immature BACE1 without affecting its ER degradation.....	79
4.3.4	TMP21 contributed to BACE1 trafficking between ER and Golgi.	80
4.3.5	P24a interacted with APP and BACE1	83
4.3.6	TMP21 increased the co-residency of APP and BACE1	85
4.3.7	TMP21 guided both the immature BACE1 and APP in detergent-resistant structures 87	
4.3.8	TMP21 didn't affect the trafficking of C99.....	91
4.4	Discussion	93
4.5	Conclusion	96
Chapter 5: Conclusion and Future Directions		97
5.1	Overall conclusions.....	97
5.1.1	Chapter 2: A novel AD-associated SNP in <i>Tmp21</i> increases TMP21 expression by potentiating the splicing efficiency.....	98
5.1.2	Chapter 3: The dysregulated TMP21 facilitates APP amyloidogenic processing	98
5.1.3	Chapter 4: TMP21 affects BACE1 maturation and trafficking	99
5.2	Significance and novelty of the research	99
5.3	Strengths and weaknesses	100

5.3.1	Elucidate the clinical relevance of TMP21 expression levels and gene polymorphisms in AD patients	100
5.3.2	Evidence the role of TMP21 in APP processing and indicates its impact on BACE1 101	
5.3.3	Examine the fundamental role of TMP21 in mice models	103
5.3.4	Characterize the TMP21/BACE1 interaction	104
5.3.5	Explore the role of TMP21 in APP/BACE1 lipid raft-like domains translocation.	105
5.4	Future directions	106
5.4.1	The effect of TMP21 on γ -secretase complex	106
5.4.2	Establish the inducible TMP21 knockout mice	110
5.4.3	Examine TMP21/GPI-anchored proteins/BACE1/APP interaction	114
References	115

List of Tables

Table 2.1 Distribution of <i>Tmp21</i> SNPs.....	34
---	-----------

List of Figures

Figure 1.1 The APP non-amyloidogenic and amyloidogenic processing.	5
Figure 1.2 APP trafficking.	9
Figure 1.3 Distinctly regulated APP and BACE1 trafficking.	11
Figure 1.4 TMP21 (p23) mediates both anterograde and retrograde transport in early secretory pathway.	19
Figure 2.1 rs12435391 had no effect on <i>Tmp21</i> pre-mRNA splicing site recognition.	36
Figure 2.2 rs12435391 increased <i>Tmp21</i> expression.	37
Figure 2.3 rs12435391 facilitated <i>Tmp21</i> pre-mRNA splicing.	40
Figure 2.4 rs12435391 had no effect on <i>Tmp21</i> transcription regulation.	42
Figure 3.1 Overexpression of TMP21 dramatically shifted the APP cleavage from non-amyloidogenic pathway to amyloidogenic pathway.	55
Figure 3.2 Knockdown of TMP21 preferentially generated more C99.	57
Figure 3.3 Disruption of TMP21 facilitated C99 and Aβ generation in 7 months old AD mice.	59
Figure 3.4 Disruption of TMP21 facilitated plaque formation in 9 months old AD mice. ...	60
Figure 3.5 Immature BACE1 increased when TMP21 overexpressed.	63
Figure 3.6 TMP21 interacted with immature BACE1.	64
Figure 3.7 Co-localization of TMP21 and BACE1.	65
Figure 3.8 TMP21 accumulated BACE1 along the peri-nuclear region.	66
Figure 4.1 Schematic representation of TMP21 constructs.	75
Figure 4.2 Multiple binding sites between TMP21 and BACE1.	76
Figure 4.3 The interaction between TMP21 and BACE1 accumulated the immature BACE1.	78
Figure 4.4 TMP21 delayed the ER export of immature BACE1 without affecting its ER degradation.	80
Figure 4.5 TMP21 contributed to BACE1 trafficking between ER and Golgi.	82

Figure 4.6 P24 interacted with APP and BACE1.....	84
Figure 4.7 TMP21 enhanced the co-residency of APP/BACE1 and the interaction APP/immature BACE1.....	86
Figure 4.8 TMP21 guided both the immature BACE1 and APP in detergent-resistant structures.	89
Figure 4.9 Lipid raft isolation of HEK and HTM cells with coexpression of APP and BACE1.	90
Figure 4.10 TMP21 did not affect the trafficking of C99.....	92
Figure 4.11 Suggested model for the essential role of TMP21 in BACE1 trafficking and maturation-----TMP21/BACE1 interaction might be the initial step.....	94
Figure 5.1 The assembly, trafficking and maturation of γ-secretase complex.....	107
Figure 5.2 TMP21/γ-secretase interaction.....	109
Figure 5.3 LoxP-flanked TMP21 vector construct.	112
Figure 5.4 Strategies for generating a loxP-flanked gene for conditional gene targeting..	113

List of Abbreviations

A β amyloid- β protein

ACT-D actinomycin D

AD Alzheimer's disease

ARF ADP-ribosylation factor

ADAM a disintegrin and metalloproteinase

AICD APP intracellular domain

ANOVA analysis of variance

Aph-1 anterior pharynx-defective 1

APP β -amyloid precursor protein

APP23 single transgenic mice carrying Swedish APP mutation (KM670/671NL)

APPwt wild type APP

APPSwe swedish APP mutation (KM670/671NL)

ARU animal research unit

BACE1 β -site APP cleaving enzyme 1

BACE2 β -site APP cleaving enzyme 2

Bp base pair

BSA bovine serum albumin

CGN cis-Golgi network

CHX cycloheximide

CoIP coimmunoprecipitate

COPI coat protein complex I

COPII coat protein complex II

CTF carboxy-terminal fragment

CTF α C-terminal fragment α (C83)

CTF β C-terminal fragment β (C99 and C89)

DMEM dulbecco's modified eagles' medium

DMSO dimethyl sulfoximine
ELISA enzyme-linked immunosorbent assay
ER endoplasmic reticulum
ERGIC ER Golgi intermediate compartment
FBS fetal bovine serum
EMP endosome membrane protein
GEFs guanine nucleotide exchange factors
GFP green fluorescent protein
GGAs γ -ear-containing ARF-binding proteins
GPI glycosylphosphatidylinositol
GSAPs γ -secretase-associated proteins
GSI γ -secretase inhibitor, L685,458
HEK293 human embryonic kidney 293 cell line
HTM HEK cells stably express human TMP21-mycHis
ISO isoginkgetin
LTP long-term potentiation
MEF mouse embryonic fibroblasts
NCT nicastrin
NFT Neurofibrillary tangle
Pen-2 presenilin enhancer 2
PBS phosphate buffered saline
PBS-Tx PBS with 0.1% Triton X-100
PBS-T PBS with 0.1% Tween-20
PCR polymerase chain reaction
PFA paraformaldehyde
PNS post-nuclear supernatant
PM plasma membrane
PS presenilin;

PS1 presenilin 1
PS2 presenilin 2
RIPA DOC radio-immunoprecipitation assay deoxycholate
RT-PCR reverse transcription polymerase chain reaction
sAPP α secretory APP α
S2P23 TMP21 hemizygous mice strain
sAPP β secreted β -amyloid precursor protein
SDS sodium dodecyl sulfate
SDS-PAGE SDS-polyacrylamide gel electrophoresis
SNP single nucleotide polymorphisms
TACE tissue necrosis factor α converting enzyme
TGN trans-Golgi network;
TEM2 transmembrane emp24 domain-containing protein
TM21 transmembrane trafficking protein, 21KD
UPR unfolded protein response

Acknowledgements

I would never have been able to finish my PhD project and crank out this thesis without the constant guidance of my supervisor, advice from my committee member, assistance from colleagues, and support from my family throughout my PhD journey.

First and foremost, I would like to express my deepest gratitude to my supervisor, Dr. Weihong Song, for his constant encouragement, guidance, caring, patience, both professionally and personally. Dr. Song provided me with a professional training, a prospective project, and a collegiality and intellectual community while being a student of his laboratory. He taught me to perform bench-work quickly yet efficiently, design experiments creatively yet rationally, and think critically yet broad-mindedly. With the support of Dr. Song, I was able to pursue my career in basic research of neuroscience, and to enrich the diversity of my knowledge and share my opinions with other experts by taking advantage of many professional conferences and academic workshops offered at UBC, nationally and internationally. I would like to offer my special thanks to Dr. Song for his understanding and support when I took parental accommodation for the birth of my son.

Advice given by the members of my supervisory committee, Dr. William Jia, Dr. Shernaz Bamji and Dr. Peter Reiner, has been a great help in guiding and progressing my research for the past several years. I was always looking forward to meet them in every annual committee meeting, not only for their enlightening insights, intellectual suggestions and great encouragements, but also for their dedication, curiosity, and passion in pursuit of science, which greatly impressed and encouraged me.

I offer my enduring gratitude to all my colleagues in Dr. Weihong Song's lab, both past and present, for the therapeutic talks and friendly atmosphere for work. I am particularly grateful for the assistance given by Dr. Kelley Bromley-Brits, Dr. Yili Wu and Dr Zhe Wang. Thanks Dr. Kelley Bromley for her initiation of this project and many preparations for the work in chapter 3,

without her contributions, I cannot quickly start this fantastic project. Dr. Yili Wu was my hands-on teacher and provided kindly and generous assistance in trouble-shooting of the bench techniques, experiments design, data analysis and always patiently revising my manuscripts. Without the help of Dr. Zhe Wang in techniques, experimental design and results interpretation, I could not finish most of the work in chapter 3 and first part of chapter 4 so quickly and efficiently. Thank you as well to Dr. Fang Cai for teaching me several techniques in cloning the LoxP-targeted TMP21 construct and culturing mouse embryonic stem cells; many thanks to Dr. Jeffrey LeDue for assisting me in live-cell imaging and confocal imaging; thanks Dr. Mingming Zhang, Dr. Qin Xu and Mr. Bruno Herculano for their critical comments and proof reading of this thesis. Also, a lot of thanks to Dr. Haiyan Zhou, Dr. Philip T T Ly, Dr. Weihui Zhou, Dr. Jing Zhang, Dr. Shuting Zhang, Dr. Qian Xu, Dr. Xiaozhu Zhang, Dr. Jiehao Zhao, Ms. Si Zhang, Ms. Juelu Wang, Ms. Xiaoling Duan and Ms. Beibei Song, it is always a great pleasure to work with them.

Last but not the least, special thanks are owed to my lovely family. I am so lucky to have all of them in my life. Thanks my mom for taking care of me during pregnancy and now my little baby; the deepest gratitude extend to my amazing husband and soul mate, Ti Chen, who provided constant love, understanding and support to pursue my career in science research. At last, thanks my little son, Lucas Chen, you are the most precious present in my life.

*I would like to dedicate my thesis
to my beloved family*

Chapter 1: General Introduction

1.1 Alzheimer's disease pathogenesis

1.1.1 An overview of Alzheimer's disease

Alzheimer's disease (AD) is the most common type of dementia. It is a syndrome that starts with gradual memory loss followed by impairment of thinking, behavior and ability to perform daily activities. As the population has been aging, the number of the AD cases has risen rapidly. According to the World Alzheimer Report in 2013 (ADI, 2013) and the World Health Organization (WHO) dementia report (Wortmann, 2012), nearly 35.6 million people worldwide live with dementia and that number is expected to be doubled by 2030 (65.7 million) and more than tripled by 2050 (from 101 to 277 million). It currently costs the world more than US\$ 604 billion per year to treat and care for people with dementia (Abbott, 2011). Among those dementia patients, around two-thirds are affected with AD (ADI, 2010). These facts make AD as a global health and social care priority, as well as a forefront of biomedical research.

1.1.2 Genetic factors predisposing to Alzheimer's disease

AD is a complex neurological disorder that occurs as a result of interactions among multiple risk factors, such as aging, family history, genetic factors and environmental factors. There is very strong evidence that genetic factors greatly contribute to the etiology of AD. Three genes, encoding amyloid β precursor protein (APP), presenilin1 (PS1) and presenilin2 (PS2), are identified as causal genes associated with familial early-onset AD (FAD), or autosomal dominant AD (ADAD) (Goate, et al., 1991; Rogaev, et al., 1995; Sherrington, et al., 1995). So far, 33 pathogenic mutations have been identified in *APP* gene and they have been estimated to be involved in up to 10% of the reported cases of FAD. 185 mutations in *PS1* and 13 mutations in *PS2* have been identified and they are estimated to account for up to 70% of FAD (see the complete list at <http://www.molgen.ua.ac.be/ADMutations>). However, FAD is less than 5% of all AD cases, and the majority of AD cases being sporadic. The late-onset AD (LOAD) with the symptoms generally begins after 65-70 years of age (Palotas & Kalman, 2006). LOAD has a

Chapter 1: General Introduction

more complex etiology with multiple genetic and environmental risk factors acting together (Pedersen, Gatz, Berg, & Johansson, 2004). For years, intensive genetic analyses have focused on identifying susceptibility or risk genes linked to AD. However, so far, *APOE4* is the only verified risk gene and it contributes to up to 30% LOAD cases (Chartier-Harlin, et al., 1994; Corder, et al., 1993), and no more *APOE4*-like signals have emerged. Additionally, the *APOE4* allele is neither necessary nor sufficient for all AD cases. About 50% of sporadic AD cases have no *APOE4* alleles and many AD cases exist with no mutation in any of the known genes. Recently, genome-wide linkage studies suggest that the multiple genetic loci on chromosome 19, 11, 8 and 1, associate with LOAD (Harold, et al., 2009; Hollingworth, et al., 2011; J. C. Lambert, et al., 2009; Naj, et al., 2011; Seshadri, et al., 2010). The identifications of these genes implicate the additional biological mechanisms for AD pathogenesis, such as lipid processing, the immune system and synaptic cell functions.

1.1.3 The amyloid hypothesis of Alzheimer's disease

Neuritic plaques and neurofibrillary tangle (NFT) are two major pathological changes in AD brains. Neuritic plaque is unique to AD whereas the profound NFT is also detected in frontotemporal dementia with Parkinsonism (Hutton, et al., 1998). The core protein of neuritic plaques is amyloid β protein ($A\beta$) (Glennner & Wong, 1984; Masters, et al., 1985), which is derived from amyloid β precursor protein (APP) (Goldgaber, Lerman, McBride, Saffiotti, & Gajdusek, 1987; Kang, et al., 1987; Robakis, Ramakrishna, Wolfe, & Wisniewski, 1987; Tanzi, et al., 1987) following sequential proteolytic cleavage by β -secretase and γ -secretase (Sun, Bromley-Brits, & Song, 2012). The primary role of $A\beta$ deposition in AD pathogenesis has been greatly bolstered by genetic studies. Most of the FAD-associated mutations in APP are at or near the cleavage sites and favor the proteolytic processing of APP by β - or γ -secretase (Citron, et al., 1992; Mullan, Crawford, et al., 1992). Pathogenesis mutations in PS1 and PS2 increases $A\beta$ generation by directly affecting γ -secretase cleavage (Borchelt, et al., 1996; Citron, et al., 1997; Scheuner, et al., 1996). *APOE4*, the major genetic risk factor for LOAD, contributes to production, clearance and aggregation of $A\beta$ (Bu, 2009). However, the plaques formation does

Chapter 1: General Introduction

not well correlate with the severity of cognitive decline in AD patients, and the synaptic and behavioral changes are documented before plaque formation in AD mice (Hsia, et al., 1999; Mucke, et al., 2000). Detailed investigations show that the diffusible, soluble oligomer of A β species are neurotoxic, they disrupt hippocampal LTP and impair the memory in rats (M. P. Lambert, et al., 1998; Selkoe, 2008; Walsh, et al., 2002). Treatments that reducing β - or γ -cleavage of APP and A β generation could significantly improve the memory deficits in AD mice, and some of these drugs are currently being tested in clinical trials (Ly, et al., 2012; Martone, et al., 2009; Siemers, et al., 2006). Thus, although the precise mechanistic relationship of A β deposition and AD pathogenesis requires to be clarified, the anti-A β therapeutics remains the most promising drug target for AD treatment.

1.1.4 APP amyloidogenic and non-amyloidogenic processing

The APP gene, located on chromosome 21, encodes three major isoforms for the APP protein with 770, 751 and 695 amino acids by alternative splicing (Cheng, et al., 1988; de Sauvage & Octave, 1989; Kitaguchi, Takahashi, Tokushima, Shiojiri, & Ito, 1988). APP695, lacking an extracellular Kunitz Protease Inhibitor domain, is predominantly expressed in neurons (Kang, et al., 1987), while APP770 and APP751 are expressed in most tissues and cells (Arai, et al., 1991; Konig, Beyreuther, Masters, Schmitt, & Salbaum, 1989; Tanzi, et al., 1987).

In the amyloidogenic pathway, APP is first cleaved by β -secretase at the amino terminal end of A β (Asp-1 site, β -site), producing a secreted form of APP (sAPP β) and membrane-bound C99 (CTF β). C99 is subsequently cleaved by γ -secretase to generate A β and intracellular carboxyl-terminal fragment (CTF γ). Beta-site APP cleaving enzyme 1 (BACE1) is β -secretase *in vivo* (Hussain, et al., 1999; Sinha, et al., 1999; Vassar, et al., 1999; Yan, et al., 1999). In BACE1-knockout neurons culture (H. Cai, et al., 2001) and BACE1-knockout mice, there is no A β or C99 could be detected (Y. Luo, et al., 2001; Roberds, et al., 2001). Notably, knockout BACE1 in AD transgenic mice reduces the A β production and rescues the memory deficits (Ohno, et al., 2004). BACE1 expression is very low due to its weak promoter activity and the low efficiency of

Chapter 1: General Introduction

translation initiation. It leads to only a minority of APP undergoes amyloidogenic processing (Y. Li, Zhou, Tong, He, & Song, 2006; Zhou & Song, 2006).

Under physiological conditions, most of APP undergoes a non-amyloidogenic cleavage process. In this pathway, APP is cleaved by α -secretase at Lys-16 site within the A β domain to produce a secreted form of APP (sAPP α) and membrane-bound C83 (CTF α) (Esch, et al., 1990; Sisodia, Koo, Beyreuther, Unterbeck, & Price, 1990). C83 is further cleaved by γ -secretase, producing extracellular fragment p3 and intracellular CTF γ (Haass, et al., 1993). The activity of α -secretase is carried out by several members of the a disintegrin and metalloproteinase (ADAM) family, including ADAM9, ADAM10, and tumour necrosis factor- α convertase (TACE, also named ADAM17), though other proteases may also contribute to α -secretase activity (Allinson, et al., 2004; Asai, et al., 2003; Parvathy, Karran, Turner, & Hooper, 1998; Slack, Ma, & Seah, 2001). Moreover, the major BACE1 cleavage site on APP is within the A β region (Glu-11 site, β' -site) (Deng, et al., 2013) to produce C89 (CTF β') and truncated amyloid species (H. Cai, et al., 2001; Chen, et al., 2000; Creemers, et al., 2001; Vassar, et al., 1999). BACE2, which is considered to be a homolog of BACE1, cleaves APP at the θ -site (Phe-19 site) within the A β region to produce C80 (CTF θ), as such precludes A β generation (Sun, He, & Song, 2006; Sun, et al., 2005) (Fig.1.1). All the CTFs are further cleaved by γ -secretase complex. The components of γ -secretase complex are Presenilin (PS)1/PS2, Nicastrin (NCT), Presenilin Enhance 2 (Pen-2) and Anterior Pharynx-defective 1 (Aph-1) (Bart De Strooper, 2003; Bart De Strooper, et al., 1998; Kimberly, et al., 2003; Sastre, et al., 2001; Takasugi, et al., 2003; Wolfe, et al., 1999).

As an overall result, the majority of APP is cleaved within the A β domain undergoes non-amyloidogenic processing. To be processed in amyloidogenic pathway, APP has to encounter BACE1 and BACE1 preferentially cleaves APP at Asp-1 site.

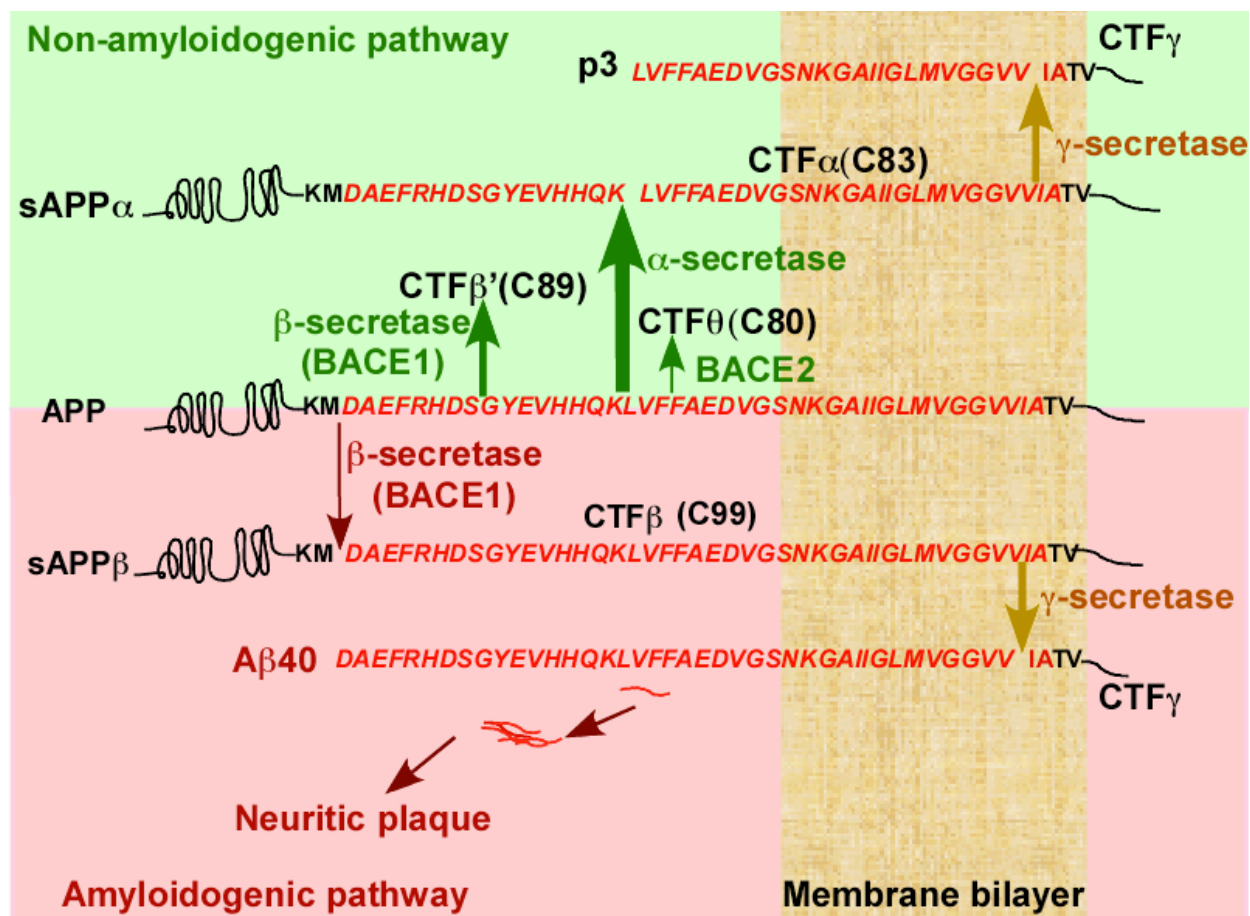


Figure 1.1 The APP non-amyloidogenic and amyloidogenic processing.

APP can be cleaved in two pathways: non-amyloidogenic pathway (Upper, green) or amyloidogenic pathway (Lower, red). Under physiological conditions, the majority of APP is cleaved within the A β domain by α -secretase to produce sAPP α and membrane-bound C83. C83 can be further cleaved by γ -secretase, producing extracellular fragment p3 and intracellular CTF γ . APP also can be cleaved at the β' site by BACE1 or at the θ site by BACE2 within the A β domain to produce truncated A β species. In the amyloidogenic pathway, APP is first cleaved by β -secretase to produce sAPP β and membrane-bound C99. Cleavage of C99 by γ -secretase yields intact A β and intracellular CTF γ . γ -secretase cleaves APP at multiple sites close to the inner membrane leaflet to produce variants of A β peptide with different length. The 40 amino acid A β peptide, A β 40, as the γ -cleavage site indicated in the figure, is the most abundant A β species. Insoluble A β deposits and aggregates to form the core of neuritic plaque in the brains, the pathological hallmark of AD (Slightly modified figure that originally published (X. Zhang & Song, 2013)).

1.2 APP and BACE1 trafficking in pathogenesis of Alzheimer's disease

1.2.1 The intracellular localization of APP and BACE1.

The nascent APP molecule matures through the constitutive secretory pathway from the endoplasmic reticulum (ER) to Golgi complex and then plasma membrane (PM). The majority of APP localizes in the Golgi complex (Caporaso, et al., 1994). Only a small proportion of APP can be detected at the cell-surface and over 50% is internalized within 10 minutes (Koo, Squazzo, Selkoe, & Koo, 1996; Perez, et al., 1999) and sorted into early endosomes (Haass, Koo, Mellon, Hung, & Selkoe, 1992; Koo & Squazzo, 1994; Lai, Sisodia, & Trowbridge, 1995), where some of APP is recycled back to the PM and others are sorted to the lysosome for degradation (Nordstedt, Caporaso, Thyberg, Gandy, & Greengard, 1993; Yamazaki, Koo, & Selkoe, 1996). The newly synthesized BACE1 also follows the classic transmembrane protein synthesis and trafficking pathway. It is transported from ER to Golgi, undergoes N-glycosylation and O-glycosylation and pro-peptide removal and finally maturing in the late Golgi or trans-Golgi network (TGN). As such, the BACE1 molecular mass increases from the immature form in the ER (~66KDa) to the fully glycosylated form (~75KDa) (Benjannet, et al., 2001; Capell, et al., 2000; Creemers, et al., 2001; Huse, Pijak, Leslie, Lee, & Doms, 2000). BACE1 transport from the ER occurs rapidly and efficiently, a minority immature BACE1 could be detected while the fully matured BACE1 is a highly stable protein with a half-life of ~16 hours (Huse, et al., 2000). BACE1 is internalized from the cell surface via its C-terminal dileucine motif (Huse, et al., 2000; Pastorino, Ikin, Nairn, Pursnani, & Buxbaum, 2002) and predominantly localized to the TGN and endosomes (Huse, et al., 2000; Vassar, et al., 1999). These acidic endosomal compartments provide a low pH environment, which is more favorable for BACE1 activity (Hook, et al., 2002). α -secretase is particularly enriched at the cell surface where it competes with BACE1 for APP processing (Parvathy, Hussain, Karran, Turner, & Hooper, 1999).

1.2.2 Subcellular localizations for A β generation.

Based on the distinct subcellular localizations of the BACE1 and α -secretase, it is likely that the majority of cell surface APP is processed through the non-amyloidogenic pathway, whereas

Chapter 1: General Introduction

intracellular APP processing would predominantly undergo the amyloidogenic pathway (Haass, et al., 1992; Koo & Squazzo, 1994). However, the active γ -secretase is suggested to broadly exist among the ER, Golgi, TGN, endosome, lysosome and cell surface (Bart De Strooper, 2003; Kim, Yin, Li, & Sisodia, 2004). Subcellular location for A β generation has been extensively studied. Multiple lines of evidence have demonstrated that A β is mainly produced in the endosomal/lysosome system. Impairing APP trafficking to the cell surface or enhancing APP internalization increases BACE1-mediated processing (Cataldo, Barnett, Pieroni, & Nixon, 1997; Haass, et al., 1992), while enhancing APP routing to, or reducing its internalization from the cell surface facilitates its α -secretase-mediated processing (Haass, Koo, Capell, Teplow, & Selkoe, 1995). APP is internalized to early endosomes via clathrin-coated vesicles; the endocytosis motif (YENPTY), located at the carboxyl terminus of APP, is responsible for its efficient internalization (Lai, et al., 1995). Deletion or mutation of this motif leads to the endocytosis-deficient APP and significantly reduces A β production (Perez, et al., 1999; Selkoe, et al., 1996). Consistently, abnormalities in the endocytotic pathway are evident in the early stage of sporadic AD brains, Down syndrome patients' brains and AD animal models, and the abnormal endocytotic pathway might contribute to AD pathogenesis by altering the trafficking of APP and BACE1. The Swedish double mutant (KM/NL) APP produced significantly more A β than wild type APP (X. D. Cai, Golde, & Younkin, 1993; Citron, et al., 1992; Mullan, Crawford, et al., 1992; Scheuner, et al., 1996); however, abolishing the endocytotic process of Swedish APP by removing its endocytotic motif still resulted in substantially more A β than with normal APP. This result indicates that β -cleavage on Swedish APP does not require an intact cytoplasmic domain and A β can be also produced in Golgi during its biosynthetic transport (Haass, Lemere, et al., 1995). What's more, inhibition of protein transport from ER to Golgi and redistributing Golgi proteins into ER by brefeldin A (BFA) treatment, or retention of APP in the ER with ER-retrieval signal, significantly reduced but not abolished intracellular A β production over 24 hours (A. S. Chyung, Greenberg, Cook, Doms, & Lee, 1997; Cook, et al., 1997). Additionally, by retaining C99 in the ER with KKQN motif or co-expression with dominant-negative mutant of the rab1B GTPas to prevent the C99 from exiting ER, A β production is almost eliminated. In

Chapter 1: General Introduction

contrast, when C99 is allowed to leave ER or targeted into Golgi and other distal compartments with QLQN motif, it normally gives a rise to substantial amounts of A β (Maltese, et al., 2001). The intracellular A β production from C99-KK can be partially restored by addition of brefeldin A (Cupers, et al., 2001). Likewise, C99-GFP accumulates in the early endosome after inhibition of γ -secretase activity (Kaether, Schmitt, Willem, & Haass, 2006). Furthermore, inhibiting the exocytosis of constitutively secretory vesicles, rather than inhibiting the clathrin-mediated endocytosis, causes the accumulation of C99-GFP in numerous small vesicles beneath PM (Cirrito, et al., 2008; Kaether, et al., 2006). These data suggest that A β production depends on the APP encounters both or sequentially β -secretase and active γ -secretase. So far, it is reported that A β could generate in multiple subcellular organelles, including ER/ER-Golgi intermediate compartment, the Golgi during its biosynthetic transport pathway and endosome/lysosome after endocytosis from plasma membrane (Fig 1.2.).

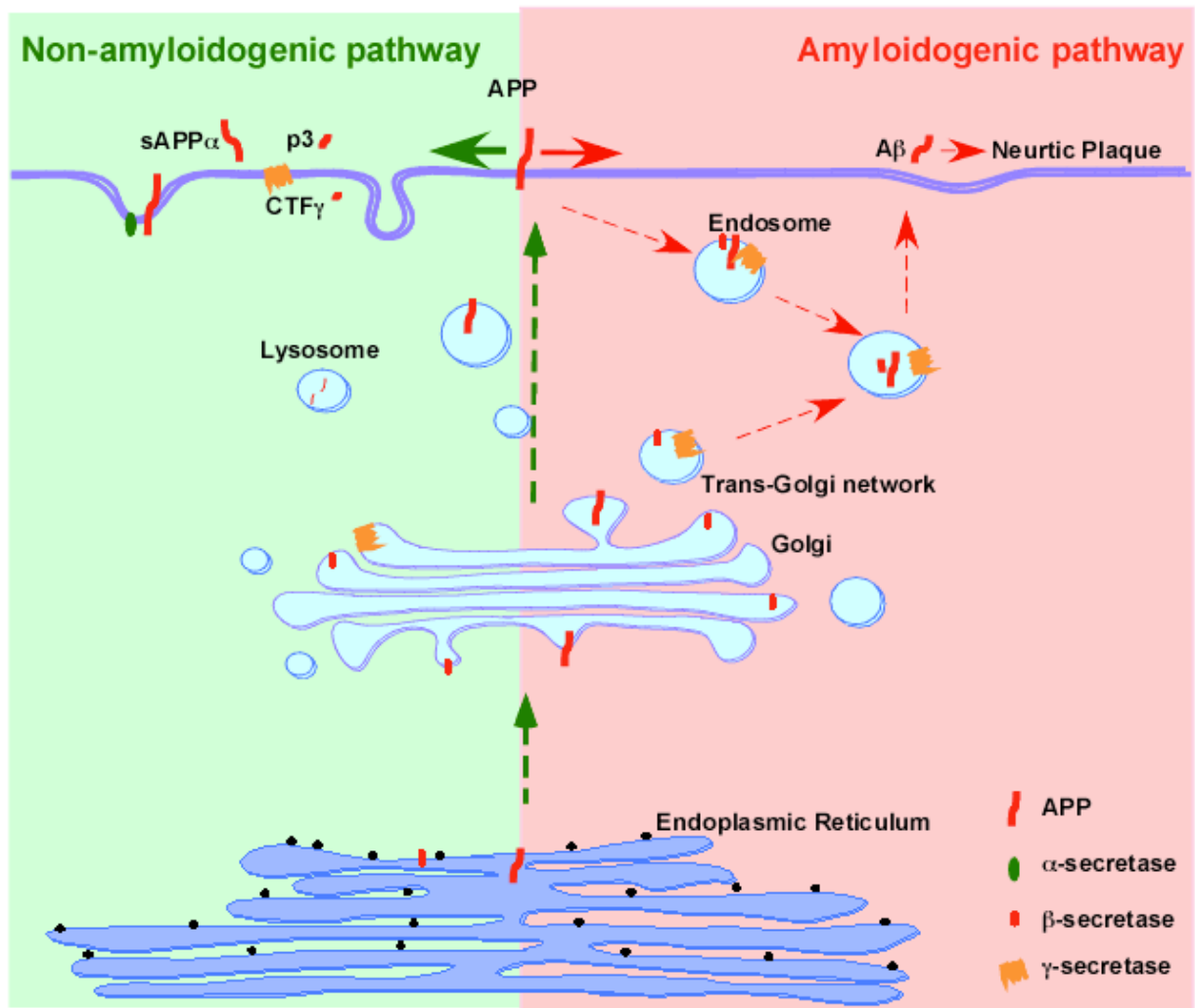


Figure 1.2 APP trafficking.

APP matures through the constitutive secretory pathway from the ER to the plasma membrane (PM). The majority of APP is then quickly internalized into early endosomes, where APP is recycled back to the PM or targeted to the lysosomal degradation pathway. Non-amyloidogenic processing (green) mainly occurs at the cell surface where α -secretase is particularly enriched. Amyloidogenic processing (red) involves APP trafficking through the secretory and recycling pathways where APP interacts with BACE1 and γ -secretases. A β is mainly generated in the subcellular compartments where the active γ -secretase complex exists (X. Zhang & Song, 2013).

1.2.3 Co-residency of APP and BACE1 increases A β production

BACE1 acts as a switch for APP amyloidogenic processing and it cleaves APP to generate C99, which is the direct precursor for A β production. The close proximity and interaction between APP and BACE1 is the prerequisite for A β production. However, in control samples from cultured hippocampus primary neurons, mice and human hippocampus region, the APP and BACE1 rarely associate in the same membrane environment (Jose Abad-Rodriguez, et al., 2004; Sakurai, et al., 2008). It has also been reported that APP and BACE1 do not co-localize at the plasma membrane where APP is generally cleaved by α -secretase (Haass, et al., 1992; Sisodia, 1992). Moreover, along the transportation from TGN to plasma membrane, and then internalization into the endosomal-lysosome system, APP and BACE1 are distinctly regulated. The internalization of APP occurs via recruitment of the adaptor-protein complex AP-2 and Dab2 for clathrin-mediated endocytosis (J. Lee, et al., 2008; Nordstedt, et al., 1993). It has been reported that AP-4 also involves in the sorting and outward transport of APP from TGN to PM (Burgos, et al., 2010; King & Scott Turner, 2004). In contrast to APP, BACE1 is internalized and sorted into rab GTPase 5-positive early endosome via a route controlled by ADP-ribosylation factor-6 (ARF6) (Sannerud, et al., 2011). The short acidic cluster-dileucine motif (DISLL) in the cytosolic domain of BACE1 specifically binds to the Golgi-localized γ -ear-containing ARF-binding proteins (GGAs), which mediate the recycling of BACE1 between TGN and early endosome (He, Chang, Koelsch, & Tang, 2002; He, Li, Chang, & Tang, 2005; He, et al., 2003; Shiba, et al., 2004; von Arnim, et al., 2004; Wahle, et al., 2005). An elegant study further proves that APP and BACE1 is not co-residency (Sakurai, et al., 2008). Mint/X11 proteins bind to munc18/syntaxin complex and contribute to synaptic vesicle transport of APP from TGN (Shrivastava-Ranjan, et al., 2008). However, BACE1 is absent from these APP-X11/munc18-syntaxin vesicles (Sakurai, et al., 2008). (Fig 1.3.).

Chapter 1: General Introduction

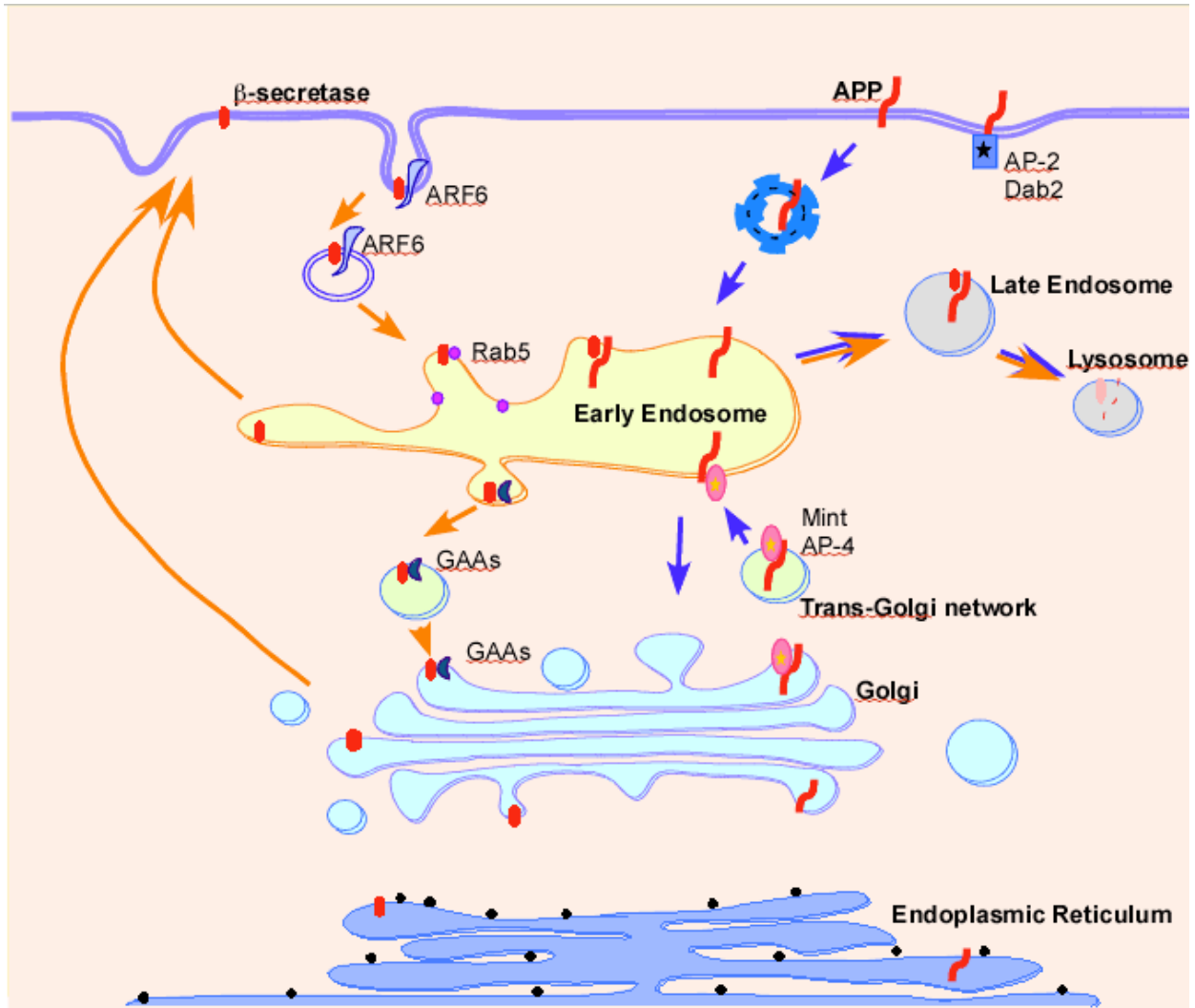


Figure 1.3 Distinctly regulated APP and BACE1 trafficking.

APP and BACE1 trafficking is differentially regulated from the site of TGN exit, internalization and further sorting into different compartments. The internalization of APP through recruitment of the adaptor-protein complex AP-2 and Dab2 for clathrin-mediated endocytosis; Mint/X11-munc18/syntaxin complex and AP-4 involve in the outward transport of APP from TGN to PM. The recycling of BACE1 from endosome is mediated by Golgi-localized γ -ear-containing ARF-binding proteins (GGAs). ARF6 mediates sorting of newly internalized BACE1 into rab5-positive early endosome and GGA3 could modulate BACE1 turnover and stability while sorting it into lysosome (X. Zhang & Song, 2013).

Chapter 1: General Introduction

Studies in AD patients and transgenic mice model consistently show that higher APP and BACE1 co-localization could be detected in the hippocampus region (Jose Abad-Rodriguez, et al., 2004) where A β mainly deposits. In cells models, facilitating the co-residency and/or the interaction between APP and BACE1 leads to increased BACE1 cleavage of APP through a regulated transport mechanism (A. Kinoshita, et al., 2003; Yan, Han, Miao, Greengard, & Xu, 2001). When both APP and BACE1 are sorted into a rab GTPase 5-positive early endosome by endocytosis induction (Rajendran, et al., 2006; Sannerud, et al., 2011), the production of sAPP β and A β are increased (Golde, Estus, Younkin, Selkoe, & Younkin, 1992; Haass, et al., 1992). The residence time of APP and/or BACE in early endosomes is essential for BACE1 cleavage. It is known that rab4 regulates sorting and cycling of early endosomes (van der Sluijs, et al., 1992). Stimulation of the recycling of cargo from the early endosome back to the PM decreases A β secretion (Rajendran, et al., 2006). Additionally, phosphorylation of munc18 facilitates APP-BACE1 interaction and shifts APP to the BACE1-associated vesicles, resulting in increased cleavage of APP by BACE1 and A β production (Sakurai, et al., 2008). Thus, enhancing the interaction between APP and BACE1, and/or increasing the co-residency of APP and BACE1 could facilitate the cleavage of APP by BACE1 and A β production.

1.2.4 BACE1 cleaves APP at two sites

BACE1 can cleave APP at two different sites to produce a 99 or 89-residue membrane-associated CTF (C99, or C89 respectively). β -cleavage at the site between Met596 and Asp597 of APP (Asp-1 cleavage site, or β site) (Lin, et al., 2000; Sinha, et al., 1999; Vassar, et al., 1999; Yan, et al., 1999) results in the release of C99 and then A β . In addition to Asp-1 site, BACE1 can also cleave APP within the A β domain between Tyr606 and Glu607 (Glu-11 cleavage site, or β' site), releasing C89 and then N-terminally truncated A β (H. Cai, et al., 2001; Creemers, et al., 2001; Huse, et al., 2002; Vassar, et al., 1999). Under physiological condition, the Glu-11 cleavage site is the major β -cleavage site (Deng, et al., 2013). Both truncated A β and p3 can be found in cerebrospinal fluid and media conditioned by cultured cells (Creemers, et al., 2001; Gouras, et al., 1998; Schenk, 1992; Seubert, et al., 1992; Vassar, et al., 1999).

Chapter 1: General Introduction

Preferential cleavage of APP by BACE1 at Asp-1 or Glu-11 site is strongly dependent on the APP sequence close to β -cleavage sites (Deng, et al., 2013) and BACE1 subcellular localization (Cordy, Hussain, Dingwall, Hooper, & Turner, 2003; Huse, et al., 2002; Vetrivel, et al., 2011). It is not simply due to the organelle's pH, oligosaccharide modification, or the amount of APP substrate. When BACE1 being tagged by an ER retrieval motif on its cytoplasmic tail, most of BACE1 is retained in the ER and expressed as the immature form, it predominately cleaves APP at Asp-1 site (Huse, et al., 2002; Vetrivel, et al., 2011). Replacing the BACE1 cytoplasmic tail with the intracellular domain of murine furin effectively causes BACE1 to be retained in the TGN, resulting in preferential generation of C89 rather than C99. Wild type BACE1 primarily exists in TGN and endosomal system, where more C89 than C99 is generated (Huse, et al., 2002). Guiding BACE1 to lipid rafts via addition of glycosylphosphatidylinositol (GPI) anchor results in the preferential cleavage of APP at Asp-1 site and secretion of more A β , and lack of cleavage at Glu-11 site (Cordy, et al., 2003; Vetrivel, et al., 2011). This shift of the β -cleavage sites is independent of the subcellular localization of APP or the pathogenic KM/NL mutation (Vetrivel, et al., 2011). Furthermore, C99 can be cleaved by BACE1 on its Glu-11 site to produce C89 (Creemers, et al., 2001; K. Liu, Doms, & Lee, 2002). However, when the APP-C99 fragment is targeted to the ER by KK motif, less C89 is processed compared to the wild type APP-C99 fragment (Cupers, et al., 2001). This data demonstrates that the C99 and C89 are processed in distinct subcellular organelles. C99 is more likely to be produced in the ER by immature BACE1 whereas C89 is predominantly processed in downstream apparatus of ER, the TGN and lysosome system.

1.2.5 Lipid rafts---platform for APP amyloidogenic processing

Lipid raft is a highly dynamic membrane structure, with a small size of 10 to 200nm. It enriches cholesterol and sphingolipids, and forms stable and ordered platforms by protein-protein and protein-lipid interaction (Pike, 2006). It could promote the interaction of APP with BACE1 and γ -secretase complex, thus facilitating the amyloidogenic cleavage of APP and contributing to A β

Chapter 1: General Introduction

production. It has been reported that BACE1, but not α -secretase, interacts with GPI-anchored proteins in lipid rafts (Sakurai, et al., 2008; Tun, Marlow, Pinnix, Kinsey, & Sambamurti, 2002). Addition of a GPI-anchor targets BACE1 into lipid raft, preferentially increasing β -site cleavage on APP and A β production (Cordy, et al., 2003; Vetrivel, et al., 2011) while targeting ADAM10 to lipid rafts competes with β -cleavage and reduces amyloidogenic APP processing (Harris, Pereira, & Parkin, 2009). Evidence also appears to support that the dynamic interaction of APP with lipid raft is critically important for APP processing. Antibody-induced co-patching of cell surface APP and BACE1 segregates them away from non-raft marker and dramatically increases A β generation, suggesting that APP is cleaved by BACE1 when it is inside raft clusters and cleaved by α -secretase when it is outside rafts (Ehehalt, Keller, Haass, Thiele, & Simons, 2003). These pieces of evidence consistently point out the important role of lipid rafts in facilitating β -cleavage of APP. Recently, a sterol-linked BACE1 transit-state inhibitor shows more effective inhibition in β -cleavage and A β production than free inhibitors (Rajendran, et al., 2008). This is not only because this inhibitor is internalized into endosome, where the β -cleavage occurred, but also because it is enriched in lipid rafts where the interaction between the inhibitors and BACE1 is enhanced. Moreover, all four γ -secretase complex components associate with lipid rafts (Vetrivel, et al., 2004). Removing the GPI proteins significantly reduces the level of A β (Sambamurti, et al., 1999). It is also shown that the PS1, PS2 and the active γ -secretase complex are located predominantly in a specialized sub-compartment called ER-MAM. ER-MAM is the extended ER compartment that is physically and biochemically connected to mitochondria (Estela Area-Gomez, et al., 2009), and it is an intracellular lipid raft-like structure intimately involved in cholesterol and phospholipid lipid metabolism, in Ca²⁺ homeostasis, and in mitochondrial function and dynamics (E. Area-Gomez, et al.). Additionally, it is reported that γ -secretase and APP CTFs, rather than CTFs derived from Notch, Jagged2, and N-cadherin, are co-reside in lipid rafts. It limits the processing of other γ -secretase substrate (Vetrivel, et al., 2005). This spatial segregation indicates that γ -secretase might specifically cleave APP in lipid rafts. Thus, lipid raft provide a specific platform for APP-BACE1 interaction and A β generation, as well as clustering the active γ -secretase complex, leading to the significantly enhanced APP

Chapter 1: General Introduction

amyloidogenic process, while outside the rafts, APP accesses α -secretase and undergoes non-amyloidogenic pathway.

Cholesterol depletion such as statins is used as a therapeutic approach to lower $A\beta$ production. However, concerns arise when there are contradictory results showed in clinic studies. Wolozin et al report that statins reduced the prevalence of AD (Wolozin, Kellman, Ruosseau, Celesia, & Siegel, 2000). Tokuda et al. report that the $A\beta$ level in plasma is not reduced in those statins-taking patients (Tokuda, et al., 2001). Further, the statins increased sAPP β , $A\beta$ and plaques in female AD mice model (Park, et al., 2003). Moderate reduction of membrane cholesterol in AD patients and transgenic mice increases $A\beta$ production, and this elevated production is associated with higher levels of BACE1-APP co-localization in hippocampus membrane (J. Abad-Rodriguez, et al., 2004). Additionally, cholesterol depletion affects Golgi morphology and apical membrane trafficking (Hansen, Niels-Christiansen, Thorsen, Immerdal, & Danielsen, 2000). Taken together, rather than reduction of membrane cholesterol level, disassociation of APP or BACE1 from lipid rafts might be better approaches for lowering $A\beta$ generation.

In summary, APP and BACE1 trafficking are critical for APP processing. Enhancing their interaction and/or increasing their chance of co-residence in the same compartment or in close proximity to each other facilitates β -cleavage of APP. BACE1 cleaves APP at two different sites, the β -site or β' -site, to produce C99 or C89, respectively, and the regulation of β -cleavage site selectively depends on the subcellular localization of BACE1. Retaining BACE1 in the ER or guiding it into lipid raft results in the preferential cleavage of APP at β -site to generate C99. However, C99 has to be further transferred into places with a mature and active γ -secretase complex and then be cleaved by γ -secretase to generate $A\beta$. The trafficking of APP and its processing enzymes, especially BACE1, plays an important role in APP processing and $A\beta$ production. Understanding how APP and these enzymes are trafficked through their secretory pathways and how the substrates encounter these enzymes with preferential activities in distinct locations will provide important insights into the development of therapeutical drugs in future.

Chapter 1: General Introduction

Valid strategies could be to prevent the A β production by altering the trafficking of APP and BACE1, or to use small molecules to block the accessibility and interaction between substrates and enzymes.

1.3 Transmembrane emp24 domain-containing protein (TMED) /P24 family proteins

P24 family proteins are small integral membrane proteins around 22-24KD. The p24 proteins play important but yet to be demonstrated roles in the early secretory transport pathway in fungi, plants and animals (G Emery, Gruenberg, & Rojo, 1999; Langhans, et al., 2008; Stamnes, et al., 1995). In agreement with their role in trafficking, p24 proteins are highly abundant in the interface between ER and Golgi (Belden & Barlowe, 1996; Blum, et al., 1999; Dominguez, Dejgaard, Fullekrug, et al., 1998; Rojo, et al., 1997b). The p24 family consists of four subfamilies (α , β , γ , and δ), whereby the exact composition varies among species. In mammals, ten p24 family proteins are identified while 6 of them are well studied: p23 (also named TMP21, TMED10, p24 δ 1), p24 (also named p24a, TMED2, p24 β 1), p25 (also named GMP25, TMED9, p24 α 2), p26 (also named p24b, TMED3, p24 γ 4) p27 (also named gp27, TMED7, p24 γ 3), and tp24 (also named T1/ST2, TMED1, p24 γ 1) (Strating & Martens, 2009; Strating, van Bakel, Leunissen, & Martens, 2009). P24 proteins share similar domain architecture: a large luminal domain of about 20KD, a single-span transmembrane domain and a highly conserved cytoplasmic domain of 12-18 amino acids. The luminal domain contains a GOLD (Golgi dynamic) domain that acts as cargo receptor between ER and Golgi (Anantharaman & Aravind, 2002), followed by a characteristic heptad repeats in coiled coils (Stamnes, et al., 1995) that interacts with other p24 family proteins (G. Emery, Rojo, & Gruenberg, 2000). The short cytoplasmic domain has binding motifs for vesicle coat complexes COPI and COPII (William J Belden & Charles Barlowe, 2001; Dominguez, Dejgaard, Fullekrug, et al., 1998; Harter & Wieland, 1998; Sohn, et al., 1996a; Weidler, Reinhard, Friedrich, Wieland, & Rosch, 2000). Mutual dependences exist among the family members. They always form heteromeric complexes, which is required for their stability, correct localization and functional expression. For example, the localization of TMP21 fully depends on heteromerization with p24a. Co-

Chapter 1: General Introduction

expression of the exogenous p24a and exogenous tagged TMP21 is both necessary and sufficient for cis-Golgi/Golgi localization of each protein (G. Emery, et al., 2000). The deletions of each member individually, especially knockdown of TMP21 leads to a general decrease of other p24 family proteins and loss of p24 complex function, but does not affect the RNA levels of other p24 family proteins (Fullekrug, et al., 1999; Jenne, Frey, Brugger, & Wieland, 2002; Marzioch, et al., 1999).

1.4 Transmembrane protein TMP21

TMP21 (Transmembrane protein, 21KD) is identified by Blum et al., they isolate this protein from rat pancreatic acinar cells. They find that TMP21 is a type I transmembrane protein and belongs to p24 family (Blum, et al., 1996c). TMP21 also named TMED10 (Transmembrane emp24 domain-containing protein 10), p23, p24 δ 1 and named Erv25p in yeast. It is encoded by the *Tmp21* gene located on Chromosome14q24.3, spanning 45179bp genomic DNA from 75.6 to 75.64Mb and including 5 exons and 4 introns. TMP21 has 219 amino acids. Similar to other p25 family proteins, TMP21 is a vesicle trafficking protein found in eukaryotes from yeast to mammals (Belden & Barlowe, 1996; Blum, et al., 1996b, 1996c; Schimmoller, et al., 1995; Stamnes, et al., 1995). In addition to its main function in protein transport between ER and Golgi, TMP21 is a major component of tubulovesicular membranes at the cis-Golgi network (CGN) (Rojo, et al., 1997b) and is essential for the integrity and proper organization of Golgi structure (Rojo, Emery, Marjomaki, et al., 2000). It mediates unfolded proteins response and quality control in the ER (W. J. Belden & C. Barlowe, 2001; Wen & Greenwald, 1999). TMP21 also selectively interacts with glycosylphosphatidylinositol-anchored proteins and contributes to their ER export and lipid rafts translocation (M. Fujita, et al., 2011; Takida, Maeda, & Kinoshita, 2008). Moreover, homozygous deletion of TMP21 results in embryonic lethality at very early stage and no homozygous embryo can be produced, indicating the fundamental role of TMP21 in the early embryonic development of mammals (Denzel, et al., 2000b).

Chapter 1: General Introduction

1.4.1 TMP21 facilitates protein transport between ER and Golgi

Protein transport between ER and Golgi is mediated by COPI- and COPII-coated vesicles (Pierre Cosson & Letourneur, 1997; Kuehn & Schekman, 1997). COPI-coated vesicles mediate the retrograde transport of Golgi-to-ER while COPII-coated vesicles mediate the anterograde transport from ER to Golgi (M. C. Lee, Miller, Goldberg, Orci, & Schekman, 2004). However, COPI vesicles in mammalian cells are also found to participate in the anterograde transport from the ER Golgi intermediate compartment (ERGIC) to the Golgi (Bethune, Wieland, & Moelleken, 2006; Lowe & Kreis, 1998). TMP21 serves as bifunctional receptor that mediates retrograde and anterograde transport between ER and Golgi (Dominguez, Dejgaard, Fullekrug, et al., 1998; Rojo, et al., 1997b). Its luminal domain is responsible for uptaking cargos into COP vesicles, and its cytoplasmic domain interacts with COPI and COPII subunits that form transport vesicles (Blum, et al., 1996c). The TMP21/p24a heteromeric complex acts as a cargo receptor in vesicle biogenesis from ER and recruits proteins in ER-derived vesicles (D. Gommel, et al., 1999; Muniz, Nuoffer, Hauri, & Riezman, 2000). TMP21 is widely implicated as an ARF-GTP receptor and/or cargo receptor for COPI-coated vesicles that bud on cis-Golgi (Letourneur, Gaynor, Hennecke, Demolliere, et al., 1994; Sohn, et al., 1996a), and it also interacts with Sec23 for COPII-coated vesicles that bud on the ER (Barlowe, et al., 1994; Belden & Barlowe, 1996; Schimmoller, et al., 1995). The budding of COPI-coated vesicles is initiated by ARF1-GDP binding to TMP21 (D. U. Gommel, et al., 2001; Sohn, et al., 1996a), and this step requires both the dilysine and diphenylalanine motifs in the cytoplasmic domain of TMP21 (P. Cosson & Letourneur, 1994a; Sohn, et al., 1996a). Binding with TMP21 leads to a conformational change in ARF1 and establishes a stable association of ARF1 with the phospholipid bilayer. The diphenylalanines motif is conserved in all p24 family members and mediates binding of Sec23 (Barlowe, 1998; Dominguez, Dejgaard, Fullekrug, et al., 1998) (Fig.1.4). Mutations of the C-terminal KKLE to SSLE on full length TMP21 significantly diminish its co-localization with COPI and interfere with the ER-Golgi trafficking of TMP21 (Blum & Lepier, 2008). Human TMP21 is ubiquitously expressed and highly expressed in the pancreas (Blum, et al., 1996c), an organ whose main task is the proteins synthesis, packaging, transport, and exocytosis.

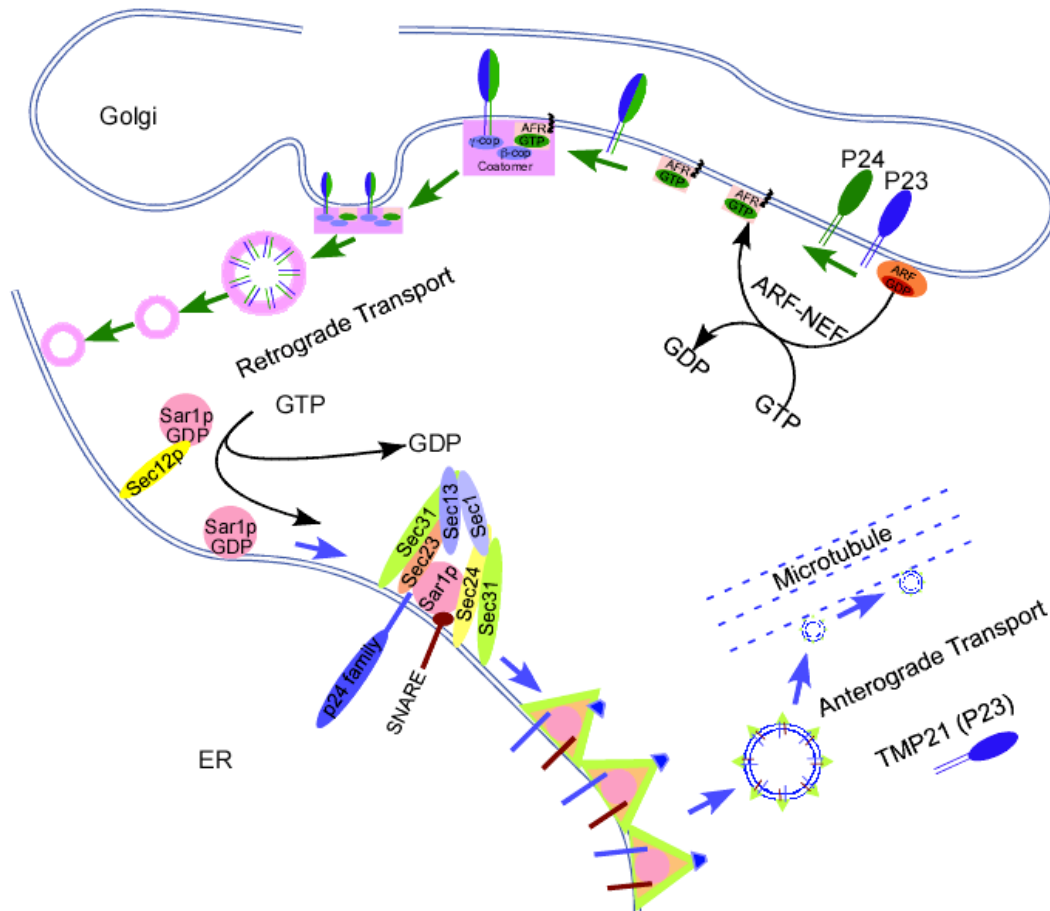


Figure 1.4 TMP21 (p23) mediates both anterograde and retrograde transport in early secretory pathway.

TMP21 belongs to the p24 ER/Golgi cargo family and plays critical roles in protein transport and organization of membrane structure. It mediates both anterograde and retrograde transport between ER and Golgi. TMP21 is widely implicated as an ARF-GTP receptor and/or cargo receptor for COPI-coated vesicle that bud on cis-Golgi, efficiency binding between p23 and COPI-coated vesicles required both the dilysine motif and a C-terminal diphenylalanine motif. The core machinery of COPI recruitment of coating proteins is initiated by ARF-GDP binding to p23, upon nucleotide exchange, ARF-GTP dissociates from p23 homooligomers and p24 homooligomers, this causes a conformational change in ARF and exposes a hydrophobic alpha-helix, resulting in a stable association with the membrane lipids, then multiple cycles of GTP hydrolysis and GDP to GTP are likely to occur, possibly causing rearrangement of p23/p24 hetero-oligomers. Cytosolic coatmer can bind in a bimodal fashion, via its β -COP and γ -COP subunits, to both ARF-GTP and p23/p24 hetero-oligomer, enhancing polymerization of the COPI vesicle coat. COPI vesicles in mammalian cells are found to participate in both the anterograde transport and retrograde transport.

Chapter 1: General Introduction

TMP21 also interacts with Sec23 for COPII-coated vesicles that bud on the ER. The diphenylalanines motif conserves in all five p24 family members and mediates binding of Sec23.

1.4.2 TMP21 contributes to the organization of Golgi apparatus

TMP21 is highly expressed in the membranes of cis-Golgi network (CGN) and accounts for up to 30% of all integral membrane proteins in CGN. These TMP21-rich membranes make the major contribution to the CGN structure (Rojo, et al., 1997b). Further evidence shows the morphogenic function of TMP21 and its contribution in generation and/or maintenance of the CGN and Golgi morphology (Denzel, et al., 2000b; Rojo, Emery, Marjomaki, et al., 2000). Maintenance of ribbon-like Golgi structure requires an optimal level of TMP21 expression. Both the overexpression and deficit of TMP21 will influence the integrity and proper organization of Golgi structure. TMP21-deficient mice show the formation of dilated saccules in the Golgi cisternae and the increased number of vacuoles surrounding the Golgi apparatus (Denzel, et al., 2000b). Overexpression of exogenous TMP21 leads to the specific relocation of endogenous TMP21 from cis-Golgi to specific membrane subdomains. This TMP21 enriched-subdomains are identified as the dynamic expansion of ER structure because of their accessibility to other ER proteins, like ER marker calnexin and Bip (Rojo, Emery, Marjomaki, et al., 2000). Using immunoelectron microscopy, it is observed that this expression-dependent TMP21 depletion leads to the expansion and clustering of the smooth ER membranes and fragmentation of Golgi ribbon (Blum, et al., 1999; D. Gommel, et al., 1999; Gong, et al., 2011). Interestingly, the relocation of TMP21 modifies the ultra-structure of the CGN and Golgi without affecting the localization of COPI and COPII as well as the anterograde and retrograde transport reactions to any significant extent *in vivo* (Rojo, Emery, Marjomaki, et al., 2000). This indicates that the function of TMP21 in vesicular trafficking is independent from its morphogenic activity. It has been noted that the major morphological changes do not affect trafficking between subcellular compartments during the biosynthetic pathway (Gahmberg, Pettersson, & Kaanainen, 1986; Sandoval & Carrasco, 1997). Thus, overexpression of TMP21-induced ER/Golgi morphological change might not affect the ER/Golgi trafficking of proteins. Also, overexpression of TMP21 retains exogenous TMP21, but not other ER proteins in these specialized ER-derived membrane, indicating this

effect is specific to TMP21. It is reasonable that the exogenous TMP21 does not exit ER because this process also requires the participation of other p24 family proteins. The p24 family proteins can exit ER when co-expression of five different p24 family proteins (Dominguez, Dejgaard, Fullekrug, et al., 1998).

1.4.3 The roles of TMP21 in ER quality control and unfolded protein response (UPR)

The ER plays an essential role in the folding and maturation in the secretory pathway. Quality control in the ER ensures that unfolded or misfolded proteins are retained before their export to ER and eventually targeted for ER-associated degradation (ERAD) by the ubiquitin/proteasome pathway (Lord, Davey, Frigerio, & Roberts, 2000). Only correctly folded, assembled and modified proteins can escape the clutches of the quality control system and can be sorted into anterograde transport vesicles (Ellgaard & Helenius, 2001, 2003). Half or more of newly synthesized wild type protein molecules fail to mature and are quickly degraded in ER at the level of nascent chains (Schubert, et al., 2000). The Unfolded Protein Response (UPR) signaling pathway is activated by ER stress, which can be induced by disturbances in the function or loss of integrity of the ER, such as the accumulation of unfolded proteins and alternations in calcium homeostasis (Lindholm, Wootz, & Korhonen, 2006; Xu, Bailly-Maitre, & Reed, 2005; Yoshida, 2007). It has been reported that the deletion of p24 proteins activates UPR in yeast and leads to increased Kar2/Bip expression (W. J. Belden & C. Barlowe, 2001). Loss of function of p24 heteromeric complex delays the transport of secretory proteins, like Gas1p and invertase, and accumulates them in ER. In contrast, ER resident proteins, as Kar2 and Bip containing an HDEL retrieval sequence, escape the ER and are secreted into the extracellular medium (W. J. Belden & C. Barlowe, 2001). Kar2/Bip are upregulated by UPR (Okamura, Kimata, Higashio, Tsuru, & Kohno, 2000). Mutants of the *C.elegans* p24 proteins facilitate the transport of proteins to cell surface via a quality control mechanism for ER/Golgi transport (Wen & Greenwald, 1999). Interestingly, the overexpression of TMP21 in cells and animal models does not significantly alter the cellular level of Kar2p/Bip/grp78, ATF4 and CHOP (Gong, et al., 2011; Rojo, Emery, Marjomaki, et al., 2000), which are all UPR marker and increase upon the induction of unfolded

protein response with the glycosylation inhibitor tunicamycin (Kozutsumi, Segal, Normington, Gething, & Sambrook, 1988). It indicates that the overexpression of TMP21, even though it accumulates in the ER, does not activate the UPR signaling pathways.

1.4.4 TMP21 facilitates the ER export of GPI-anchored proteins and guides them into lipid rafts

In eukaryotic cells, glycosylphosphatidylinositol (GPI) anchoring of proteins is a highly conserved posttranslational modification. In mammalian cells, more than 150 proteins are modified by GPI. The biosynthesis of glycosylphosphatidylinositol (GPI) precursors occurs in the ER. The GPI anchoring to newly synthesized proteins is also processed in the lumen of the ER (Ikezawa, 2002; Taroh Kinoshita, Fujita, & Maeda, 2008; T. Kinoshita & Inoue, 2000). After attachment to proteins, the lipid and glycan parts of GPI are structurally remodeled (Moriyama Fujita & Jigami, 2008; Moriyama Fujita & Kinoshita, 2008). Both reactions are required for the efficient transport of GPI-anchored proteins from ER to Golgi (M. Fujita, et al., 2011). Upon exiting from the ER, the GPI-anchored proteins are sorted into COPII-coated vesicles (Morsomme, Prescianotto-Baschong, & Riezman, 2003; Morsomme & Riezman, 2002). However, GPI proteins are localized in the lumen and lack the cytosolic domains, so that they cannot directly interact with cytosolic COPII components and must either use membrane-spanning cargo receptors or alternative mechanism for ER export. Further studies find that TMP21 forms a hetero-oligomer with p24a and recognizes the remodeled-GPI anchors signal, and the TMP21-p24a complex mediates the specific sorting of the correctly remodeled GPI proteins into the COPII-coated vesicle, thus facilitating the ER export of these GPI-anchored proteins (Bonnon, Wendeler, Paccaud, & Hauri, 2010; M. Fujita, et al., 2011). This process depends on the GOLD domain in the luminal of p24 family proteins (Anantharaman & Aravind, 2002). TMP21 and p24 family proteins are co-precipitated with GPI-anchored proteins. Knockdown of TMP21 impairs the packaging of GPI-anchored proteins into COPII-coated vesicles and delays their transit from ER to Golgi (M. Fujita, et al., 2011). It greatly slows down the maturation process of GPI-anchored proteins, without affecting non-GPI-linked proteins

Chapter 1: General Introduction

(Bonnon, et al., 2010; Takida, et al., 2008). Association of p24 family proteins with GPI-anchored proteins is pH dependent; neutral pH promotes interactions while acidic pH induces the disassociation of cargo and p24 family proteins. This fact suggests that these proteins bind in the ER and disassociate in acidic compartments, such as ERGIC or cis-Golgi (M. Fujita, et al., 2011). Furthermore, it has been reported that early lipid-raft-like structures can be observed in the ER (Browman, Resek, Zajchowski, & Robbins, 2006; Sevlever, et al., 1999), where sterols and sphingolipids are expressed at low concentrations (van Meer & Lisman, 2002). TMP21-p24a complex co-partitions with GPI-anchored proteins into this biosynthetically early raft-like structures (Bonnon, et al., 2010).

1.5 TMP21 and Alzheimer's disease

The *Tmp21* gene is located on chromosome 14q24.3, from 75.6 to 75.64Mb. By linkage studies in 1992, Chr14q24.3 is defined as a minimal cosegregating region that containing the major gene predisposing to early onset AD (Mullan, Houlden, et al., 1992; Schellenberg, et al., 1992; St George-Hyslop, et al., 1992; Van Broeckhoven, et al., 1992). At least 19 different transcripts are isolated from this region. One of these transcripts, PS1, encoded by the gene *PS1* from 73.6 to 73.69Mb (R.F. Clark, 1995; Sherrington, et al., 1995), is identified as the core member of the γ -secretase complex and responsible for proteolytic cleavage of APP (Bergmans & De Strooper; Bart De Strooper, 2003). *PS1* knockout mice showed a markedly reduced activity in γ -secretase cleavage of APP and A β production (B. De Strooper, et al., 1998). *Tmp21*, located in the region highlighted by AD linkage studies and close to the *PS1* gene, is possibly involved in the etiology of AD. However, the genetic association between *Tmp21* and AD remains elusive.

TMP21 is widely expressed in the brain and highly expressed in the neocortex and hippocampus (Vetrivel, et al., 2008). These brain regions are crucial for learning and memory and are most severely affected in AD as observed by the high number of plaques deposited (Braak & Braak, 1991; Braak, Braak, & Bohl, 1993; Dolcini, et al., 2008). TMP21 level is at its highest during

Chapter 1: General Introduction

embryonic development and declines with age. Aging is the greatest risk factor for AD. Patients with AD show a reduced level of TMP21 in the frontal cortex and hippocampus, but not in the cerebellum, which is less affected by AD (Vetrivel, et al., 2008). Our lab has recently characterized the promoter of human *Tmp21* gene and found that it contains an NFAT1 response element (S. Liu, et al., 2011), which activation is briefly increased early in the early stage of cognitive decline and falls under normal levels as the disease progresses (Abdul, et al., 2009) et al., 2009). These results imply the potential relevant between TMP21 and AD pathogenesis. It is known that endogenous TMP21 is highly expressed during the embryonic development stage and shortly after birth but declines with age, which indicates a high demand of TMP21 at early stage in life and suggests it is indispensable to early stage development (Denzel, et al., 2000b; Vetrivel, et al., 2008). However, while transgenic mice expressing human TMP21 display a sustained high level of TMP21 expression during post-natal development, they begin to show complex neurological problems when endogenous TMP21 begins to decline (Gong, et al., 2011). This evidence suggests that tightly controlling TMP21 expression level is critically important for facilitating mammalian development and maintaining proper neuronal function.

Recently, by using a higher-dimension analytic method (LA) to investigate the dynamic nature of genes co-expression at the genome-wide scale, Li et al found the positive co-expression of TMP21 and APP. In the same system, they observed the positive co-expression of PS1 and APP, as well as the negative co-expression of BACE2 and APP (K.-C. Li, Liu, Sun, Yuan, & Yu, 2004). Following this study, TMP21 was found to play a pivotal role as a regulator of the γ -secretase complex. TMP21 could co-precipitate with other members of the γ -secretase complex, PS1/PS2, NCT, Pen -2 and Aph-1 (F. S. Chen, et al., 2006). More importantly, TMP21 is co-localized with PS1 in human brain (Vetrivel, et al., 2008). Similar to the components of the γ -secretase complex and BACE1, TMP21 can be degraded by the ubiquitin-proteasome pathway (S. C. Liu, et al., 2008). TMP21 can be pulled down by a high affinity compound biotin-linked- γ -secretase inhibitor (Teranishi, et al., 2009) and is identified as one of the γ -secretase-associated proteins (GSAPs) in detergent resistant membrane from rat brains; those GSAPs regulate APP

Chapter 1: General Introduction

and Notch processing differently (Hur, et al., 2012). TMP21 selectively regulates the APP cleavage at the γ -site without affecting ϵ -site cleavage on APP or Notch (F. S. Chen, et al., 2006; Dolcini, et al., 2008). Notch is another known substrate of the γ -secretase complex (B. De Strooper, et al., 1999; Song, et al., 1999); Notch is essential for cell fates determination, cell proliferation and cell death in development (Artavanis-Tsakonas, Rand, & Lake, 1999; Bray, 2006). The transmembrane domain of TMP21 binds to the γ -secretase complex and decreases γ -secretase proteolytic processing thus reducing the A β production (Pardossi-Piquard, et al., 2009). Knockdown of TMP21 expression enhances APP maturation efficiency, producing more mature APP for amyloidogenic pathway thereby generating more A β (Vetrivel, et al., 2007). This evidence shows a dual role of TMP21 in the modulation of A β production by controlling APP trafficking and γ -secretase activity. The negative regulation of A β production by TMP21 suggests that increasing TMP21 expression might be a potential strategy to reduce A β level and consequently, prevent AD pathogenesis. However, transgenic mice with neuron-specific expressed human TMP21 showed severe neurological problems, growth retardation, infertility and premature death (Gong, et al., 2011; Gong, et al., 2012). Still, it remains to be determined the causal linkage between TMP21 levels and AD pathogenesis.

1.6 Overall goals of this research

The trafficking of APP and all its enzymes, BACE1, α - and γ -secretase, is essential for APP cleavage. Especially, APP encountering BACE1 in lipid rafts facilitates APP amyloidogenic processing and immature BACE1 cleaving APP at Asp-1 site is the first step for A β generation. However, BACE1 mainly cleaves APP at Glu-11 site to generate truncated A β . TMP21, the vesicular trafficking protein, mediates proteins ER/Golgi transport and facilitates GPI-anchored protein ER export and lipid raft translocation. The effects of TMP21 on γ -secretase activity and APP trafficking have been reported recently and as such are attracting more attentions to the investigation of the role of TMP21 in AD pathogenesis. However, there is no genetic study of *Tmp21* in AD patients, the exact role of TMP21 in BACE1 cleavage and APP processing is still unknown. The overall goals of this research are to analyze the genetic linkage between *Tmp21*

Chapter 1: General Introduction

SNPs and AD and investigate the role of AD-associated SNP in TMP21 expression, to explore the role of TMP21 in APP processing by emphasizing the impact of TMP21 on BACE1 Asp-1 site cleavage, and to understand the mechanism through which TMP21 affects BACE1 maturation and trafficking thus facilitating APP amyloidogenic processing.

1.6.1 Genetic analysis of *Tmp21* SNPs in AD patients

The genetic association between *Tmp21* and AD remains elusive. In chapter 2, we screened genomic DNA of *Tmp21* from more than 400 AD patients and controls and identified an AD-associated SNP in *Tmp21*. Then we explored a novel strategy to study the effect of this SNP on TMP21 expression *in vitro*; furthermore, we investigated the mechanism through which this SNP alters TMP21 expression.

1.6.2 Explore the role of TMP21 in APP processing

Downregulation of TMP21 increases A β generation by selectively modulating γ -secretase activity without affecting Notch cleavage, suggesting that TMP21 is a negative modulator of A β production (F. S. Chen, et al., 2006). However, upregulated TMP21 leads to Golgi fragmentation and severe neurological problems in human *Tmp21* transgenic mice (Gong, et al., 2011). We identify that a novel AD-associated SNP significantly increased the expression of TMP21 at both mRNA and protein levels. In chapter 3, we explored the roles of both up- and down-regulated TMP21 in APP amyloidogenic processing and first implied the potential impact of TMP21 on BACE1.

1.6.3 Investigate the effect of TMP21 in BACE1 maturation and trafficking

BACE1 is mainly presented as its mature form and cleaves APP within the A β region at Glu-11 site to generate C89 then truncated A β species (Deng, et al., 2013; Huse, et al., 2002). Preferential cleavage of APP by BACE1 at Asp-1 or Glu-11 site is strongly dependent on BACE1 subcellular localization. The Asp-1 site cleavage on APP for producing C99 and intact A β is enhanced by retaining BACE1 in the ER or guiding BACE1 into lipid rafts (Cordy, et al.,

Chapter 1: General Introduction

2003; Huse, et al., 2002; Vetrivel, et al., 2011). TMP21, a vesicular trafficking protein, mediates proteins ER/Golgi transport and maturation process (Dominguez, Dejgaard, Fullekrug, et al., 1998; Nickel, Sohn, Bunning, & Wieland, 1997). It also facilitates GPI-anchored proteins ER export and lipid rafts translocation (M. Fujita, et al., 2011; Takida, et al., 2008). Preliminarily, our data suggests that TMP21/immature BACE1 interaction in the ER might alter the trafficking and maturation processing of BACE1. In chapter 4, we revealed how the TMP21 affected APP and BACE1 trafficking, thus the underlying mechanism for TMP21 facilitating APP amyloidogenic processing.

Chapter 2: A Novel AD-associated SNP in *Tmp21* Increases TMP21 Expression by Potentiating the Splicing Efficiency

2.1 Introduction

TMP21 is recently identified as a modulator of γ -secretase and it selectively regulates the cleavage at the γ -site of APP without affecting the ϵ -site cleavage on APP or Notch (F. S. Chen, et al., 2006; Dolcini, et al., 2008). It suggests that TMP21 could be a potential therapeutic target to specifically reduce A β generation without affecting Notch signaling pathway. Our lab has characterized the promoter of human TMP21 and found that it contains an NFAT1 response element (S. Liu, et al., 2011), and similar to BACE1 and other members of γ -secretase complex, TMP21 can be degraded by the ubiquitin-proteasome pathway (S. C. Liu, et al., 2008). TMP21 is encoded by the *Tmp21* gene located on Chr14q24.3. This region is highlighted by AD linkage studies (Schellenberg, et al., 1992; St George-Hyslop, et al., 1992; Van Broeckhoven, et al., 1992). However, the genetic association between *Tmp21* and AD remains elusive. In this chapter, we screened the *Tmp21* Single-Nucleotide Polymorphisms (SNPs) in 261 AD patients and 236 controls. We firstly identified that rs12435391 (IVS4-28T>C) located in intron 4 of *Tmp21* was an AD-associated SNP. Next we investigated the role of this AD-associated SNP in TMP21 pre-mRNA processing and mRNA protein expression *in vitro*. Although rs12435391 (IVS4-28T>C) did not affect the splicing site recognition, it significantly increased TMP21 expression at both mRNA and protein levels. Furthermore, we found that this SNP significantly increased the splicing efficiency of *Tmp21* pre-mRNA, leading to the elevation of mature mRNA. However, the stability of *Tmp21* pre-mRNA and transcription activity of *Tmp21* was not affected. Taken together, our study identified a novel AD-associated *Tmp21* SNP and also indicated that the upregulation of TMP21 contributed to AD pathogenesis.

2.2 Methods

2.2.1 Subjects.

Genomic DNA was extracted from 261 sporadic AD patients and 236 healthy controls (The National Cell Repository for Alzheimer's Disease [NCRAD], Indianapolis, Indiana) of Caucasian. The mean (SD) age of AD patients was 82.97 (9.00) years for 174 females and 77.83 (9.49) years for 87 males, and the mean (SD) age of AD patients was 85.81 (9.99) years for 135 females and 84.47 (9.36) years for 101 males, respectively (Zhou, et al.).

2.2.2 SNP detection.

Five pairs of TMP21 gene-specific primers were used to amplify 5 amplicons of TMP21 entire coding sequence, from exon1 to exon 5, which covered over 40kb region on chromosome 14. The forward primers, EXON1 F 5'-ACGGCATCAGAAGGTCAGAG, EXON2 F 5'-TGGGGATGGTTGGAACATAG, EXON3 F 5'-GAGGAGTTGTGGCTGTTTCC, EXON4 F 5'-AGCGATGTTTTTCAGAGAGCTG or EXON5 F 5'-AGCGATGTTTTTCAGAGAGCTG, and reverse primers, EXON1 R 5'-CTCCACCGCACGTCCTTT, EXON2 R 5'-GGTGCTCCAAAGACTACAAGG, EXON3 R 5'-CCCGGCTAAGGCTGTTAATAC, EXON4 R 5'-CCCAGCCAGGATAATGAACT or EXON5 R 5'-CCTTGATGGTGCTGTTGGTA were used to amplify exon1 to exon 5 including the flanking intronic sequence. PCR reactions were carried out by using Platinum Taq DNA Polymerase (Invitrogen, Carlsbad, CA), 0.2 mM of each dNTP, 1.5 mM of Mg²⁺, 0.3% DMSO and 0.3 μM of each primer. Samples were initially denatured at 94°C for 5 min, followed by 40 cycles with denaturing at 94°C for 30 s, annealing for 30 s at 57°C, then extending at 72°C for 1 min, followed by a final extension at 72°C for 5 min. PCR products were cleanup by Shrimp Alkaline Phosphates (SAP) and Exonuclease (EXO1) (New England Biolab) at 37°C for 45min to remove the excess dNTPs and PCR primers, then both enzymes were inactivated by heating at 80°C for 15min. BigDye v.3.1 ready reaction mixture and the forward primers were used in DNA sequencing reactions. Cycle sequencing was performed in Eppendoff thermal cyclers (MJ Research, Waltham, MA) and the samples were sequenced by NAPS unit in UBC (<http://dnalims.msl.ubc.ca/>).

2.2.3 Plasmids constructions.

The human *TMP21* promoter plasmid pTMP21-3151+175 contains -3151 to +175 region of *TMP21* gene promoter upstream of firefly luciferase reporter gene in the pGL3-basic. The *TMP21* expression plasmid pcDNA4-TMP21mycHis was generated as previously described (S. Liu, et al., 2011). The 593bp fragment including exon1-4 of *Tmp21* was amplified from pcDNA4-TMP21mycHis by PCR using the forward primer TMP-fullcDNA-F 5'-GCCACCATGTCTGGTTTGTCTGGCCCAC and reverse primer TMP-E4-R 5'-GCATCTCCTCTTCTCTTCTTCTTC. The 978bp fragment consisting of intron4 and exon5 was amplified from gDNA from SH-SY5Y cells with primer TMP-E4-F 5'-CCATTAGAGGTAGAGCTGCG and TMP-E5-myc-stop-Xbal-R 5'-GCTCTAGATTACAGATCCTCTTCTGAGATGAGTTTTTGTTCCTCAATCAATTTCTTGG CCTTG. As the template, these two fragments with 90bp overlapped were amplified to produce 1480bp *Tmp21* fragment including exons1-4, intron4 (755bp), and exon5 by PCR, using primers at the very ends: TMP-fullcDNA-F and TMP-E5-myc-stop-Xbal-R. The Luciferase reporter gene was replaced by exons1-4, intron4 (755bp), and exon5. The intron4 Single-nucleotide Polymorphism (*TMP21*-Intron4 SNP) was introduced by PCR-based site mutagenesis method. *TMP21*-Intron4 Negative plasmid was constructed by cloning *Tmp21* coding sequence into the same vector without intron4. pB1P-A contains -4941 to +292 region of *BACE1* gene promoter upstream of firefly luciferase reporter gene in pGL3-basic (Christensen, et al., 2004). The human *RACN1* promoter pRACNLuc-A contains -1651 to +45 region of *RCAN1* gene promoter upstream of firefly luciferase reporter gene in pGL3-basic (Sun, et al.). *TMP21* wild type intron4 and intron4 with SNP, amplified with the primers 5'-GGGGTACCGTGAGGGGGAAGGCGACTC and 5'-GCTAGCTAGCCTAAAAAAAACAAAAGCA, were inserted into the upstream of *RCAN1* promoter and *BACE1* promoter, respectively.

2.2.4 Cell culture, transfection and drug treatments.

HEK293 cells and SH-SY5Y cells were cultured in in Dulbecco's modified eagle medium (DMEM) supplemented with 10% fetal bovine serum (FBS), 1mM sodium pyruvate, 1mM L-glutamine, and 50U/mL penicillin G sodium and 50µg/mL streptomycin sulfate (Invitrogen, Carlsbad, CA USA). All cells were cultured in an incubator at 37°C containing 5% CO₂. Cells were seeded in 24-well plates or 35mm plates 24 hours before transfection and grown to near 70% confluence by the day of transfection. Cells were transfected with 0.5ug TMP21 plasmid DNA per well using 1µl Lipofectamine 2000 (Invitrogen). Plasmid pcDNA3.1-RCAN1mycHis or peGFP-N2 was cotransfected to normalize for transfection efficiency. Actinomycin D (ACT-D) (10µM) (Sigma) and isoginkgetin (ISO) (33µM) (Abcam) were dissolved in acetone and DMSO, respectively.

2.2.5 Immunoblotting.

Cells were harvested and washed with ice-cold PBS and lysed in a modified RIPA-DOC buffer (150mM NaCL, 50mM Tris-HCL, 1% Triton X-100, 2% SDS, and 1% sodium deoxycholate) with the presence of protease inhibitor cocktail complete (04693116001; Roche, Indianapolis, IN, USA). After briefly sonication and centrifugation at 14,000rpm for 10 mins, supernatants were collected and protein assay was performed with the Bio-Rad Dc protein assay kit (Bio-Rad, Richmond, CA, USA). Whole-cell lysates were diluted in 4XSDS-sample buffer and separated on 12% Tris-glycine SDS-PAGE gel and transferred to polyvinylidene fluoride (PVDF-FL) membranes. Membranes were blocked in PBS containing 5% non-fat dried milk and incubated with the primary antibodies diluted in the blocking buffer at 4°C overnight. The primary antibody 9E10 (1:100) and AC-15 (1:5000) (Abcam, Cambridge, MA, USA and Sigma) were used to detect myc-tagged TMP21 and β-actin. The near-infrared fluorescence-labeled secondary antibodies were IRDyeTM 680 Goat Anti-Rabbit IgG (1:100,000) and IRDyeTM 800 Goat Anti-Mouse IgG (1:100, 000) (Lincoln, NE, USA). Detection and quantification were performed with the LI-COR Odyssey imaging system.

2.2.6 Semi-quantitative RT-PCR.

Total RNA was isolated from cells using TRI reagent (Sigma) and treated by DNase in TURBO DNA-free Kit (Invitrogen) as described in instructions. ThermoScrip™ RT-PCR system (Invitrogen) was used to synthesize the first strand cDNA using 1µg of total RNA as template following the manufacturer's instructions. The newly synthesized cDNA templates were amplified by Platinum Taq DNA polymerase (Invitrogen) in a 10µl reaction. Twenty to 35 cycles of PCR were performed to cover the linear range of the PCR amplification. The human TMP21 gene specific primers TMP-E4-F2 5'-TGCCTACATGAAGAAGAGAGAAGAG, or TMP-E4-F 5'-CCATTAGAGGTAGAGCTGCG and myc-tag specific reverse primer Myc-stop-XbaI-R 5'-CTAGACAGATCCTCTTCTGAGATGAGTTTTTGTCTAG, were used to amplify a 185-bp or 240-bp fragment of the TMP21 coding region covering the splicing site between exon4 and exon5, respectively. TMP21 Intron4 or Exon5 sequencing primers TMP-Int4-seq-F 5'-TGTTAGACCTAGGGACAGAGT forward and myc-tag specific reverse primers Myc-stop-XbaI-R were used to amplify a 242-bp fragment of the TMP21 gDNA. pcDNA3.1-RCAN1mycHis or peGFP-N2 was used as a transfection efficiency control. RCAN1 gene-specific primers were: forward: 5'-GTCCATGTATGTGAGAGTGATCAAG; myc-tag specific primers Myc-stop-XbaI-R and amplified a 130bp fragment of the RCAN1 coding region. β-actin primers were: forward: 5'-GGACTTCGAGCAAGAGATGG; reverse: 5'-CTAGAAGCATTGCGGTGGACG to amplify a 466bp fragment cross exon4 to 6 of β-actin. Or β-actin primers: forward: 5'-ATCATTGCTCCTCCTGAGCGC; reverse: 5'-CTAGAAGCATTGCGGTGGACGA amplified a 144bp fragment of the β-actin exon 6. The forward primer 5'-TGTTAGACCTAGGGACAGAGT and reverse primer 5'-CTAGACAGATCCTCTTCTGAGATGAGTTTTTGTCTAG were used to amplify *Tmp21* pre-mRNA with 242bp. All PCR products were analyzed on 1%~2% agarose gels.

2.2.7 Luciferase assay.

Cells were transfected with 0.5µg plasmid in a well of 24-well plate. The Renilla luciferase vector pCMV-RLuc (Promega, Madison, WI, USA) was cotransfected to normalize the

Chapter 2: A Novel AD-associated SNP in *Tmp21*

transfection efficiency. Cells were harvested at 48 hour after transfection and lysed in 50 μ L 1X passive lysis buffer (Promega) per well. Firefly luciferase activities and Renilla luciferase activities were assayed using the Dual-luciferase reporter assay system (Promega). The firefly luciferase activity was normalized according to Renilla luciferase activity and expressed as relative luciferase units to reflect the promoter activity.

2.2.8 Statistical analysis.

Statistical analysis was performed using GraphPad Prism version 5.0 for Macintosh. Allele frequency and genotype distribution of AD patients and controls were calculated by Pearson's chi-square test. The association of TMP21 SNP and AD risk was evaluated with chi-square test with odds ratios (ORs) by comparing allele frequency and genotype frequency between AD cases and controls. Quantifications were performed from 3 or more independent experiments. Values represent Means \pm SEM. ANOVA, Student's t test or linear regression was used for statistical analysis. $P < 0.05$ was considered as statistically significant.

2.3 Results

2.3.1 Identification of a novel AD-associated SNP in intron4 of TMP21

To investigate the association between *Tmp21* SNPs and AD, we screened the exonic regions including the 5' UTR and 3' UTR, and the flanking intronic regions in 261 sporadic AD patients and 236 controls. Due to the limitation of sequencing, 482 samples with excellent signals, 248 AD cases and 236 controls, were included for this study. Five single nucleotide polymorphisms (SNPs) were identified. Four SNPs were in non-coding region, rs3832966 (IVS2-75-/GGGC) and IVS2-71G>A in intron2, rs12435391 (IVS4-28T>C) and rs175444 (IVS4-73C>G) in intron 4, and one synonymous substitution rs4649 (585C>T) in exon 5 (Table 2.1). IVS2-71G>A is a novel SNP, which has not been reported. The distribution of the genotypes in both AD patients and controls was in Hardy–Weinberg equilibrium.

Chapter 2: A Novel AD-associated SNP in *Tmp21*

SNP	n	Genotype			χ^2	P	Allele		χ^2	P
IVS2-71G>A*		GG	GA	AA			G	A		
	AD	246 147(0.60)	93(0.38)	6(0.02)	2.76	P>0.05	0.79	0.21	0.11	P>0.05
	Controls	234 132(0.56)	100(0.43)	2(0.01)			0.78	0.22		
rs3832966										
IVS2-75-/GGGC		-/-	-/GGGC	GGGC/GGGC			-	GGGC		
	AD	246 160(0.65)	21(0.09)	65(0.26)	27.09	P<0.01	0.69	0.31	1.04	P>0.05
	Controls	234 124(0.53)	62(0.26)	48(0.21)			0.66	0.34		
rs4649										
c.585C>T		CC	CT	TT			C	T		
	AD	248 221(0.89)	26(0.10)	1(0.00)	1.55	P>0.05	0.94	0.06	0.48	P>0.05
	Controls	236 216(0.92)	18(0.08)	2(0.01)			0.95	0.05		
rs12435391										
IVS4-28T>C		TT	TC	CC			T	C		
	AD	248 74(0.30)	115(0.46)	59(0.24)	9.40	P<0.01	0.53	0.47	8.50	P<0.01
	Controls	236 102(0.43)	90(0.38)	44(0.19)			0.62	0.38		
rs175444										
IVS4-73C>G		CC	CG	GG			C	G		
	AD	248 84(0.34)	113(0.46)	51(0.21)	0.97	P>0.05	0.57	0.43	1.04	P>0.05
	Controls	236 72(0.31)	108(0.46)	56(0.24)			0.53	0.47		

* IVS2-71G>A (dbSNP database did not include)

Table 2.1 Distribution of *Tmp21* SNPs.

rs12435391 (IVS4-28T>C) in intron 4 showed different genotype and allele frequency between AD patients and controls. The frequency of the TT, TC or CC genotype was 29.84%, 46.37% or 23.79% in AD patients compared with 43.22%, 38.14% or 18.64% in controls ($X^2 = 9.40$, $P=0.01$), respectively. The effect size (odds ratio, OR) of TC or CC genotype in AD was 1.761, (95% confidential interval is 1.172 to 2.646) or 1.848 (95% confidential interval is 1.130 to 3.023), respectively. The frequency of T allele was 53.02% in AD patients and 62.29% in controls, while the frequency of C allele was 46.98% and 37.71% ($X^2 = 8.5$, $P<0.01$). The effect size (odds ratio) of C allele in AD is 1.463, 95% confidential interval is 1.132 to 1.891. The ORs of rs12435391 are higher than the other risk genes that previously reported (Harold, et al., 2009; Hollingworth, et al., 2011; J. C. Lambert, et al., 2009; Naj, et al., 2011; Seshadri, et al., 2010). For rs3832966 (IVS2-75-/GGGC), the frequency of the -/-, -/GGGC or GGGC/GGGC genotype

Chapter 2: A Novel AD-associated SNP in *Tmp21*

was 65.04%, 8.54% or 26.42% in AD patients compared with 52.99%, 26.50% or 20.51% in controls ($X^2 = 27.09$, $P < 0.01$), respectively. However, the frequency of (-) allele was 69.30% in AD patients and 66.24% in controls, while the frequency of GGC allele was 30.69% and 33.76% ($X^2 = 1.04$, $P = 0.31$). For rs4649 (c.585C>T), the frequency of the CC, CT or TT genotype was 89.11%, 10.48% or 0.40% in AD patients compared with 91.53%, 7.63% or 0.85% in controls ($X^2 = 1.55$, $P = 0.46$), respectively. The frequency of C allele was 94.35% in AD and 95.34% in controls, while the frequency of T allele was 5.65% in AD and 4.66% in controls ($X^2 = 0.48$, $P = 0.49$). For rs175444 (IVS4-73C>G), the frequency of the CC, CG or GG genotype was 33.87%, 45.56% or 20.56% in AD patients compared with 30.51%, 45.76% or 23.73% in controls ($X^2 = 0.97$, $P = 0.61$), respectively. The frequency of C allele was 56.65% in AD and 53.39% in controls, while the frequency of G allele was 43.35% in AD and 46.61% in controls ($X^2 = 1.04$, $P = 0.31$). For the novel SNP IVS2-71G>A, the frequency of the GG, GA or AA genotype was 59.76%, 37.81% or 2.44% in AD patients compared with 56.41%, 42.74% or 0.85% in controls ($X^2 = 2.76$, $P = 0.25$), respectively. The frequency of G allele was 78.66% in AD and 77.78% in controls, while the frequency of A allele was 21.34% in AD and 22.22% in controls ($X^2 = 0.11$, $P = 0.74$). Our results indicated that there is a significant genetic association between AD and rs12435391 (IVS4-28T>C), not other SNPs.

2.3.2 rs12435391 had no effect on *Tmp21* splicing site recognition

Next, we investigated whether this AD-associated SNP affects TMP21 expression. *Tmp21* coding sequence without intron4, with 753bp wild type intron4 or with intron4 containing rs12435391 was cloned into an expression vector to generate TMP21-Intron4 negative, TMP21-Intron4 WT or TMP21-Intron4 SNP, driven by the endogenous promoter of TMP21. (Fig. 2.1 A). Three plasmids were transfected into HEK cells. 48 hours later, RT-PCR was performed to determine the size of exogenous *Tmp21*. To distinguish exogenously expressed *Tmp21* mRNA from endogenous mRNA, the myc-tag primer specifically amplifying the exogenous mRNA was applied. Compared with TMP21-Intron4 negative, a positive control of mature *Tmp21* mRNA, TMP21-Intron4 WT can be recognized by splicing machinery and processed into mature mRNA

Chapter 2: A Novel AD-associated SNP in *Tmp21*

with the migration rate as same as TMP21-Intron4 negative (Fig. 2.1A). Sequencing results showed the correct TMP21 coding sequence, ACT/AGT, at the boundary of exon4 and exon5, indicating intron 4 of TMP21-Intron4 WT was precisely spliced by endogenous machinery (Fig.2.1 B). Moreover, compared with TMP21-Intron4 negative and TMP21-Intron4 WT, RT-PCR product of TMP21-Intron4 SNP transfected cell also showed the same migration rate and the sequence, ACT/AGT, around the splicing sites between exon4 and exon5 was as same as the sequence of TMP21-Intron4 WT (Fig. 2.1 A and B). The results indicated that TMP21-Intron4 SNP pre-mRNA could be spliced at right sites as TMP21-Intron4 WT.

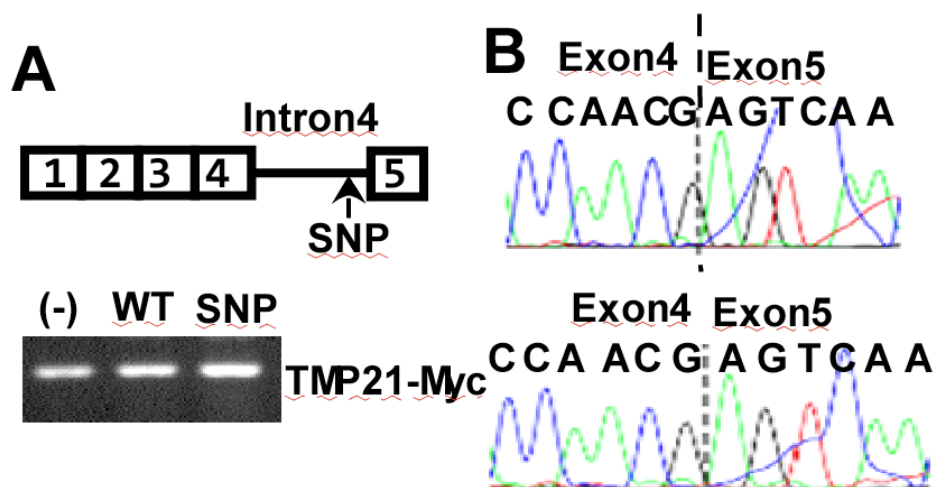


Figure 2.1 rs12435391 had no effect on *Tmp21* pre-mRNA splicing site recognition.

(A) TMP21 coding sequences, coding sequence with wild type intron 4 or intron 4 with SNP was cloned into the expression vector under the control of endogenous TMP21 promoter, named as TMP21-Intron4 negative (Con), TMP21-Intron4 WT (WT) or TMP21-Intron4 SNP (SNP). HEK cells were transfected with these three constructs, respectively. Mature mRNA from the transfected TMP21 constructs was examined by RT-PCR. PCR products were resolved on 2.0% agarose gel. (B) Sequencing results of the cDNA from TMP21-Intron4 WT (top panel) or TMP21-Intron4 SNP (bottom panel) transfected cells showed that both wild type intron 4 and Intron 4 with SNP was spliced at the same site that is as same as that in UCSC database.

2.3.3 rs12435391 increased *Tmp21* expression

Although rs12435391 did not alter *Tmp21* intron4 splicing site, it may affect TMP21 mRNA expression at multiple steps. To determine the effect of rs12435391 on TMP21 expression, the levels of *Tmp21* mRNA in those cells transfected with TMP21-Intron4 WT and TMP21-Intron4 SNP plasmids were examined by semi-quantitative RT-PCR. eGFP served as a control for the transfection efficiency. We found that Intron4 SNP rs12435391 dramatically increased the mRNA level of *Tmp21* compared to TMP21-Intron4-WT, 1.00 ± 0.08 vs. 1.46 ± 0.05 ($p=0.0049$)(Fig 2.2 A and B.). Correspondingly, the increased protein level of TMP21 was detected in TMP21-Intron4-SNP transfected cells compared with TMP21-Intron4-WT transfected cells, 1.00 ± 0.28 vs. 1.92 ± 0.44 ($p=0.0347$) (Fig. 2.2 C and D).

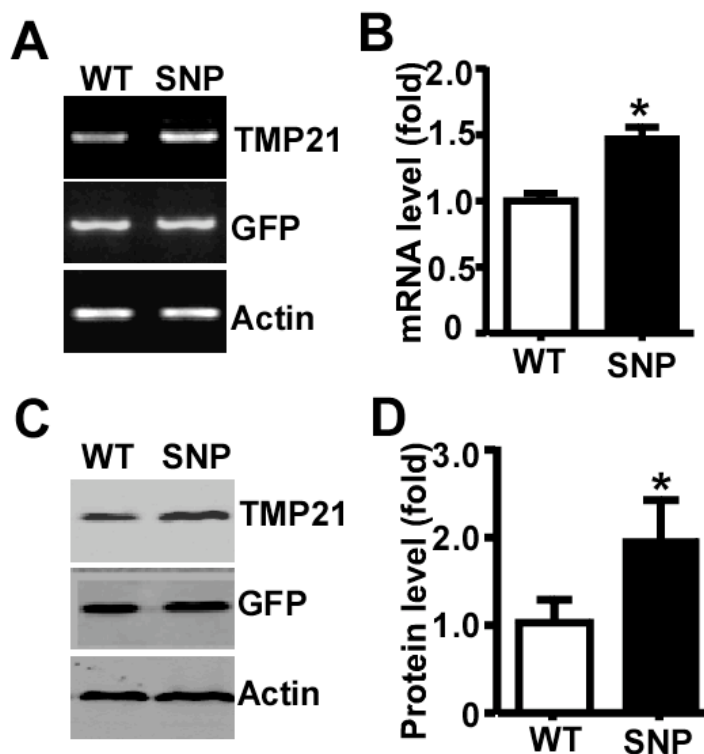


Figure 2.2 rs12435391 increased *Tmp21* expression.

(A) TMP21 WT or SNP plasmids were cotransfected with eGFP construct into HEK293 cells. Mature mRNA of exogenous TMP21 was amplified by RT-PCR with specific primers. GFP served as the control of transfection efficiency and β -actin was a loading control. (B) Quantification of *Tmp21* mRNA levels in (A). The mRNA level

Chapter 2: A Novel AD-associated SNP in *Tmp21*

was normalized to GFP and the ratio was further normalized to that of WT. Values are expressed as Mean \pm SEM. N=3, *p<0.05 by student's *t*-test. (C) TMP21 WT or SNP plasmids were co-transfected with eGFP construct into HEK293 cells. 48 hours later, cells were lysed in RIPA-DOC buffer and cell lysate were subjected to 12% SDS-PAGE. Mys-tagged TMP21 was detected by anti-myc antibody 9E10. β -actin was a loading control, detected by actin antibody (AC-15, Sigma). (D) Quantification of *Tmp21* mRNA levels in (C). TMP21 level was normalized to GFP and the ratio was further normalized to that of WT. Values are expressed as Mean \pm SEM. N=3, *p<0.05 by student's *t*-test.

2.3.4 rs12435391 increased *Tmp21* pre-mRNA splicing efficiency

The elevation of mRNA can be caused by increased RNA generation or reduced RNA degradation. Since rs12435391 is located in intron 4 of *Tmp21* and it does not alter the splicing site, the mature mRNA generated from both TMP21-Intron4-WT and TMP21-Intron4-SNP should have the same sequence, indicating there is no degradation difference between two mature mRNAs. Next we examine whether TMP21-Intron4-SNP-induced increase of *Tmp21* mRNA is caused by increased mature mRNA generation. The alteration of RNA transcription, pre-mRNA degradation or splicing efficiency may contribute to the enhancement of TMP21 expression induced by rs12435391. To explore the underlying mechanism of rs12435391-induced TMP21 increase, we first examined the degradation rate of TMP21 pre-mRNA in TMP21-Intron4-WT and TMP21-Intron4-SNP transfected cells. HEK cells were transfected with TMP21-Intron4-WT and TMP21-Intron4-SNP, respectively. 24 hours later, both transcription inhibitor Actinomycin D (ACT-D) and splicing inhibitor Isoginkgetin (ISO) were applied to the cells and the cells were harvest at 0, 1, 2.5 and 5 hours after treatments. Total RNA was extracted and treated with overdosed DNase to remove gDNA contamination. Unspliced pre-mRNA was amplified by RT-PCR. Pre-mRNA levels of both TMP21-Intron4-WT and TMP21-Intron4-SNP transfected cells were significantly decreased at 1, 2.5, 5-hour time points compared with 0 time point (Fig. 2.3 A and B). The half-life of TMP21-Intron4-WT or TMP21-Intron4-SNP pre-mRNA was around 2 hours (Fig. 2.3 C). It indicated that rs12435391 did not affect the pre-mRNA stability.

Chapter 2: A Novel AD-associated SNP in *Tmp21*

Although rs12435391 did not affect the splicing site recognition, it may have an effect on splicing efficiency as multiple putative branch sites are around rs1243539 (Fig. 2.3 D). Since pre-mRNA stability was not affected by TMP21-Intron4-SNP, the alteration of pre-mRNA treated with transcription inhibitor ACT-D will reflect the effect of intron 4 SNP on pre-mRNA splicing rate. TMP21-Intron4-WT and TMP21-Intron4-SNP were transfected into HEK cells, respectively. 24 hours later, the transcription inhibitor ACT-D was applied to the cells and the cells were treated for 2.5 hours. Unspliced pre-mRNA was amplified by RT-PCR. As expected, pre-mRNA levels of both TMP21-Intron4-WT and TMP21-Intron4-SNP transfected cells were significantly decreased to $41\% \pm 6\%$ and $19\% \pm 2\%$, ($p=0.0021$ and $p=0.0020$, relative to the control, respectively), respectively (Fig. 2.3 E, F), and significantly more reduced *Tmp21* pre-mRNA level in TMP21-Intron4-SNP cells, compared with TMP21-Intron4-WT cells, $59\% \pm 6\%$ vs $81\% \pm 2\%$, $p=0.023$ (Fig. 2.3 G). According to our previously results, the similar pre-mRNA stabilities showed between TMP21-Intron4-WT and TMP21-Intron4-SNP, it was probably that much more TMP21-Intron4-SNP pre-mRNA was spliced than TMP21-Intron4-WT, leading to more reduced pre-mRNA level of TMP21-Intron4-SNP. This result suggested that TMP21-Intron4-SNP significantly increased the splicing efficiency of pre-mRNA.

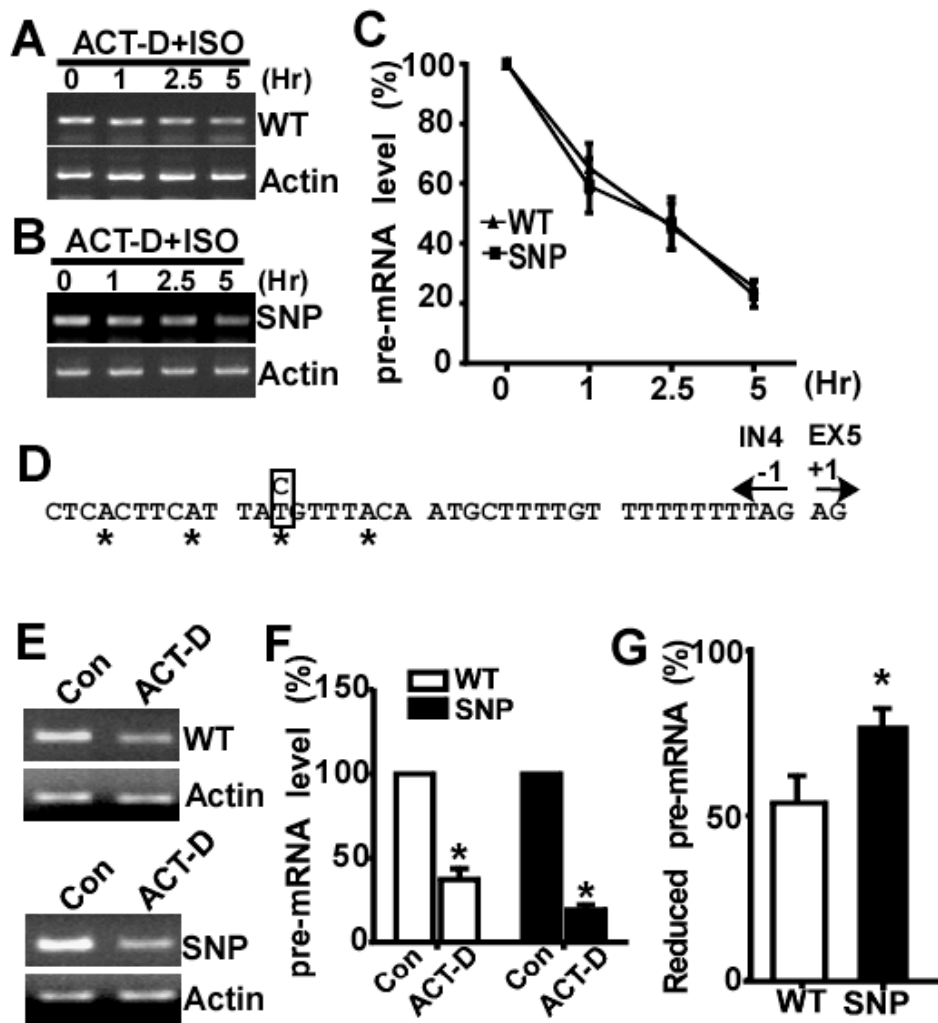


Figure 2.3 rs12435391 facilitated *Tmp21* pre-mRNA splicing.

HEK293 cells were transfected with TMP21-Intron4-WT (A) or TMP21-Intron4-SNP (B). 48 hours later, cells were treated with transcription inhibitor Actinomycin D (ACT-D) (10 μ M) and pre-mRNA splicing inhibitor isoginkgetin (ISO) (33 μ M). At 0, 1, 2.5 or 5-hour time points, the levels of pre-mRNA were assessed by RT-PCR with specific primers. PCR products were resolved on 2% agarose gel. (C) Quantification of (A) and (B). The levels of *Tmp21* pre-mRNA were normalized to actin and plotted as the percentage of the control at 0-hour point. Values represent Mean \pm SEM. N=3 by two-way ANOVA. (D) The sequence of *Tmp21* intron 4 upstream of the exon 5. Putative branch sites are marked by *. TMP21-Intron4-WT or TMP21-Intron4-SNP (E) was transfected into HEK293 cells. After 48 hours, 10ug/ml ACT-D was applied to cells for 2.5 hours. The levels of pre-mRNA were assessed by RT-PCR. PCR products were resolved on 2% agarose gel. (F) and (G) Quantification of (E). Values represent Mean \pm SEM. N=4, *<0.05 by student's *t*-test.

2.3.5 rs12435391 had no effect on *Tmp21* transcription

A SNP in a regulatory DNA binding site may alter the affinity with transcription regulatory factors, resulting different gene expression (Liao, 2010). It is possible that this intron 4 might contain *cis*-regulatory elements and rs12435391 might alter *Tmp21* gene expression at transcription level. As pre-mRNA stability was not affected by TMP21-Intron4-SNP, any difference of pre-mRNA between TMP21-Intron4-WT and TMP21-Intron4-SNP transfected cells with splicing inhibitor Isoginkgetin (ISO) treatment will reflect their differential transcription activity. The level of unspliced pre-mRNA was measured in ISO treated cells transfected with TMP21-Intron4-WT and TMP21-Intron4-SNP, respectively. No significant difference between TMP-intron4-SNP and TMP-intron4-WT was detected, 1.47 ± 0.25 vs. 1.34 ± 0.15 ($p=0.67$) (Fig 2.4 A, B and C). To further confirm the effect of Intron4-SNP on *Tmp21* transcription, we cloned wild type intron4 or intron 4 with the SNP upstream of BACE1 promoter or RCAN1 promoter in pGL3-Basic construct, respectively. The effect of TMP21-Intron4-SNP on transcription activity is measured by luciferase activity. The plasmids containing BACE1 promoter (pB1), BACE1 promoter with wild type intron 4 (I4-WT-pB1), BACE1 promoter with intron 4-SNP (I4-SNP-pB1), RCAN1 promoter (pR1), RCAN1 promoter with wild type intron 4 (I4-WT-pR1) or intron 4-SNP (I4-SNP-pR1), were transfected into HEK cells respectively. Intron 4 SNP of TMP21 did not alter the promoter activities of either BACE1, 1.00 ± 0.03 vs. 0.84 ± 0.05 ($p=0.06$) (Fig.2.4 D) or RCAN1, 1.00 ± 0.10 vs. 0.80 ± 0.09 ($p=0.22$) (Fig. 2.4 E). Our data clearly demonstrated that the SNP had no significantly impact on *Tmp21* transcription.

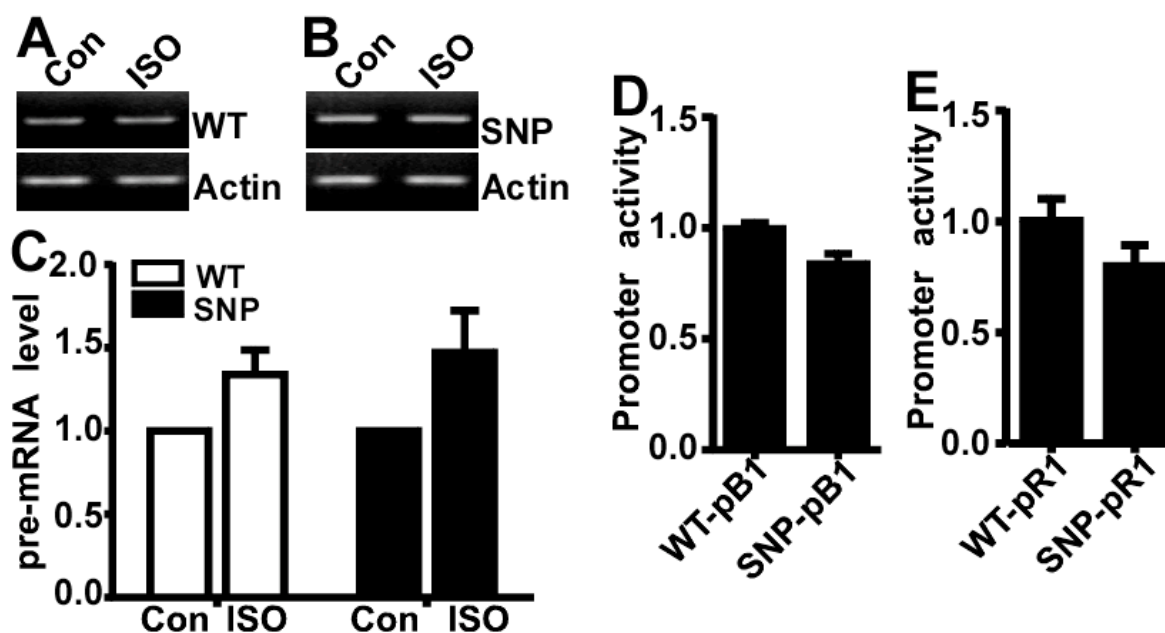


Figure 2.4 rs12435391 had no effect on *Tmp21* transcription regulation.

HEK293 cells were transfected with TMP21-Intron4-WT (A) or TMP21-Intron4-SNP (B). 48 hours after transfection, cells were treated with 33 μ M pre-mRNA splicing inhibitor Isoginkgetin (ISO) for 2.5 hours. Unspliced pre-mRNA was amplified by RT-PCR with specific primer. Actin served as loading control. PCR products were resolved in 2% agarose gel (C) Quantification of (A) and (B) with Image J software. Values represent Mean \pm SEM. N=3 by student's *t*-test. (D) BACE1 promoter with *Tmp21* wild type intron 4 (I4-WT-pB1) or intron 4 SNP (I4-SNP-pB1) was cloned into pGL-3 basic to drive the expression of firefly luciferase. I4-WT-pB1 or I4-SNP-pB1 was co-transfected with pRLuc (encoding Renilla luciferase) into HEK cells, respectively. The activity firefly luciferase was normalized to Renilla luciferase activity to control the transfection efficiency. Values represent Mean \pm SEM. N=3 by student's *t*-test. (E) RCAN1 promoter with *Tmp21* wild type intron 4 (I4-WT-pR1) or intron 4 SNP (I4-SNP-pR1) was cloned into pGL-3 basic. I4-WT-pR1 or I4-SNP-pR1 was co-transfected with pRLuc into HEK cells, respectively. The activity firefly luciferase was normalized to Renilla luciferase activity to control the transfection efficiency. Values represent Mean \pm SEM. N=3 by student's *t*-test.

2.4 Discussion

TMP21 has been shown to modulate γ -secretase activity and APP trafficking, leading to increased A β production (F. S. Chen, et al., 2006; Vetrivel, et al., 2007). Intriguingly, TMP21 specifically regulated γ -secretase activity on APP processing without affecting Notch cleavage

Chapter 2: A Novel AD-associated SNP in *Tmp21*

(F. S. Chen, et al., 2006), which makes TMP21 a seductive target for AD treatment. However, upregulated TMP21 leads to Golgi fragmentation and sever neurologic problems in human *Tmp21* transgenic mice (Gong, et al., 2011). These findings suggest that TMP21 levels are significantly altered in disease state and that TMP21 may play an integral, clinically relevant role in AD pathogenesis. However, the mechanism of TMP21 dysregulation and the association between TMP21 and AD remain elusive.

In this study, we first identified an AD-associated *Tmp21* SNP in intron 4, rs12435391, which demonstrated the genetic impact of TMP21 on the risk to develop AD and the clinical relevance of TMP21 expression levels in AD pathogenesis. Using gDNA bank from AD patients and controls (Zhou, et al.), we screened *Tmp21* SNPs in exonic regions excluding the 5' UTR and 3' UTR, and the flanking intronic regions. Five SNPs were identified. Four SNPs were in non-coding region and one synonymous substitution in exon 5. IVS2-71G>A is a novel SNP, which has not been reported. *rs12435391* (IVS4-28T>C) in intron 4 showed significantly difference of allele and genotype frequency in AD patients and controls. This is the first study in elucidating the *Tmp21* gene polymorphisms in AD patients since 1992.

The intron 4 of TMP21 has only 755bp and *rs12435391* located 28bp before exon5. To further examine the role of this intronic SNP on pre-mRNA processing and TMP21 expression levels, we firstly engineered an expression construct consist of all coding exons and the intron of interest, driven by the endogenous promoter. The results showed that this construct was recognized by splicing machinery, properly processed into mRNA, and subsequently expressed as protein of the proper size. This in vitro approach was used to study how rs12435391 affected TMP21 pre-mRNA processing and expression levels. A T/C point mutation was introduced by PCR-based site-directed mutagenesis to mimic *rs12435391*. Using PCR, RT-PCR and Western blot, we detected TMP21 in DNA, mRNA and proteins levels after transfection. Compared with wild type construct, the transcript size, mRNA and resulting protein from SNP plasmid revealed the effect of this SNP on TMP21 pre-mRNA processing, mRNA and protein expression. The

Chapter 2: A Novel AD-associated SNP in *Tmp21*

traditional approach to analysis RNA alternative splicing is minigene assay involving serials intronic and exonic regions from multiple genes (F. Pagani, Baralle, FE, 2010; F. Pagani, et al., 2002). However, our expression construct consists of all coding exons and the intron of interest, driven by its endogenous promoter, it removes many of the confounding variables. More importantly, our novel construct was recognized by endogenous splicing machinery, and expressed mRNA and protein at proper size. It provides an effective application to assess the intronic SNPs in future research.

As intronic SNP can affect gene expression at multiple levels including gene transcription, pre-mRNA splicing and pre-mRNA degradation, we further determined the effect of rs12435391 on *Tmp21* expression and the underlying mechanism. Since previous study showed that intronic SNPs contribute to diseases through alternative splicing of pre-mRNAs (F. Pagani & Baralle, 2004; F. Pagani, et al., 2002), we first examine whether rs12435391 disrupts the splicing site recognition. The high fidelity of pre-mRNA splicing is critically dependent on the recognition of exon-intron and intron-exon boundary signals by U1 snRNP (Zhuang & Weiner, 1986), U2 snRNP and U2 auxiliary factors (Hartmann, Theiss, Niederacher, & Schaal, 2008). The consensus sequence of exon-intron boundary consists of MAG/GURAGU (M=C or A, R=purine, and “/” denotes the exon-intron board) including the last 3 nucleotides of the upstream exon and the first 6 nucleotides of the downstream intron (Freund, et al., 2003). The intron-exon boundary, termed as 3'splice site (3'ss), consists of three signal parts, the branch point sequence (BPS), polypyrimidine tract and the most 3' intronic dinucleotide, AG (Moore, 2000), crossing a variable region from 18-40 nucleotides to hundreds of nucleotides upstream of the intron-exon board (Gooding, et al., 2006; Helfman & Ricci, 1989). As this *Tmp21* SNP is located at 28-nucleotide upstream of intron4-exon5 board, within the region of 3'splice site, it may affect 3'splice site recognition resulting in disruption of *Tmp21* pre-mRNA splicing. Since the intron 4 of *Tmp21* only contains 753bp, we explored a novel strategy to study this intronic SNP by cloning the full length wild type intron 4 or intron 4 with the SNP into the expression plasmid consisting of all *Tmp21* coding exons, in which intron 4 was located between exon 4 and 5. If the

Chapter 2: A Novel AD-associated SNP in *Tmp21*

splicing sites in intron 4 are correctly recognized, standard-sized mature *Tmp21* mRNA should be produced, otherwise the longer unspliced mRNA will be detected. Indeed, the wild type intron 4 in TMP21 expression construct was recognized by the splicing machinery, and properly processed into mature mRNA. Compared with wild type intron 4, intron 4 with rs1243539 produced the same size mature mRNA. Sequencing of the mature mRNA further confirmed that both wild type intron 4 and intron 4 with rs1243539 can be precisely recognized and processed by the splicing machinery. Our work not only demonstrated that rs1243539 did not disrupt splicing site recognition but also provided a viable approach to study intronic SNPs.

Although the SNP rs1243539 did not disrupt the recognition of pre-mRNA splicing site, it significantly increased TMP21 expression at both mRNA level and protein level. Previous studies showed that intronic SNP can affect splicing efficiency (F. Pagani, et al., 2002). Moreover, as many putative branch sites around or right at this SNP position, particularly the strongest one, rs1243539 may increase the splicing efficiency by affecting branch sites usage or efficiency, resulting in increased mature mRNA level. Our data demonstrated that increased splicing efficiency of intron 4 was involved in rs1243539-induced *Tmp21* overexpression. In addition to its effect on pre-mRNA splicing, considering intronic SNPs may disturb pre-mRNA degradation or the function of cis-regulatory elements within this region (Liao, 2010; Orr & Chanock, 2008), the half-life of *Tmp21* pre-mRNA and its effect on *Tmp21* transcription activity was examined. We found that the half-life of *Tmp21* pre-mRNA was 2 hours, which was not altered by rs1243539. Moreover, rs1243539 had no effect on *Tmp21* transcription. As the endogenous *Tmp21* promoter drove all of the TMP21 constructs, our results clearly demonstrated that rs1243539-induced TMP21 overexpression was not attributed to the increase of *Tmp21* transcription. Most studies on disease-associated SNPs focus on the SNPs in promoter region that alter the gene transcription, or the intronic SNPs disrupting splicing site recognition, yet overlook the effect of intronic SNPs on altering the level of gene expression. Our study provides a new mechanism of disease-associated intronic SNPs regulating gene expression in addition to splicing site recognition.

Chapter 2: A Novel AD-associated SNP in *Tmp21*

This novel AD-associated *Tmp21* SNP, rs1243539, significantly increased TMP21 expression by potentiating its splicing efficiency, indicating that TMP21 upregulation might contribute to AD pathogenesis. Consistently, a more recent study showed that even 50% increase of TMP21 in transgenic mice leads to the severe neurological problems and premature death (Gong, et al., 2012). However, previous reports showed that TMP21 downregulation increases γ -cleavage of APP and A β production (F. S. Chen, et al., 2006; Dolcini, et al., 2008; Hasegawa, Liu, & Nishimura, 2010; Vetrivel, et al., 2007). The controversial results suggest TMP21 may play a complex role in biological processes, which is not rare for biological molecules. For example, regulator of calcineurin 1 (RCAN1) plays a dual role in regulating calcineurin activity, both low level or knockout of RCAN1 and overexpression of RCAN1 dramatically inhibiting calcineurin activity (Hilioti, et al., 2004; Kingsbury & Cunningham, 2000; Sanna, et al., 2006; Shin, Yang, Kim, Do Heo, & Cho, 2011; Vega, et al., 2003). As a modulator of γ -secretase activity, TMP21 may also play a dual role in regulating γ -secretase activity, both TMP21 downregulation and upregulation impairing γ -secretase activity. Moreover, both decreased expression and overexpression of p24 family proteins may result in defects in membrane trafficking events of early endosomes, which might lead to the enhanced APP processing and A β biogenesis (Rojo, Emery, Marjomäki, et al., 2000; Tang, 2009; Vetrivel & Thinakaran, 2006). As a member of the p24 family, increased TMP21 or reduced TMP21 may disturb APP trafficking to affect APP processing and A β generation. Regardless, the precise control of TMP21 expression is crucial to maintain its physiological functions, avoiding its pathogenic effects.

2.5 Conclusion

Here, we first identified that rs12435391 (IVS4-28T>C) located in intron 4 of *Tmp21* was an AD-associated SNP by screening 248 AD patients and 236 controls. Our results showed that rs12435391 (IVS4-28T>C) did not alter the splicing site between exon 4 and exon 5, but it significantly increased TMP21 expression by potentiating the splicing efficiency of intron 4. Our study suggested that upregulation of TMP21 may contribute to AD pathogenesis.

Chapter 3: The Dysregulated TMP21 Facilitates APP Amyloidogenic Processing

3.1 Introduction

TMP21 was found to play a pivotal role as a regulator of the γ -secretase complex. TMP21 could co-precipitate with other members of the γ -secretase complex, PS1/PS2, NCT, Pen -2 and Aph-1 (F. S. Chen, et al., 2006). More importantly, TMP21 is co-localized with PS1 in human brain (Vetrivel, et al., 2008). TMP21 selectively regulates the APP cleavage at the γ -site without affecting ϵ -site cleavage on APP or Notch (F. S. Chen, et al., 2006; Dolcini, et al., 2008). The transmembrane domain of TMP21 binds to the γ -secretase complex and decreases γ -secretase proteolytic processing thus reducing the A β production (Pardossi-Piquard, et al., 2009). Knockdown of TMP21 expression enhances APP maturation efficiency, producing more mature APP for amyloidogenic pathway thereby generating more A β (Vetrivel, et al., 2007). This evidence shows a dual role of TMP21 in the modulation of A β production by controlling APP trafficking and γ -secretase activity, suggesting that the increased TMP21 expression might be a potential strategy to reduce A β level and consequently, prevent AD pathogenesis. However, transgenic mice with neuron-specific expressed human TMP21 showed Golgi fragmentation, and severe neurological problems, growth retardation, infertility and premature death (Gong, et al., 2011; Gong, et al., 2012). We identified a novel AD-associated SNP that significantly increased the expression of TMP21 at both mRNA and protein levels. However, it remains to be determined the causal linkage between TMP21 levels and APP processing and AD pathogenesis. In this chapter, we further examined the roles of TMP21 in APP amyloidogenic processing. Here, we found that both the overexpression and downregulation of TMP21 significantly increased C99 level. C99 is the BACE1 cleavage product of APP at Asp-1 site. Thus, in addition to modulating γ -secretase activity, TMP21 might also affect BACE1.

3.2 Methods

3.2.1 Plasmids constructions.

The TMP21 expression plasmid pcDNA4-TMP21mycHis was previously generated in our lab (S. Liu, et al., 2011). Using this plasmid as template, TMP21 cDNA with stop codon was amplified by forward primer TMP F Bam: 5'-CGGGATCCGCCACCATGTCTGGTTTGTCTGGCCCAC and reverse primer TMP R Stop Eco: 5'-GGAATTCTTACTCAATCAATTTCTTGGCCTTG, generating TMP21 no tag expression plasmid. GFP-TMP21 plasmid was constructed by GFP being inserted between TMP21 signal peptide and luminal domain, using two pairs of primers: TMP-sig+GFP-F: 5'-CCCCAGATTGGTCCTTGCCATGGTGAGCAAGGGCG and TMP-sig+GFP-R: 5'-CGCCCTTGCTCACCATGGCAAGGACCAATCTGGGG, TMPlum-FBamHI: 5'-CGGGATCCATCTCCTTCCATCTGCCC and TMPlum-REcoRI: CGGAATTCTTAGGTATCACGCATCTCCTC. By fusing Dsred at the C-terminal of BACE1 in pzBACE1 plasmid (Zhou, Qing, Tong, & Song, 2004), we generated BACE1-Dsred plasmid. pBACE1-EGFP was cloned by the cDNA of BACE1 inserted into pEGFP-N1 (Sun, Tong, Qing, Chen, & Song, 2006).

3.2.2 Cell culture and transfections.

HTM is the stable cell-line that overexpression TMP21-mycHis in HEK293. All cells were cultured in Dulbecco's modified eagle medium (DMEM) supplemented with 10% fetal bovine serum (FBS), 1mM sodium pyruvate, 1mM L-glutamine, and 50U/mL penicillin G sodium and 50µg/mL streptomycin sulfate (Invitrogen, Carlsbad, CA USA), and were maintained at 37°C in an incubator containing 5% CO₂. HTM cell media also contained 60mg/mL zeocin. Cells were seeded in 24-well plates or 35mm plates 24 hours before transfection and grown to near 70% confluence by the day of transfection. Transient transfections were performed using the calcium phosphate method, and cells were allowed to grow for an additional 48 to 72 h until confluent. Or cells were transfected with 2µg plasmid DNA in 35mm plate using 2µl of lipofectamine 2000 Reagent (Invitrogen) according to the manufacturer's instructions. Unless otherwise stated, all

Chapter 3: The Dysregulated TMP21 Facilitates APP Amyloidogenic Processing

cells were harvested in PBS and lysed in a modified RIPA-DOC buffer (150mM NaCl, 50mM Tris-HCL, 1% Triton X-100, 2% SDS, and 1% sodium deoxycholate) with the presence of protease inhibitor cocktail complete (04693116001; Roche, Indianapolis, IN, USA). After briefly sonication and centrifugation at 14,000rpm for 10 mins, supernatants were collected and protein assay was performed with the Bio-Rad Dc protein assay kit (Bio-Rad, Richmond, CA).

3.2.3 Immunoblotting.

Whole-cell lysates were diluted in 4XSDS-sample buffer and separated on 12% Tris-glycine SDS-PAGE gel and transferred to polyvinylidene fluoride (PVDF-FL) membranes. Membranes were blocked in PBS containing 5% non-fat dried milk and incubated with the primary antibodies diluted in the blocking buffer at 4°C overnight. Rabbit anti-TMP21 antibody T21 (1:1000) was generated by inoculating rabbit with synthetic peptide HKDLLVTGAYEIHK, this peptide shared 100% sequence homology with both mouse and human TMP21. Rabbit anti-C20 (1:1000) recognized the last twenty amino acids on the C-terminal end of human APP and Mouse 9E10 (1:200) recognized the Myc tag were made in-house as well. Human p24a was detected by mouse monoclonal antibody TMED2 (1:2000) (C-8) (Santa Cruz Biotechnology). Golph4 (1:2000), for Golgi marker detection, was a rabbit polyclonal antibody from Abcam. The antibody AC-15 (1:5000) (Abcam, Cambridge, MA, USA and Sigma) was used to detect β -actin. Then the membranes were rinsed in PBS-T and incubated with near-infrared fluorescence-labeled secondary antibodies IRDyeTM680-labeled goat anti-rabbit (1:100,000) and IRDyeTM800-labeled goat anti-mouse antibodies (1:100,000) (Lincoln, NE, USA) in PBS-T at room temperature for 1 h, after further rinsed in PBS-T the membranes was scanned by LI-COR Odyssey R system. All quantification measurements were preformed using ImagJ software.

3.2.4 A β 40 enzyme linked-immunosorbent assay (ELISA).

HEK or HTM cells with APPwt and BACE1 coexpression were cultured in cell culture medium supplemented with 5% FBS. At 24 or 48 hours after transfection, the conditioned medium was collected; the mice brains tissue was weighted and treated by 5M Guanidine HCl for 3 hour at

Chapter 3: The Dysregulated TMP21 Facilitates APP Amyloidogenic Processing

room temperature. Then the concentration of A β 40 was detected using β -amyloid 1-40 Colorimetric ELISA kit (Invitrogen) according to manufacturer's instructions.

3.2.5 Coimmunoprecipitation.

Cells were harvested in PBS 48 h after transfection and lysed in 0.3ml NP-40 lysis buffer (20mM Tris.HCl pH 7.5, 150mM NaCl, 1mM MgCl₂, 1mM EDTA, 1% NP-40) and protease inhibitor cocktail Complete on ice for 30mins. Samples were spun at top speed for 15 min and supernatants were transferred to a new tube. Immunoprecipitation antibody was added in 60ul protein A/G coupled to agarose beads (Santa Cruz Biotechnology) and gently mixed at 4°C for 3 h to overnight. Beads were washed by NP-40 lysis buffer and added into samples supernatant. After mixing overnight at 4°C, the beads were washed three times in lysis buffer and boiled in 1xSDS sample buffer for 5 min. Further short centrifugation to spin down the beads. The samples were loaded on 16% Tris-Tricine gels (for CTFs) or 8%-10% glycine gel for immunoblotted. The cells transfected with myc-tagged expression plasmids were immunoprecipitated with anti-myc antibody 9E10 (1:20) and immunoblotted with anti-TMP21 antibody T21 or anti-eGFP (1:1000); for APP and CTF samples were immunoprecipitated with anti-APP-CTF antibody C20 (1:100), then immunoblotting was performed using 9E10 (1:500).

3.2.6 Subcellular fractionation.

Cells were harvested in 1ml PBS, spinned down at 1000xg for 60 sec and resuspended in homogenization buffer (10mM HEPES, pH 7.4, 1mM EDTA, 0.25M sucrose (8.56%)), supplemented with a protease inhibitor mixture. Then the cells were disrupted using 10 strokes in a Dounce homogenizer. Then nuclei and intact cells were precipitated in pellet by low-speed centrifugation at 1000xg for 10 minutes. Collect equal volume of Post-nuclear fraction (PNS) and load on fresh-prepared sucrose density gradient (10~50%, w/v). After centrifugation at 28,000xg for 2 hr at 4°C in a swinging bucket rotor MLS50 (Beckman), 16~20 fractions were collected, proteins samples were concentrated for gel analysis by adding trichloroacetic acid

Chapter 3: The Dysregulated TMP21 Facilitates APP Amyloidogenic Processing

(TCA) to 20%. Immunoblot analyses of these fractions were performed, using Golph4 (1:1000), C20 (1:1000) and 9E10 (1:200) antibodies.

3.2.7 Immunocytochemistry.

Cells were seeded onto glass cover slips in 24 well plates the day before transfection, 24 hours after transfection cells were rinsed in PBS, fixed in 4% PFA or methanol at -20°C for 20 min, blocked in 5% BSA in PBS-Tx for 30 min, and incubated with or without primary antibodies in 1% BSA in PBS-Tx overnight at 4°C. The next day cells were rinsed, incubated for 1 h with goat anti-rabbit Alexa Fluor 488 (green) or goat anti-mouse Alexa Fluor 568 (red), rinsed in PBS-Tx, and mounted using Fluoromount-G (Southern Biotech). Cells transfected with GFP-TMP and BACE1-RFP were fixed 24 hours after transfection and then mounted. Cells were imaged with a 100x oil objective lens on a Carl Zeiss Axiovert-200 epi fluorescent microscope.

3.2.8 Confocal imaging and time-lapse live cell image analysis.

Cells were transfected with GFP-TMP and BACE1-RFP and incubated in phenol red-free DMEM (Invitrogen) supplemented with 10% FBS, sodium pyruvate, L-glutamine and penicillin/streptomycin as regular complete medium. Cells were fixed by methanol or the live cell image analysis were performed 24 hours after transfection. Confocal images were recorded with the Axiovert 200M microscope using an AxioCam HRm Rev.2 camera. The objective lens of the microscope was Plan Apochromat 63x/1.40 Oil (DIC III). The time-lapse images were acquired every 500 milliseconds, 30 frames in total.

3.2.9 SiRNA knockdown.

Synthetic siRNA duplexes against the conserved sequence ATACCTGACCAACTCGTGA (nt 416-434 of NM-006827) present in human and mouse *Tmp21* mRNA was purchased from Dharmacon (Vetrivel, et al., 2007). Scramble control siRNA against the sequence CTGCAGAGCTCGACCACTC (Vetrivel, et al., 2007) and p24a siRNA against the sequence CCGGATGTCCACCATGACT (W. Luo, Wang, & Reiser, 2007) were synthesized by

Chapter 3: The Dysregulated TMP21 Facilitates APP Amyloidogenic Processing

Dharmacon. Cells were given fresh medium, and siRNA was prepared with lipofectamine 2000 in Opti-medium as per the manufacturer's protocol (Invitrogen). Cells were harvested 48 to 72 h after siRNA treatment.

3.2.10 Mice breeding

APP23 transgenic mice were shipped from Novartis in Switzerland. APP23 transgenic mice carry human APP751 cDNA with the Swedish mutation at positions 670/671(KM/NL) driven by Thy1.2 promoter which has a neuronal specific expression pattern (Sturchler-Pierrat, et al., 1997). The S2P23 mice, which display hemizygous knockdown of TMP21 in a C57BL/6 background were shipped to our facility from Transgenic Services at Cancer Research UK (Denzel, et al., 2000a). These mice were bred in the Animal Research Unit (ARU) at the University of British Columbia Hospital.

3.2.11 Genotyping.

Mice were weaned at 3 weeks of age, after that they were anesthetized using isoflourance. The ear punch biopsies were collected and digested in 300 μ L lysis buffer (10mM Tris HCl pH 8.0; 10mM EDTA pH 8.0; 150mM NaCl; 0.5% SDS) with 100ng/ml proteinase K (New England Biolabs) overnight at 55°C while rotating. The next day, samples were centrifuged at 14,000rpm for 10mins to spin down the insoluble hair or tissue. Supernatant were collect and added equivalent volume of phenol/chloroform, followed by vortex. Samples were centrifuged to separate the aqueous and organic layers, and the aqueous layer was carefully removed. DNA was purified again using phenol/chloroform and precipitated with 0.7X volume of isopropanol, and pelleted by centrifugation at 14,000rpm for 15 mins. The pellet was washed twice with 70% ethanol, air dried, and dissolved in 50 μ L TE buffer (pH 7.4).

For the genotyping of APP23 mice, gDNA was subjected to PCR with Thy1E2 forward primer 5'-CACACAGAATCCAAGTCGG and APP1082 reverse primer 5'-CTTGACGTTCTGCCTCTTCC by PCR method. The 1kb band from PCR indicates the

existence of the human APP gene. For genotyping of S2P23 mice, the PCR preformed using forward primer G-TMP21 mice-F (5'-CCGGACTCTAGGTCCGCCAA), and reverse primers G-TMP21 mice-R (5'-TCTGGTTTGTGGCCCACTCTCCG) and G-TMP21mice-Neo (5'-AATTCGCCAATGACAAGACGCT), the S2P23 mice displayed the positive band being 260 bp in size. All procedures used in this study were in accordance with guidelines established by the Canadian Council on Animal Care and approved by the University of British Columbia Animal Care Committee.

3.2.12 Neuritic plaque staining.

Mice were sacrificed and half of the brain was fixed in 4% paraformaldehyde (PFA) for more than 48 hours at 4°C and followed by 30% sucrose solution around 48 hours at 4°C. Brains were embedded in OCT solution at -20°C and sectioned with a Leica cryostat (Deerfield, IL) to 30µM thickness. Slices were collected into D'Olomos solution and store at -20°C. Every 6th slice with the same reference position was mounted onto the slides fro staining. As previously described (Ly, Cai, & Song, 2011), slices were immunostained with biotinylated mono- clonal 4G8 antibody (recognizes the 17 to 24 amino acid residues of A β) (Signet Laboratories, Dedham, MA) at 1:1000 dilutions. Plaques were visualized by the avidin-biotin-peroxidase complex (ABC) (Elite ABC, Vector Laboratories) and diaminobenzidine tetrahydrochloride (DAB) (Vector Laboratories) method, and counted under microscopy with 40X magnification. Thioflavin S staining for β -sheet is also used to detect A β -containing neuritic plaques. It was performed with 1% thioflavin S in 80% ethonal. Upon binding, thioflavin S undergoes a characteristic blue shift of its emission spectrum and the green fluorescence-stained plaques could be visualized with fluorescent microscopy (Ly, et al., 2011). Plaques were quantified by average plaque count per slices for each mouse, and the data were analyzed by student *t*-test.

3.3 Results

3.3.1 Upregulation of TMP21 shifted the APP processing from non-amyloidogenic to amyloidogenic pathway

We have identified an AD-associated SNP in the exon 4 of TMP21 gene, and this SNP promoted TMP21 expression at both mRNA and protein levels *in vitro*. To examine the effect of TMP21 upregulation on APP processing, we transfected pTMP21-mycHis into the Human Embryonic Kidney 293 cells (HEK293) and established a stable cell line HTM (S. C. Liu, et al., 2008). When cotransfection of APP^wt and BACE1 into HEK and HTM cells, C83 level was significantly reduced, 1.00 ± 0.11 vs. 0.42 ± 0.03 ($p=0.0046$), but C99 level was increased in HTM cells, 1.00 ± 0.07 vs. 1.75 ± 0.26 ($p=0.045$), no statistic difference of C89 levels between HEK and HTM cells 1.00 ± 0.12 vs. 0.72 ± 0.09 ($p=0.0842$) was observed (Fig.3.1 A). The ratio of C99 to C83 was increased by over three fold in HTM cells, 1.00 ± 0.06 vs. 3.56 ± 0.53 ($p=0.0150$) (Fig 3.1 B). Interestingly, we also found that there are more C99, rather than C89 production in HTM cells. The ratio of C99/C89 was significantly increased in HTM cells 1.00 ± 0.10 vs. 2.00 ± 0.18 ($p=0.0057$). (Fig.3.1 B.). ELISA assay showed the increased A β level in the HTM medium, 1.00 ± 0.06 vs. 2.06 ± 0.14 ($p=0.025$). (Fig. 3.1 C). It suggested that overexpression of TMP21 shifted APP processing from α -secretase cleavage, as indicated by the decrease in C83, towards BACE1 cleavage, and specifically, overexpression of TMP21 augmented the C99 generation, rather than C89 generation, and the increased C99 may provide more substrate of γ -secretase, thus led to increased A β production.

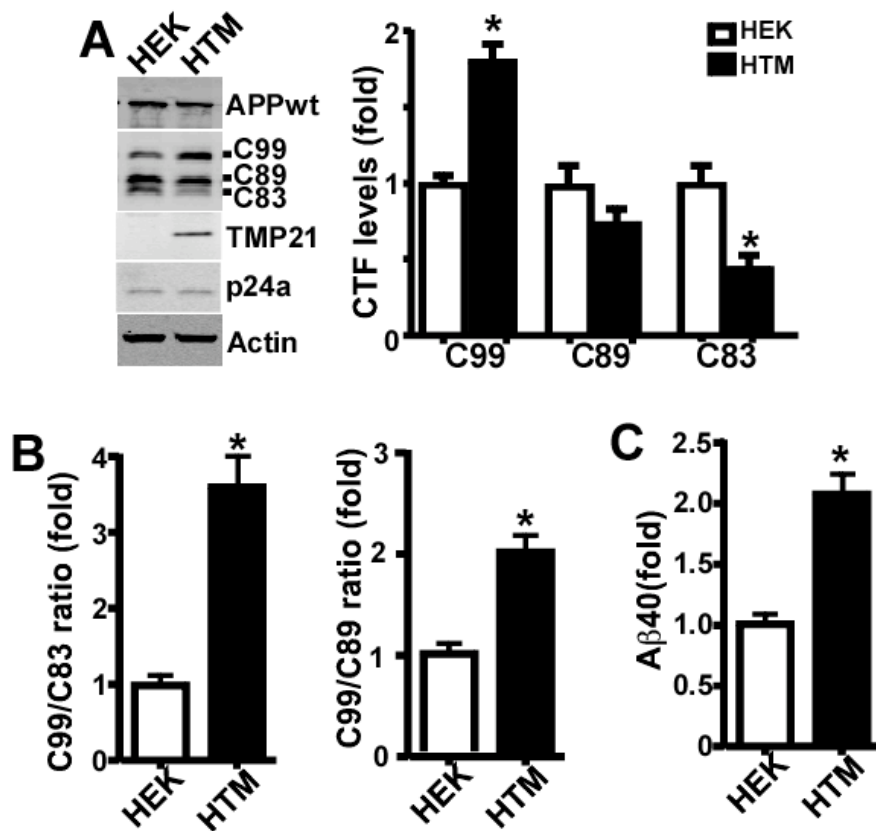


Figure 3.1 Overexpression of TMP21 dramatically shifted the APP cleavage from non-amyloidogenic pathway to amyloidogenic pathway.

(A) Transient transfection of APPwt and BACE1 expression plasmid into HEK and TMP21 stable overexpression cell line HTM, equal quantities of total proteins were loaded onto 16% tricine gels for immunoblot analysis to detect full-length APP, actin, TMP21-myc and CTFs. The CTFs levels in HEK and HTM were quantified and values are expressed as Mean±SEM. N>=3, *p<0.05 by student's *t*-test. When TMP21 was stably upregulated, there was a significant increase in C99 levels (*p<0.05) and decrease in C83 levels as well (*p<0.05). (B) The ratios of C99/C83 and C99/C89 from experiments in (A) were also analyzed by Graphpad Prism version 5 and values are expressed as Mean±SEM. N=3, *p<0.05 by student's *t*-test. (C) Conditioned medium of HEK and HTM cells cotransfected with APPwt and BACE1 from (A) was collected, the secreted Aβ40 was quantified by ELISA assay. Values are expressed as Mean±SEM. N>=3, *p<0.05 by student's *t*-test.

3.3.2 Knockdown of TMP21 also preferentially enhanced C99 generation.

To further investigate the role of TMP21 in APP processing, we transfected the TMP21 siRNA (Vetrivel, et al., 2007) into HEK cells. The TMP21 siRNA transfected cells showed around 20~70% reduction of TMP21, and p24a decreased correspondingly. A decrease of TMP21 was also found in p24a siRNA transfected cells. P24a siRNA or TMP21 siRNA significantly increased C99 production, rather than C83 or C89 in APPwt and BACE1 co-expressing cells (Fig 3.2 A), resulting in the dramatically increased ratio of C99/C89 compared to scramble siRNA control cells 1.00 ± 0.14 vs. 1.62 ± 0.19 ($p=0.0029$) or 1.00 ± 0.14 vs. 1.31 ± 0.17 ($p=0.0240$), respectively. The ratio of C99/C83 ratio was dramatically increased in p24a knockdown cells and TMP21 knockdown cells, comparing to scramble siRNA control cells 1.00 ± 0.26 vs. 2.92 ± 0.44 ($p=0.0070$) or 1.00 ± 0.26 vs. 1.79 ± 0.27 ($p=0.0172$), respectively. APP Swedish mutation (KM670/671NL), leading to a increased β -site cleavage and A β generation, is identified in a Swedish family with early-onset AD (Citron, et al., 1992; Mullan, Crawford, et al., 1992). Studies in our lab show that APP^{swe} generates more C99 and higher C99/C89 ratio compared to APP^{wt} (Deng, et al., 2013). Upon co-expression of APP^{swe} and BACE1 in p24a siRNA or TMP21 siRNA transfected cells, C99 level was specifically increased (Fig 3.2 B). The ratio of C99/C89 ratio was dramatically increased in p24a knockdown cells and TMP21 knockdown cells, comparing to scramble siRNA control cells, 1.00 ± 0.07 vs. 2.27 ± 0.49 ($p=0.0339$) or 1.00 ± 0.07 vs. 1.76 ± 0.33 ($p=0.0342$), respectively. The ratio of C99/C83 ratio was dramatically increased in p24a knockdown cells and TMP21 knockdown cells, comparing to scramble siRNA control cells, 1.00 ± 0.07 vs. 3.73 ± 0.88 ($p=0.0176$) or 1.00 ± 0.07 vs. 2.94 ± 0.46 ($p=0.0073$), respectively (Fig 3.2 B). This *in vitro* data showed that suppression of TMP21 also facilitated APP amyloidogenic processing by specifically increasing C99 levels. The increased C99 was because of the enhanced BACE1 cleavage at Asp-1 site on APP. It also suggested the impact of TMP21 on BACE1 cleavage.

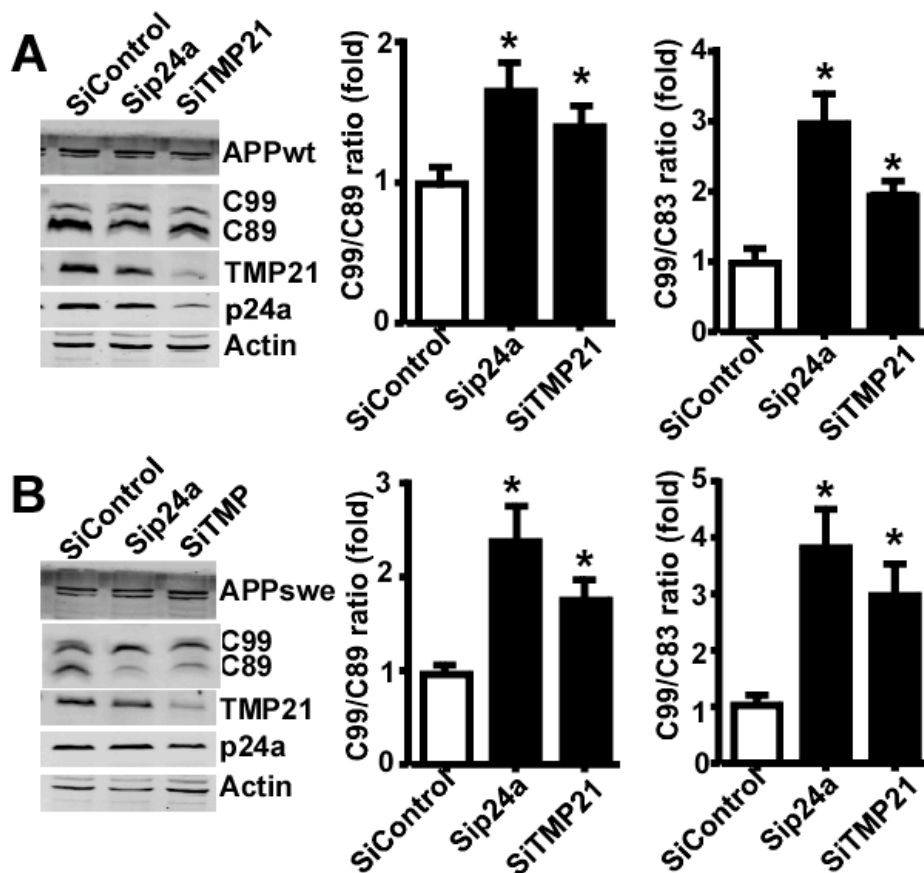


Figure 3.2 Knockdown of TMP21 preferentially generated more C99.

(A) The cells expressed both APPwt and BACE1 and then were treated by TMP21 siRNA, scramble control siRNA and p24a siRNA, respectively. 48-72 hours after siRNA treatment, the cells were harvest in PBS and the same amounts of total proteins were loaded on 16% Tris-Tricine gel, the holoAPP and CTFs levels were detected by C20 antibody. Endogenous TMP21 was detected by T21 antibody and endogenous p24a was detected by TMED2 antibody. The pattern of C99/C89 and C99/C83 were analyzed using Graphpad Prism version 5. Values were expressed as Mean±SEM. N>=3, *p<0.05 by student's *t*-test. (B) The cells expressed both APPswe and BACE1 and then were treated by TMP21 siRNA, scramble control siRNA and p24a siRNA, respectively. 48-72 hours after siRNA treatment, the cells were harvest in PBS and the same amounts of total proteins were loaded on 16% Tris-Tricine gel, the CTFs levels were detected by C20 antibody and the pattern of C99/C89 and C99/C83 were analyzed using Graphpad Prism version 5. Values were expressed as Mean±SEM. N>=3, *p<0.05 by student's *t*-test.

3.3.3 Disruption of TMP21 facilitated plaque formation in AD transgenic mice.

To determine the role of TMP21 in AD pathology *in vivo*, we crossed the TMP21-deficient mice with AD mice. The *Tmp21* hemizygous mice strain S2P23 is established by disrupting one *Tmp21* allele. The mRNA level of TMP21 and the protein level of TMP21 is significantly reduced in these mice (Denzel, et al., 2000a). Homozygous TMP21 knockout mice are not viable, suggesting that the TMP21 is essential for early stage of mammalian development (Denzel, et al., 2000a). APP23 transgenic mice express the human APP751 isoform with the Swedish mutation specifically in neurons and begin to develop neuritic plaques at 6 months (Sturchler-Pierrat, et al., 1997). The APP23XS2P23 double crossed mice appeared smaller than their littermate controls. Total of 214 pups from 15 breeding cages were analyzed. The genotyping ratio of APP23: S2P23: C57BL/6: APP23XS2P23 was 0.46: 0.50: 1: 0.18, instead of the expected 1:1:1:1 Mendelian ratio. In total, 18 double crossed mice were produced: 10 female and 8 male. Among them, 12 died before the age of 3 months. Few APPXS2P23 mice can survive after 6 months. Brain tissue from two mice at the age of 7 months were collected and there were only 4 female and 1 male reached at the age of 9 months. The limited numbers curtailed our further study in behaviors. The fatality of the APP23XS2P23 mice is detrimental and the fundamental function of TMP21 demands further attention.

Even though the fluorescent detection using thioflavin S were unable to detect the A β plaques in either APP23XS2P23 double crossed mice or APP23 littermate controls at 7 months old, we still can observe the relatively increased C99 level and the trend of increased A β level in APP23XS2P23 double crossed mice (Fig 3.3). After 2 more months later, in 9 months-old mice brain, consistently, there was significantly increased the C99 generation, compared APP23XS2P23 double crossed mice to littermate controls, 1.00 ± 0.14 vs. 2.06 ± 0.14 ($p=0.0023$). We also detected the increased A β levels in APP23XS2P23 double crossed mice, compared to their littermate controls, 1.00 ± 0.10 vs. 2.30 ± 0.42 ($p=0.0210$). Moreover, using the immunohistochemical staining with anti-human A β antibody 4G8 and fluorescent detection using thioflavin S, we clearly saw the increased plaques in the cortex of the APP23XS2P23

Chapter 3: The Dysregulated TMP21 Facilitates APP Amyloidogenic Processing

mice, compare to the APP23 mice, 1.00 ± 0.08 vs. 2.19 ± 0.09 ($p=0.0002$) (Fig 3.4). This evidence was consistent with the *in vitro* results from previous published paper of other groups (F. S. Chen, et al., 2006; Vetrivel, et al., 2007) and strongly supported that the deficiency in TMP21 can exacerbate A β production and AD pathogenesis *in vivo*.

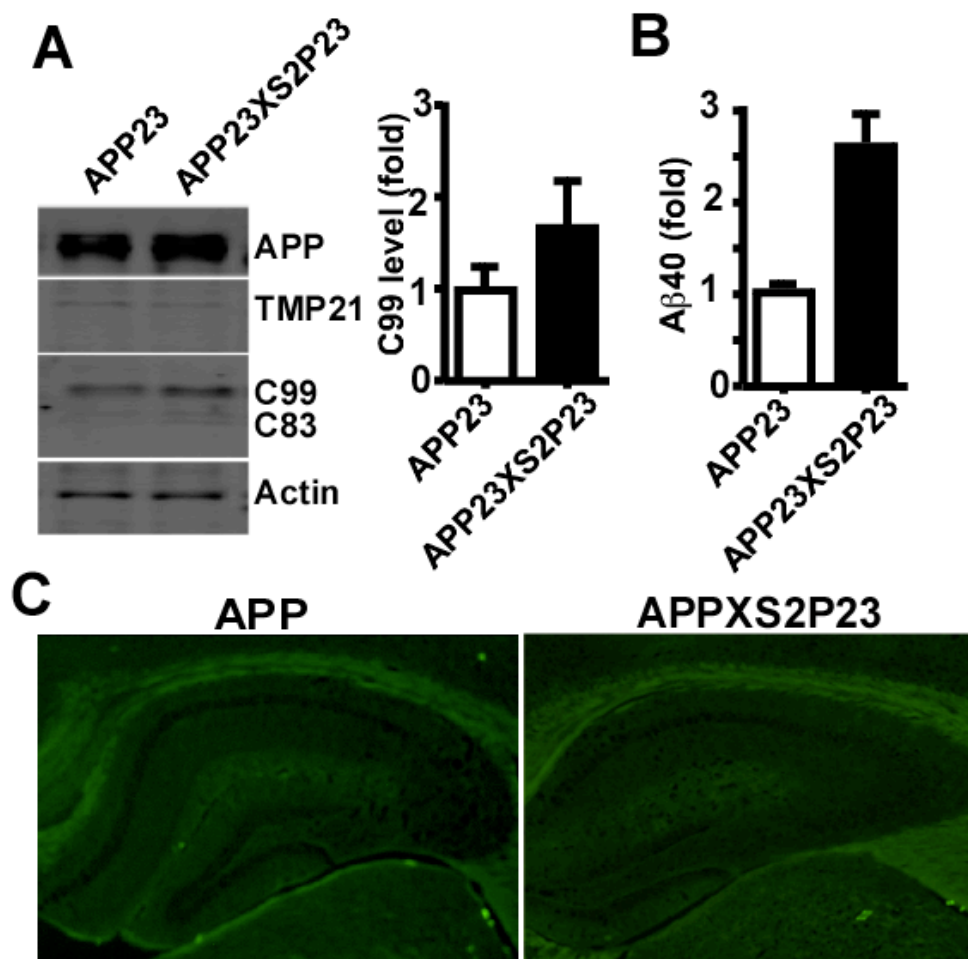


Figure 3.3 Disruption of TMP21 facilitated C99 and A β generation in 7 months old AD mice.

The TMP21 hemizygous knockdown mice S2P23 were crossed breeding with classic AD mice APP23, the double-crossed mouse APP23XS2P23 and its littermate controls were sacrificed at 7 months. Half of the brain was used for Western blot and ELISA analysis, and the other half was used for plaques staining. (A) Brains tissue the same amount of tissue from the same brain region was lysed in 2% SDS RIPA-DOC buffer. The same amounts of total proteins were loaded on 16% Tris-Tricine gel. The full-length APP and CTFs levels were detected by C20 antibody.

Chapter 3: The Dysregulated TMP21 Facilitates APP Amyloidogenic Processing

Endogenous TMP21 was detected by T21 antibody. C99 levels were analyzed using Graphpad Prism version 5. Values were expressed as Mean \pm SEM. N=2. (B) Brains tissue were lysed in Guanidine HCl according to A β ELISA Kit instructions (Invitrogen) for A β 40 ELISA analysis. Values were expressed as Mean \pm SEM. N=2, (C) The other half of the brain was dissected, fixed, and sectioned. The plaques were detected by immunohistochemical staining with fluorescent detection using thioflavin S to detect the A β plaques. Plaques were visualized by microscopy with 40 \times magnification.

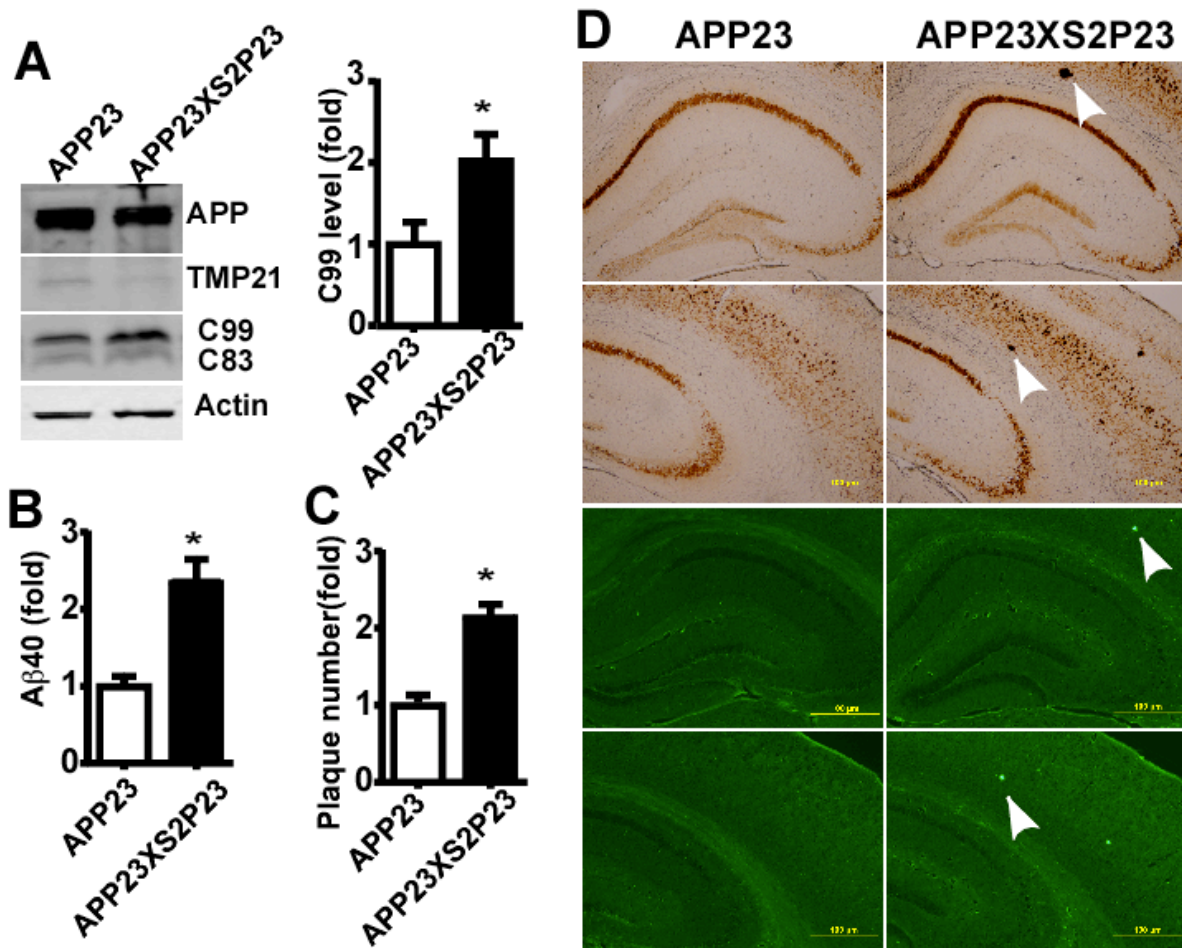


Figure 3.4 Disruption of TMP21 facilitated plaque formation in 9 months old AD mice.

The TMP21 hemizygous knockdown mice S2P23 were crossed breeding with classic AD mice APP23, the double-crossed mouse APP23/S2P23 and its littermate controls were sacrificed at 9 months. Half of the brain was used for Western blot and ELISA analysis, and the other half was used for plaques staining. Half of the brain was used for Western blot and ELISA analysis, and the other half was used for plaques staining. (A) Brains tissue were be

Chapter 3: The Dysregulated TMP21 Facilitates APP Amyloidogenic Processing

isolated from half of the brain, the same amount of tissue from the same brain region was lysed in 2% SDS RIPA DOC buffer. The same amounts of total proteins were loaded on 16% Tris-Tricine gel. The full-length APP and CTFs levels were detected by C20 antibody. Endogenous TMP21 was detected by T21 antibody. C99 levels were analyzed using Graphpad Prism version 5. Values were expressed as Mean \pm SEM. N=5, * p <0.05 by student's *t*-test. (B) Brains tissue were lysed in Guanidine HCl according to A β ELISA Kit instructions (Invitrogen) for A β 40 ELISA analysis. Values were expressed as Mean \pm SEM. N=5, * p <0.05 by student's *t*-test. (D) The other half of the brains from APP23XS2P23 and its littermates control APP23 were used for plaque staining. The brain was dissected, fixed, and sectioned. The plaques in brains slices were immunohistochemical staining with anti-human A β antibody 4G8 (upper lanes) and fluorescent detection using thioflavin S (bottom lanes). Plaques were visualized by microscopy with 40 \times magnification. (C) Plaques were quantified by average plaque count per slices for each mouse, and the data were analyzed Graphpad Prism version 5. Values were expressed as Mean \pm SEM. N=5, * p <0.05 by student's *t*-test.

3.3.4 TMP21 accumulated immature BACE1 and interacted with immature BACE1.

Our results suggested that overexpression and downregulation of TMP21 facilitated APP amyloidogenic processing, which indicated by the increased C99 levels. The preferential increased C99 level cannot be explained by the alteration of γ -secretase activity. It indicated that the BACE1, cleaved APP at Asp-1 site to produce C99, might play major role. Therefore, to determine whether TMP21 affects BACE1, we first detected the BACE1 in TMP21 overexpressed and downregulated cells. It's known than the newly synthesized BACE1 followed the classic transmembrane protein synthesis and trafficking pathway from ER to Golgi. The trafficking of BACE1 between ER and Golgi can be traced by the alteration of the BACE1 molecular mass from the immature form in the ER (~66KDa) to the mature form (~75KDa) (Benjannet, et al., 2001; Capell, et al., 2000; Creemers, et al., 2001; Huse, et al., 2000). So we transfected BACE1 into HEK cells and HTM cells. Western blot analysis showed that overexpression of TMP21 significantly accumulated the immature form of BACE1, leading to increased ratio of immature BACE1 to mature BACE1, 1.00 \pm 0.09 vs. 4.00 \pm 0.39 (p =0.0066). The cytoplasmic domain of TMP21 is very essential for its ER/Golgi trafficking. To exclude the artifact that induced by the mycHis tag at the cytoplasmic tail of TMP21, we transfected BACE1 in GFP-TMP21 (with GFP inserted between signal peptide and luminal domain of TMP21)

Chapter 3: The Dysregulated TMP21 Facilitates APP Amyloidogenic Processing

expression cells (Fig.3.5 B.), and also transfected BACE1 in cells expressed TMP21 without tag (Fig 3.5 C). Consistently, the increased immature BACE1 can be detected and the ratio of immature BACE1 to mature BACE1 was significantly increased when cotransfected with TMP21 with or without tags. These results showed that the mycHis at the C-terminal of TMP21 or the GFP tag ahead of TMP21 presented the similar effects on accumulation immature BACE1 as TMP21 without any tag. We also found the increased immature BACE1 could be detected in TMP21 or p24a knockdown cells, 1.00 ± 0.07 vs. 2.48 ± 0.30 ($p=0.0223$) or 1.00 ± 0.07 vs. 3.18 ± 0.35 ($p=0.0041$), respectively. The downregulated TMP21 retained BACE1 in ER as its immature form, which is consistent with the function of TMP21 in ER-to-Golgi trafficking.

Further, we found the interaction between TMP21 and BACE1 by coimmunoprecipitation (CoIP) assay, and specifically, only the immature form of BACE1 could be co-precipitated with TMP21. It indicated the interaction between TMP21 and the immature BACE1 (Fig. 3.6 A.). The reverse Co-IP also showed the TMP21 can be co-precipitated by BACE1 (Fig. 3.6 B). These results suggested that TMP21 may regulate BACE1 maturation or ER export through this TMP21/immature BACE1 interaction. The immature BACE1 existed in ER, where BACE1 preferentially cleaved APP at Asp-1 site and produce more C99. It was possible that TMP21 affected the BACE1 maturation processing through ER, thus contributed to the enhanced C99 level.

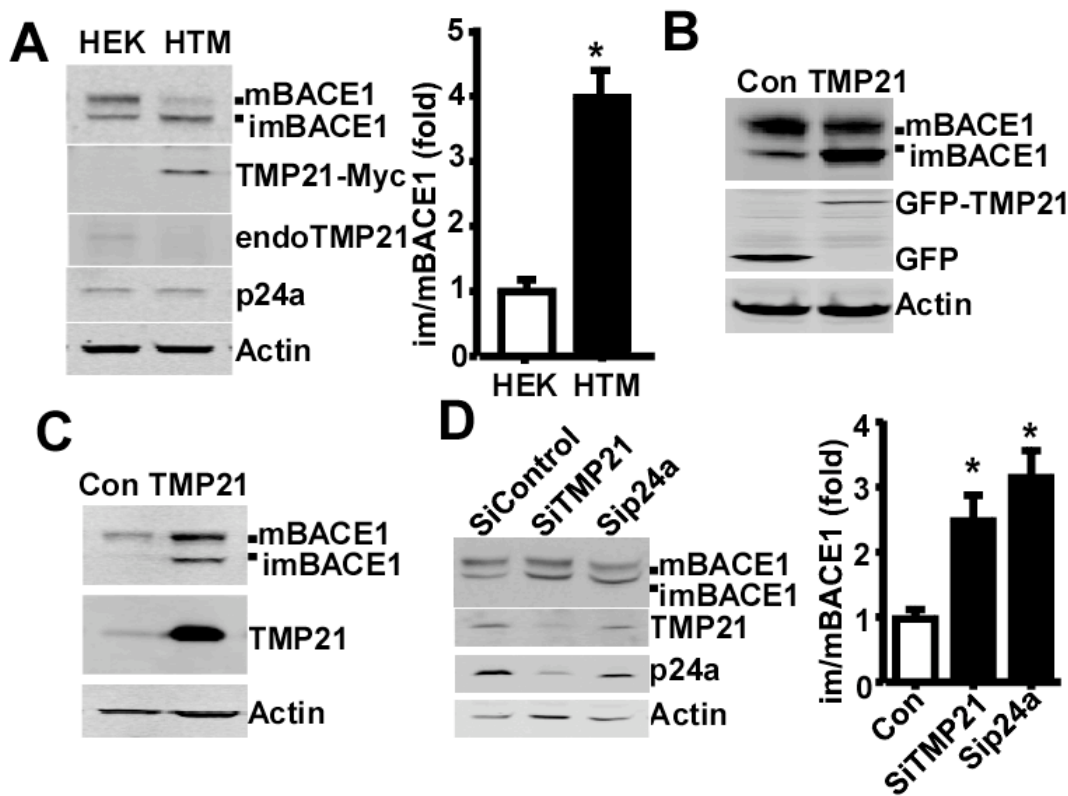


Figure 3.5 Immature BACE1 increased when TMP21 overexpressed.

(A) BACE1-myc expression plasmid was transfected into HEK cells and HTM cells. Equal amount of total proteins from each sample were loaded on the 8% glycine gel and the pattern of mature form and immature form of BACE1 could be visualized by 9E10 antibody. The mycHis tagged TMP21 could be detected by 9E10 antibody. Endogenous TMP21 and p24a were blotted by T21 antibody and TMED2 antibody, respectively. The patterns of immature and mature BACE1 were analyzed using ImagJ and Prism 5. Values were expressed as Mean±SEM. N>=3, *p<0.05 by student's *t*-test. (B). GFP-tagged TMP21 plasmids was transfected into the cells expressed with BACE1-myc plasmid. GFP-TMP21 and GFP control could be detect by anti-GFP antibody. (C) TMP21 no tag plasmid was transfected into the cells expressed with BACE1-myc plasmid. Endogenous TMP21 was blotted by T21 antibody. (D) The cells expressed BACE1 were treated by TMP21 siRNA, scramble control siRNA and p24a siRNA, respectively. 48-72 hours after siRNA treatment, the cells were harvest in PBS and the same amounts of total proteins were loaded on 8% glycine gel and the pattern of mature and immature of BACE1 was detected by 9E10 antibody. The patterns of immature and mature BACE1 were analyzed using ImagJ and Prism 5. Values were expressed as Mean±SEM. N>=3, *p<0.05 by student's *t*-test.

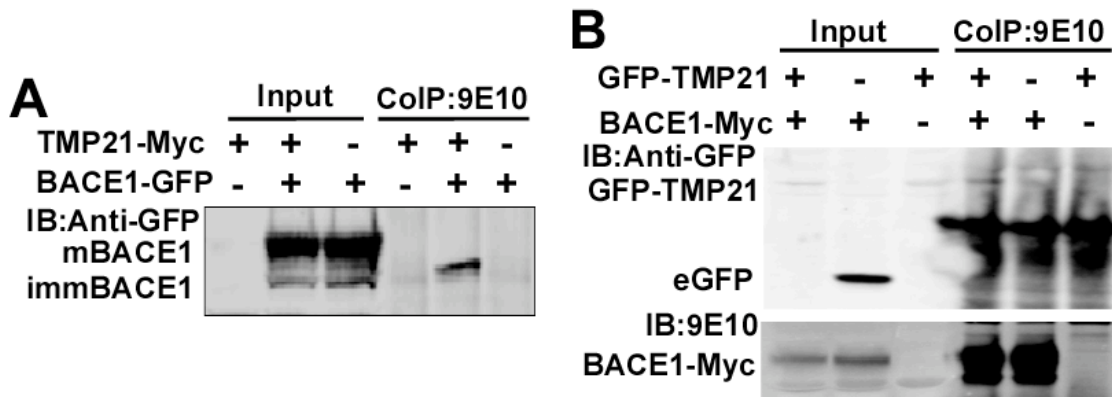


Figure 3.6 TMP21 interacted with immature BACE1.

(A) HEK cells were transfected with myc-tagged expression plasmid of TMP21 and GFP tagged-BACE1, eGFP or pcDNA4 vectors as negative controls. After 24 hours, cells were harvested in PBS and lysed in NP-40 buffer. Lysates were immunoprecipitated with anti-myc antibody 9E10 and analyzed by immunoblot using anti-GFP antibody. The immature form of BACE1 can be coimmunoprecipitated with TMP21. (B) HEK cells were transfected with myc-tagged expression plasmid of BACE1 and GFP tagged-TMP21, eGFP or pcDNA4 vectors as negative controls. Lysates were immunoprecipitated with anti-myc antibody 9E10 and analyzed by immunoblot using anti-GFP antibody. The GFP-TMP21 can be coimmunoprecipitated with BACE1.

3.3.5 Overexpression of TMP21 altered trafficking of BACE1 and its subcellular distribution

TMP21 is a critical protein that mediates anterograde and retrograde transport between ER and Golgi (Dominguez, Dejgaard, Füllekrug, et al., 1998; Rojo, et al., 1997a). To investigate the effect of TMP21 on BACE1 subcellular distribution and trafficking along biosynthetic pathway, we cotransfected HEK cells with pTMP21-mycHis and BACE1myc and disrupted the cells in non-detergent buffer using Dounce homogenizer. The subcellular organelles with different density were separated through sucrose gradient as described in methods. In subsequent Western Blot analysis, the co-fractionation of TMP21 and BACE1 was detected in heavy-density sucrose gradient fractions, fraction 10-13. Immature BACE1 began to exist in these fractions. To further examine the subcellular distribution. GFP tagged-TMP21 and DsRed tagged-BACE1 were transfected into HEK cells and immunocytochemistry and confocal imaging were performed.

Chapter 3: The Dysregulated TMP21 Facilitates APP Amyloidogenic Processing

Consistent with previous observation, TMP21 and BACE1 were co-localized in a juxtannuclear region (Fig. 3.3). Furthermore, BACE1 was accumulated along TMP21 transport pathway and cotransport with TMP21 in the live cell imaging. It also showed that the BACE1 was concentrated in the region around the nuclear envelope (Video. 3.1). All these evidence proved that TMP21 affected BACE1 trafficking and contributed to the maturation process of BACE1.

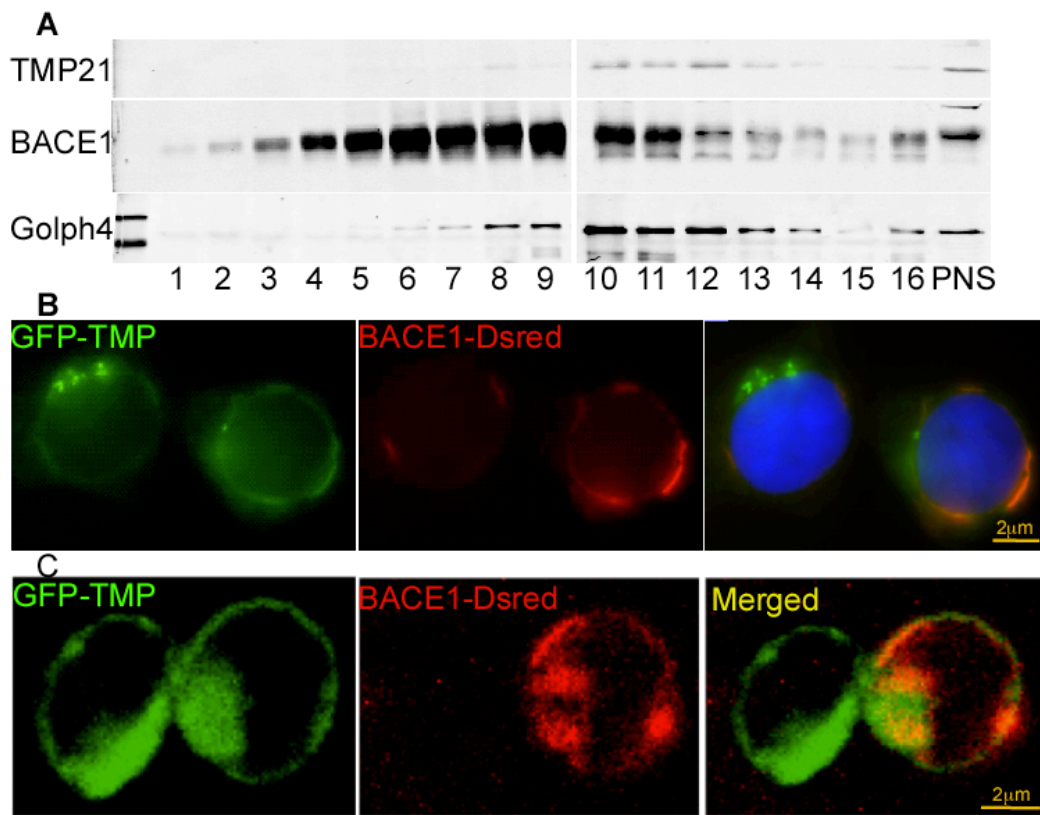


Figure 3.7 Co-localization of TMP21 and BACE1.

(A) 16 fractions from 10~50% sucrose density gradient were collected and concentrated by TCA precipitation as described in methods, 9E10 antibody was used to detect TMP21-Myc and BACE1-Myc. Golph4 was used as Golgi markers. The immunocytochemistry (B) and confocal imaging (C) was used to detect the localization of GFP fused between the signal peptide and luminal domain of TMP21 (GFP-TMP21) and BACE1-Dsred.

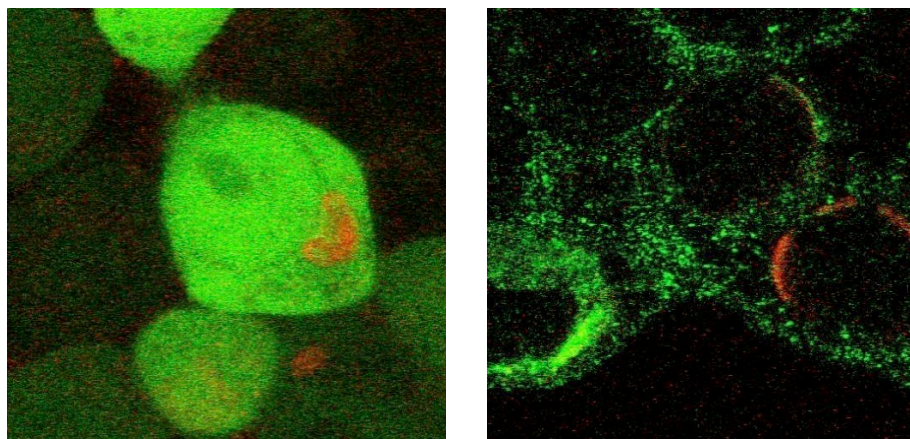


Figure 3.8 TMP21 accumulated BACE1 along the peri-nuclear region

The eGFP control plasmid and GFP-TMP21 and BACE1-Dsred were cotransfected into HEK cells using Calcium Phosphate transient transfection. Cells were cultured in phenol red-free complete DMEM medium. Live cell image analysis was performed 24h after transfection. Time-lapse images were acquired every 500 ms, 30 frames in total. These are the images taken from videos.

3.4 Discussion

Previous reports showed that the downregulation of TMP21 increased γ -cleavage of APP and A β production (F. S. Chen, et al., 2006; Dolcini, et al., 2008; Hasegawa, et al., 2010; Vetrivel, et al., 2007). It suggested that a deficiency in TMP21 might exacerbate AD pathology. In this chapter, we identified a novel AD-associated SNP in TMP21, and this SNP significantly increased TMP21 mRNA and protein expression *in vitro*, which indicated that increase in TMP21 expression might contribute to AD pathogenesis. We found the abnormal expression of TMP21, either by downregulating and overexpressing, increased the β -cleavage on APP, and specifically generated more C99.

To investigate the exact role of TMP21 expression levels in AD pathogenesis, multiple lines of the transgenic mice harbored human *Tmp21* at various expression levels were established (Gong, et al., 2011). Even a 50% increase of TMP21 overexpression in central nervous system leads

Chapter 3: The Dysregulated TMP21 Facilitates APP Amyloidogenic Processing

post-natal growth retardation, severe neurologic problems and early death, and the onset and severity of the symptoms are highly correlated with the TMP21 expression levels. Moreover, premature death of these transgenic mice lines occurred before they reached sexual maturity, resulting in no offspring generated beyond F1 (Gong, et al., 2011). Interestingly, the newborn human *Tmp21* transgenic mice are normal and show no symptom in the first two weeks after birth (Gong, et al., 2011). While the *Tmp21* homozygous knockout results in early embryonic lethality at E4.5, no homozygous knockout embryos or blastocysts could be detected and no homozygous knockout ES cell clones could be obtained (Denzel, et al., 2000b). These evidences suggest that the endogenous TMP21 expression levels are precisely controlled. The high expression level of TMP21 is essential for the development of embryonic and early post-natal stage but it begins to decline after birth. However, when sustained high-level TMP21 expressed during post-natal development, especially when endogenous TMP21 declines in human *Tmp21* transgenic mice, the mice begin to show complex neurological problems. Patients with AD show the reduced level of TMP21 (Vetrivel, et al., 2008). Certain amount of TMP21, at least, is required for facilitate normal trafficking and the reduction of TMP21 might contribute to the abnormal trafficking of AD-linked proteins, such as APP and its cleavage enzymes. Additionally, TMP21 levels declined with aging. When the low steady-state level of TMP21 is interrupted by increased expression of exogenous TMP21, it might also results in neurological problems.

Previous studies showed that the downregulation of TMP21 increases γ -secretase activity thus A β production (F. S. Chen, et al., 2006; Dolcini, et al., 2008; Hasegawa, et al., 2010; Vetrivel, et al., 2007). However, the activation of the γ -secretase activity and/or the increased β -site cleavage leads to the increased A β level. Therefore, without thoroughly examination of all CTFs, we cannot rule out the possibility that TMP21 alters APP processing not only by its regulation on γ -secretase activity, but also by its effects on BACE1. When we co-expression of APP and BACE1 in TMP21 overexpressed cells, we found the decreased in C83 level and surprisingly and the increased in C99 level, indicating the shift of APP processing from α -cleavage to the β -cleavage.

Chapter 3: The Dysregulated TMP21 Facilitates APP Amyloidogenic Processing

Moreover, overexpression of TMP21 preferentially enhanced BACE1 cleavage At Asp-1 site to produce more C99, rather than C89. The specific increased in Asp-1 site cleavage indicated that TMP21 enhanced β -cleavage. Furthermore, we found that the upregulation of TMP21 accumulated immature BACE1, and this effect is not the artifacts induced by additional tags. More interestingly, we identified the interaction between TMP21 and BACE1, specifically, TMP21 interacting with immature BACE1. Further, we observed the co-localization of TMP21/BACE1 around the nuclei region and BACE1 co-transport with TMP21, indicating the role of TMP21 in BACE1 maturation and trafficking. Similarly, our results showed the accumulated immature BACE1 in TMP21 knockdown cells, as a consequence, enhanced β -cleavage on APP and preferentially more C99 generated. When TMP21 knockdown in AD mice model, the increased A β level and plaques were detected. Again, our studies emphasized the impact of TMP21 on BACE1 maturation and thus APP amyloidogenic processing. Here, we could not totally exclude the effect of TMP21's regulation on γ -secretase activity based on our data; we can not distinguish that the increase A β is absolutely from increased C99 level or also from the upregulated γ -secretase activity in our cell model and mouse model. Further investigations are necessary.

3.5 Conclusion

In this chapter, we demonstrate that the proper expression level of TMP21 is essential in APP processing. The dysregulation of TMP21 facilitated APP amyloidogenic processing by increasing C99 generation, indicating the effect of TMP21 on β -cleavage. Moreover, interaction of TMP21/immature BACE1, the accumulation of immature BACE1, and the alteration of BACE1 subcellular distribution and transport, indicated the potential role of TMP21 on BACE1 maturation and trafficking.

Chapter 4: TMP21 Affects BACE1 Maturation and Trafficking

4.1 Introduction

TMP21, a vesicular trafficking protein, mediates proteins ER/Golgi transport and maturation process (Dominguez, Dejgaard, Fullekrug, et al., 1998; Nickel, et al., 1997). It also facilitates GPI-anchored proteins ER export and lipid rafts translocation (M. Fujita, et al., 2011; Takida, et al., 2008). BACE1 mainly presents as its mature form and cleaves APP within A β region at Glu-11 site to generate C89 and then truncated A β species (H. Cai, et al., 2001; Creemers, et al., 2001; Deng, et al., 2013; Huse, et al., 2002; Vassar, et al., 1999). Preferential selection of APP cleavage by BACE1 at Asp-1 or Glu-11 site is strongly dependent on BACE1 trafficking and localization. The Asp-1 site cleavage on APP to produce C99 and A β are enhanced by retaining BACE1 in ER or guide BACE1 into lipid raft (Cordy, et al., 2003; Huse, et al., 2002; Vetrivel, et al., 2011). Our study in Chapter 3 has found that TMP21 preferentially enhanced Asp-1 site cleavage of APP to generate more C99 by accumulating immature BACE1 and interacting with immature BACE1. These results suggested that TMP21 might alter the trafficking and maturation processing of BACE1. In this chapter, we further examined how the TMP21 affects BACE1 trafficking and maturation processing. Here, we would like to characterize the TMP21/BACE1 interaction first and hypothesize that the TMP21/BACE1 interaction might contribute to the immature BACE1 accumulation. TMP21 accumulates immature BACE1 by delaying the maturation of BACE1 and affecting its ER/Golgi trafficking. Furthermore, TMP21 enhances the interaction and co-residency of APP/BACE1, might translocate both the immature BACE1 and APP into lipid raft-like structures.

4.2 Methods

4.2.1 Plasmids constructions.

For the TMP21 plasmids cloning, we used TMP21 expression plasmid pcDNA4-TMP21mycHis as template. TMP21 signal peptide was fused to the N-terminal of GFP then the different domains of TMP21 from human TMP21 cDNA sequence will be fused to the C-terminal of GFP

Chapter 4: TMP21 Affects APP and BACE1 Trafficking

as indicated in Fig 4.1. All chimeras included sequential deletions of cytoplasmic domain, transmembrane domain and luminal domain, mutation of KKLIE motif to SSLIE, and mutation of FFKAK motif to AAKAK. The mutant TMP21 cDNA were amplified by primers TMP FF/AA F: 5'-TGCGACGCGCTGCTAAGGCCAAG and TMP FF/AA R: 5'-CTTGGCCTTAGCAGCGCGTCGCA, TMP KK/SS F: 5'-AAGGCCTCCTCATTGATTGAG and TMP KK/SS R: 5'-CTCAATCAATGAGGAGGCCTT. To generate p24a-myc plasmid, cDNA from HEK293 cells was used as template, forward primer p24a-fHind: 5'-GCCAAGCTTGCCACCATGGTGACGCTTGCTGAACTGC and reverse primer p24a-rXba: 5'-GCCTCTAGAAACAACCTCTCCGGACTTCAAAAATC were used for PCR, the coding sequence p24a was subcloned into pcDNA4 vector. Using this plasmid as template, GFP-p24a plasmid was constructed by GFP being inserted between p24a signal peptide and luminal domain, using two pairs of primers: p24-sig+GFP-R: 5'-CGCCCTTGCTCACCATGCCCCGAGACCGTGGCCAGGA and p24-sig+GFP-F: 5'-TCCTGGCCACGGTCTCGGGCATGGTGAGCAAGGGCG, p24lum-RBamHI: 5'-GCGTCGATGCTAACGAAATACTTGTACAGCTCGTCC and p24lum-FEcoRI: GGACGAGCTGTACAAGTATTTTCGTTAGCATCGACGC. Using pzBACE1 as template, BACE1 mutant plasmids BACE1D93A and BACE1D93/289A were generated by primers B1 D93A F: 5'-GACGCTCAACATCCTGGTGGCCACAGGCAGCAGTAACTTTG and B1 D93A R: 5'-CAAAGTTACTGCTGCCTGTGGCCACCAGGATGTTGAGCGTC, B1 D289A F: 5'-CAACTATGACAAGAGCATTGTGGCCAGTGGCACCACCAACCTTC and B1 D289A R: 5'-GAAGGTTGGTGGTGGCCACTGGCCACAATGCTCTTGTCATAGTTG. APP C99 cDNA were amplified by PCR and then cloned into pcDNA3 vector to generate expression plasmid pAPP-C99.

4.2.2 Cell culture and transfections.

All cells were cultured in Dulbecco's modified eagle medium (DMEM) supplemented with 10% fetal bovine serum (FBS), 1mM sodium pyruvate, 1mM L-glutamine, and 50U/mL penicillin G sodium and 50ug/mL streptomycin sulfate (Invitrogen, Carlsbad, CA USA), and

Chapter 4: TMP21 Affects APP and BACE1 Trafficking

were maintained at 37°C in an incubator containing 5% CO₂. HTM cell media also contained 60mg/mL zeocin. Cells were seeded in 24-well plates or 35mm plates 24 hours before transfection and grown to near 70% confluence by the day of transfection. Transient transfections were performed using the calcium phosphate method, and cells were allowed to grow for an additional 48 to 72 h until confluent. Or cells were transfected with 2µg plasmid DNA in 35mm plate using 2µl of lipofectamine 2000 Reagent (Invitrogen) according to the manufacturer's instructions. Unless otherwise stated, all cells were harvested in PBS and lysed in a modified RIPA-DOC buffer (150mM NaCl, 50mM Tris-HCL, 1% Triton X-100, 2% SDS, and 1% sodium deoxycholate) with the presence of protease inhibitor cocktail complete (04693116001; Roche, Indianapolis, IN, USA). After briefly sonication and centrifugation at 14,000rpm for 10 mins, supernatants were collected and protein assay was performed with the Bio-Rad Dc protein assay kit (Bio-Rad, Richmond, CA).

4.2.3 Immunoblotting.

Whole-cell lysates were diluted in 4XSDS-sample buffer and separated on 12% Tris-glycine SDS-PAGE gel and transferred to polyvinylidene fluoride (PVDF-FL) membranes. Membranes were blocked in PBS containing 5% non-fat dried milk and incubated with the primary antibodies diluted in the blocking buffer at 4°C overnight. Rabbit anti-TMP21 antibody T21 was generated by inoculating rabbit with synthetic peptide HKDLLVTGAYEIHK, this peptide shared 100% sequence homology with both mouse and human TMP21. Rabbit anti-C20 (1:1000) recognized the last twenty amino acids on the C-terminal end of human APP and Mouse 9E10 (1:200) recognized the Myc tag were made in-house as well. Human and mouse p24a was detected by mouse monoclonal antibody TMED2 (C-8) (1:2000) (Santa Cruz Biotechnology). Purified mouse anti-calnexin antibody was purchased from BD Bioscience. Lipid raft associated protein flotillin2 was detected using rabbit anti-flotillin2 (Sigma) (1:1000) and β-actin was detected using monoclonal antibody AC-15 (1:5000) (Abcam, Cambridge, MA, USA and Sigma). Then the membranes were rinsed in PBS-T and incubated with near-infrared fluorescence-labeled secondary antibodies IRDyeTM680-labeled goat anti-rabbit (1:100,000) and

Chapter 4: TMP21 Affects APP and BACE1 Trafficking

IRDyeTM800-labeled goat anti-mouse antibodies (1:100,000) (Lincoln, NE, USA) in PBS-T at room temperature for 1 h, after further rinsed in PBS-T the membranes was scanned by LI-COR Odyssey R system. All quantification measurements were preformed using ImagJ software.

4.2.4 Coimmunoprecipitation.

Cells were harvested with 1XPBS 48h after transfection and lysed in 0.3mL NP-40 lysis buffer (20mM Tris.HCl pH 7.5, 150mM NaCl, 1mM MgCl₂, 1mM EDTA, 1% NP-40) with protease inhibitor cocktail complete (04693116001; Roche, Indianapolis, IN, USA) on ice for 30mins. Samples were spun at 14,000rpm for 15 min and supernatants were transferred to a new tube. Immunoprecipitation antibody was added in 60µl protein A/G coupled to agarose beads (Santa Cruz Biotechnology) and gently mixed at 4°C for 3 h to overnight. Beads were washed by NP-40 lysis buffer and then added into samples supernatant. After mixing overnight at 4°C, the beads were washed three times in lysis buffer and boiled in 1xSDS sample buffer for 5 min. The cells transfected with myc-tagged expression plasmids were immunoprecipitated with anti-myc antibody 9E10 (1:20) and immunoblotted with anti-TMP21 antibody T21 or anti-eGFP (1:1000); The cells expressed with APP and CTF were immunoprecipitated with anti-APP-CTF antibody C20 (1:100), then immunoblotting was performed using 9E10 (1:500).

4.2.5 Immunocytochemistry.

Cells were seeded onto glass cover slips in 24 well plates the day before transfection, 24 hours after transfection cells were rinsed in PBS, fixed in 4% PFA or methanol at -20°C for 20 min, blocked in 5% BSA in PBS-Tx for 30 min, and incubated with or without primary antibodies in 1% BSA in PBS-Tx overnight at 4°C. The next day cells were rinsed, incubated for 1 h with goat anti-rabbit Alexa Fluor 488 (green) or goat anti-mouse Alexa Fluor 568 (red), rinsed in PBS-Tx, and mounted using Fluoromount-G (Southern Biotech). Cells transfected with GFP-TMP and BACE1-RFP were fixed 24 hours after transfection and then mounted. Cells were imaged with a 100x oil objective lens on a Carl Zeiss Axiovert-200 epi fluorescent microscope.

4.2.6 Pharmacological treatment.

L-685,458 (Sigma), a potent, structurally novel γ -secretase inhibitor, was dissolved in DMSO and applied to cell culture medium at 1 μ M final concentration for 3h to overnight. Cycloheximide (CHX) (Sigma), a proteins synthesis inhibitor at translational level, was added into the medium at 100 μ g/mL final concentration and chased at different time points.

4.2.7 Lipid raft isolation.

Cells were washed in PBS and scraped into 0.5ml of lysis buffer containing different detergents: 0.5% Lubrol WX (Lubrol 17A17; Serva) in 25mM Tris-HCl (pH 7.4), 150mM NaCl, and 5mM EDTA or 1% Triton X-100 (Sigma) in 25mM Tris-HCl (pH 8) and 140mM NaCl. All the lysis buffers were supplemented with a protease inhibitor cocktail complete (Roche). Cells were homogenized by five passages through a 25-gauge needle. The lysates were adjusted to 45% final concentration of sucrose and transferred to the ultracentrifuge tube. A discontinuous sucrose gradient is then formed by sequentially layering 35% sucrose and 5% sucrose, and the tubes were subject to ultracentrifugation at 39,000 rpm for 19 h in Beckman MLS50 rotor at 4 °C. Twelve to sixteen fractions were collected from the top of the gradient and equal volume of each fraction was analyzed by Western blotting (Chang, et al., 1994; Elortza, et al., 2003; Foster, De Hoog, & Mann, 2003; Sargiacomo, Sudol, Tang, & Lisanti, 1993; Smart, Ying, Mineo, & Anderson, 1995). Lipid raft associated protein flotillin2 was detected using rabbit anti-flotillin2 (Sigma) (1:1000) and purified mouse anti-calnexin antibody was used as the soluble proteins marker and purchased from BD Bioscience.

4.3 Results

4.3.1 Multiple binding sites between TMP21 and BACE1

The luminal domain, transmembrane domain and cytoplasmic domain of TMP21 show different functions during its transport pathway, respectively. For instants, majority of TMP21 is located in the cis-Golgi, while it is also found on the plasma membrane (Blum, et al., 1996b; Sohn, et al., 1996b). The large 156 amino acids luminal domain of TMP21 contributes to the transient

Chapter 4: TMP21 Affects APP and BACE1 Trafficking

appearance of TMP21 on cell surface (Blum, 2007; Blum & Lepier, 2008), while a short C-terminal cytoplasmic tail facilitates TMP21 cycling between Golgi and ER (Dominguez, Dejgaard, Füllekrug, et al., 1998). Cytoplasmic domain of TMP21 carries a KKLIE motif similar to ER retention and retrieval KKXX motif (Blum, et al., 1996a). This motif is essential for COPI vesicle budding from the cis-Golgi then directed to the ER (P. Cosson & Letourneur, 1994b; Jackson, Nilsson, & Peterson, 1990; Letourneur, Gaynor, Hennecke, Démollière, et al., 1994). The diphenylalanine motif FFKAK in cytoplasmic domain mediates the interaction with Sec23 that contributes to COPII vesicle budding (Dominguez, Dejgaard, Füllekrug, et al., 1998). This FFKAK motif is also similar to F/YXXXXF/Y motif, the strong AP-2 binding motif (Dominguez, Dejgaard, Füllekrug, et al., 1998). The transmembrane domain of TMP21 promotes its association with the PS1 and Nicastrin, and contributed to the decreased γ -secretase activity for APP processing (Pardossi-Piquard, et al., 2009). To further demonstrate the mechanism that how the TMP21 delays the transport of immature BACE1, we constructed a series of GFP-tagged TMP21 plasmids. They included sequential deletions of cytoplasmic domain, transmembrane domain and luminal domain, mutation of KKLIE motif to SSLIE (Blum & Lepier, 2008), and mutation of FFKAK motif to AAKAK (Sohn, et al., 1996b). The schematic representations of these GFP tagged-TMP21 domains are showed in Figure 4.1. To map the APP or BACE1 binding motif on TMP21, we used Co-IP to assess interaction between BACE1 and wild type or these TMP21 domains, respectively. The results showed that there are multiple binding site of BACE1 in luminal domain and transmembrane domain of TMP21, correspondingly, and multiple TMP21 binding sites on BACE1 (Figure 4.1 and Figure 4.2). It suggests that the conformation of TMP21 and BACE1 is an important contribution of the interaction between these two proteins.

Chapter 4: TMP21 Affects APP and BACE1 Trafficking

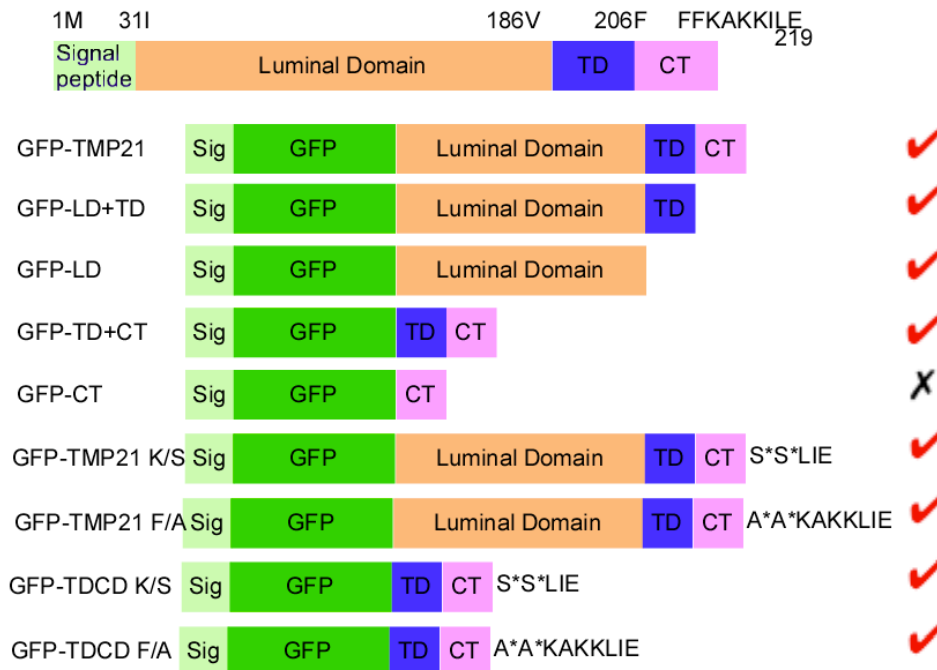


Figure 4.1 Schematic representation of TMP21 constructs.

To map the BACE1-binding motif in TMP21, we construct a series of GFP-tagged TMP21 domains. The scheme outlines the organization of the different TMP21 domains; sig, ER translocation signal peptide (M-31 ~I1); luminal, luminal domain (I1~L156), TD, single-span transmembrane domain (L156~F174); CT, cytoplasmic tail peptide (L177~L188) containing the KKXX motif (KKILE, 184~188). In the GFP-TMP21 constructs, the different TMP21 domains were tagged with signal peptide-tag GFP as indicated, then the different domains of TMP21 from human TMP21 cDNA sequence will be fused to the C-terminal of GFP. All chimeras included sequential deletions of cytoplasmic domain, transmembrane domain and luminal domain, mutation of KKLIE motif to SSLIE, and mutation of FFKAK motif to AAKAK. Using BACE1-myc and GFP-TMP21 cotransfected cells as positive control. All of these GFP-TMP21 constructs were cotransfected with BACE1-myc, the lysate was immunoprecipitated with anti-myc antibody 9E10 and analyzed by immunoblot using anti-GFP antibody. Here we summarized the results and labeled as “V” or “X”, it meant that all of these constructs interacted with BACE1-myc except the GFP-CT. The multiple TMP21 binding sites in BACE1 can be detected by immunoprecipitated the TMP21-LD with different BACE1 fragments, correspondingly. Detailed results see Figure 4.2.

Chapter 4: TMP21 Affects APP and BACE1 Trafficking

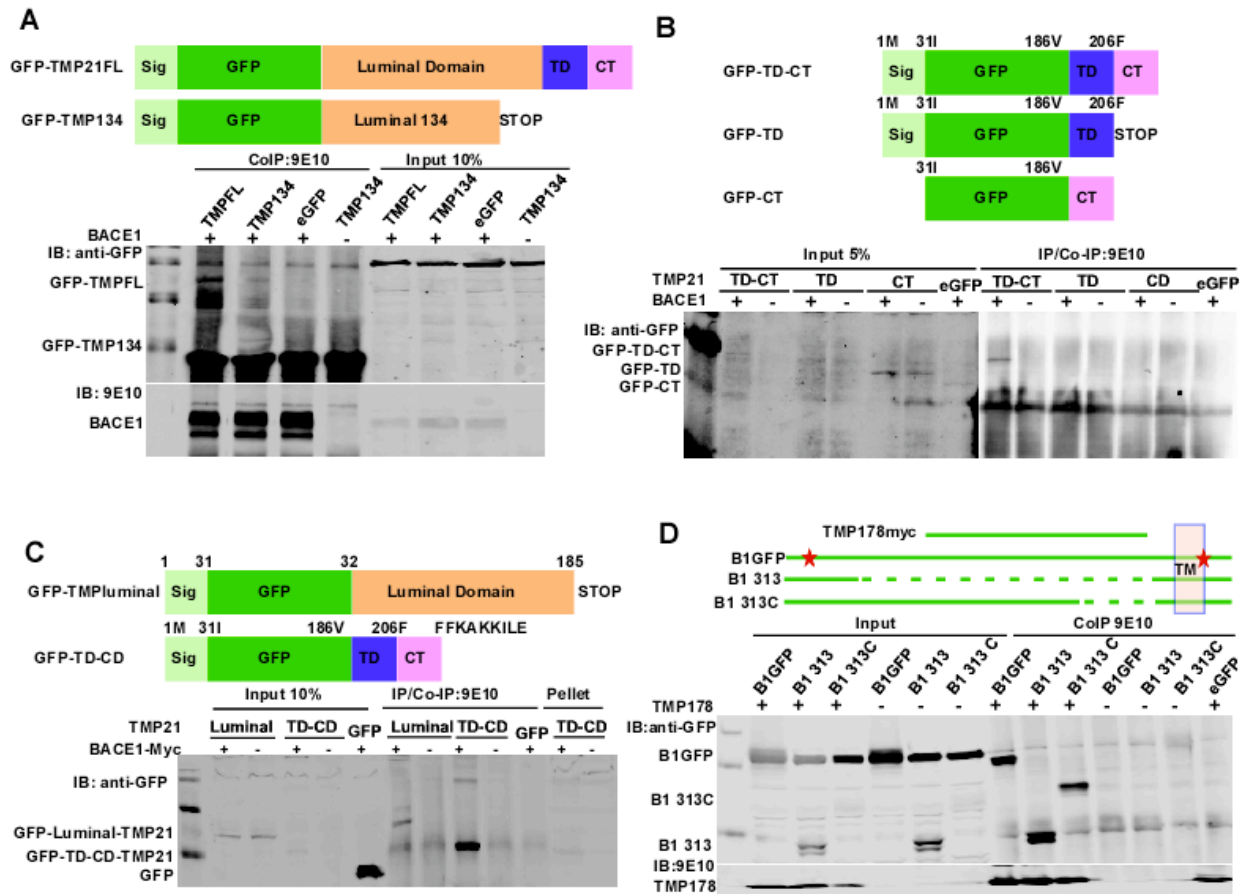


Figure 4.2 Multiple binding sites between TMP21 and BACE1.

(A) GFP-TMPFL and GFP-TMP134 were cotransfected with BACE1myc into HEK cells, respectively; (B) GFP-TMP TD-CT, GFP-TMP TD and GFP-TMP CT were cotransfected with BACE1myc into HEK cells, respectively; (C) GFP-TMP luminal and GFP-TMP TD-CT were cotransfected with BACE1myc into HEK cells, respectively. The GFP-TMP21FL/BACE1myc cotransfection was considered as positive control, the TMP21/pcDNA4 and BACE1myc/eGFP cotransfections were negative controls. The interaction between different TMP21 constructs and BACE1 were detected by coimmunoprecipitated with anti-myc antibody 9E10 and analyzed by immunoblot using anti-GFP antibody. (D) BACE1-GFP, BACE1 313 and BACE1 313C were cotransfected with TMP178myc into HEK cells, respectively. The BACE1-GFP/pcDNA4, BACE1 313/pcDNA4 and BACE1-313C/pcDNA4 cotransfections were negative controls. The interaction between TMP178 and different BACE1 constructs were detected by coimmunoprecipitated with anti-myc antibody 9E10 and analyzed by immunoblot using anti-GFP antibody. The red stars represented the potential binding sites of TMP21 on BACE1.

4.3.2 The interaction between TMP21 and BACE1 accumulated the immature BACE1

We hypothesized that the conformations of TMP21 and BACE1 contribute to the BACE1/TMP21 interaction. To examine this issue, we tagged a large protein, GFP at the C-terminal of TMP21. Tagging GFP at the C-terminus of TMP21 almost abolished the interaction of BACE1 with TMP21, and we could not detect the strong TMP21 band in the BACE1 antibody-co-immunoprecipitated samples. Furthermore, when we analyzed the BACE1 maturation, we found that GFP-TMP, TMP21myc and no-tag TMP21, but not TMP21-GFP showed the strong interactions with BACE1, resulting in more immature BACE1. These evidence suggested that the GFP tagged at the C-terminal of TMP21 might significantly interference the conformation of TMP21, thus abolished the TMP21 and BACE1 interaction. Abolishing the TMP21/BACE1 interaction decreased the immature BACE1 accumulation (Figure 4.3). Additionally, there was no significant endogenous TMP21 that can be coimmunoprecipitated by BACE1 (Fig 4.3 B). It is possible that TMP21/BACE1 interaction is weak and/or transient under physical condition. Alternatively, it is possible that TMP21 did not directly interact with BACE1, as we observed in *in vitro* binding assay using bacterial recombinant TMP21 protein (Data was not shown here).

Chapter 4: TMP21 Affects APP and BACE1 Trafficking

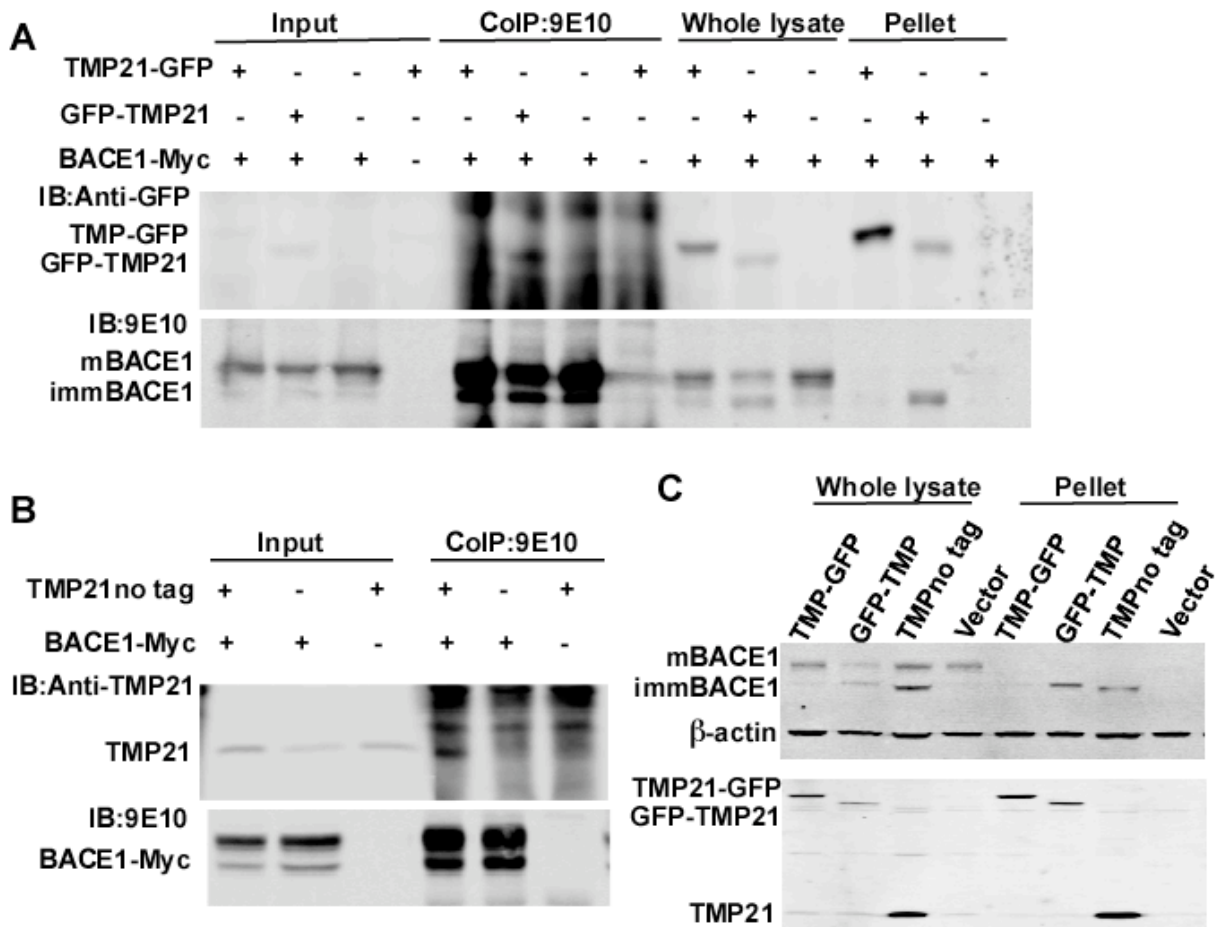


Figure 4.3 The interaction between TMP21 and BACE1 accumulated the immature BACE1.

(A) We tagged the GFP at the C-terminal of TMP21 named TMP21-GFP. The TMP21-GFP, GFP-TMP21 and eGFP control were cotransfected with BACE1-myc or pcDNA4 vector, respectively. The interaction of BACE1 and TMP21 can be accessed by coimmunoprecipitated with anti-myc antibody 9E10 and analyzed by immunoblot using anti-GFP antibody. Proteins in whole lysates and Triton X-100 resistant pellets from the same samples were loaded on the same 8% glycine gel. (B) BACE1-myc was cotransfected with no-tag TMP21 or vector control, lysate was immunoprecipitated with anti-myc antibody 9E10 and analyzed by immunoblot using TMP21 antibody T21 on 12% glycine gel. (C) BACE1-myc expressed cells were transfected with TMP-GFP, GFP-TMP, TMP no-tag and vector control, respectively. Then the whole lysate and Triton X-100 resistant pellets were collected and loaded on 8% glycine gel. The pattern of mature and immature BACE1 was detected by 9E10 antibody. The TMP21 was visualized by T21 antibody.

4.3.3 TMP21 delayed the ER export of immature BACE1 without affecting its ER degradation

We further investigated the maturation process of BACE1. We did pulse chase experiment by treating cells with the protein synthesis inhibitor---Cycloheximide (CHX) (Ennis & Lubin, 1964; Wettstein, Noll, & Penman, 1964). We harvested the cells and collected proteins at different time points, the results showed that almost all of the immature BACE1 disappeared within 1 hour. However, overexpression of TMP21 increased the immature BACE1 level and the immature BACE1 was detectable for more than 3 hours. This evidence suggested that the maturation of BACE1 was affected by TMP21 and it led to the accumulation of immature BACE1 (Fig 4.4 A). Furthermore, we asked how TMP21 increased immature BACE1 level. It is probably because of the TMP21 prevents the transport of immature BACE1. However, it is also possible that TMP21 also contributes to the degradation of immature BACE1. We then investigated whether TMP21 affect ER degradation of immature BACE1. After tagging the C-terminal of BACE1 with KCLK---the ER retrieval motif, most detectable BACE1 is immature form. The pro-peptide of BACE1 is cleaved after entering Golgi. HEK cells transfected BACE1kclk (BACE1-ER) with or without TMP21 were treated by CHX to inhibit proteins synthesis. Western blot analysis showed there is no significant difference between the BACE1-ER levels in the CHX treated cells with and without TMP21 co-expression (Fig 4.4 B), indicating the TMP21 did not affect the degradation of immature BACE1 in ER. What's more, we can detect a small portion of mature BACE1 in these BACE1-ER transfected cells because BACE1-ER can be posttranslationally modified when it cycles between ER and Golgi, and with the co-expression of TMP21 the mature BACE1 was significantly block, it provided further support that TMP21 delays the immature BACE1 exit from ER. As expected, we could also detect the interaction between BACE1-ER and TMP21 (Fig 4.4 C). The facts demonstrated that rather than affecting immature BACE1 ER degradation, TMP21 delayed the immature BACE1 exit from ER, resulting the delaying of BACE1 maturation processing and accumulation of immature BACE1.

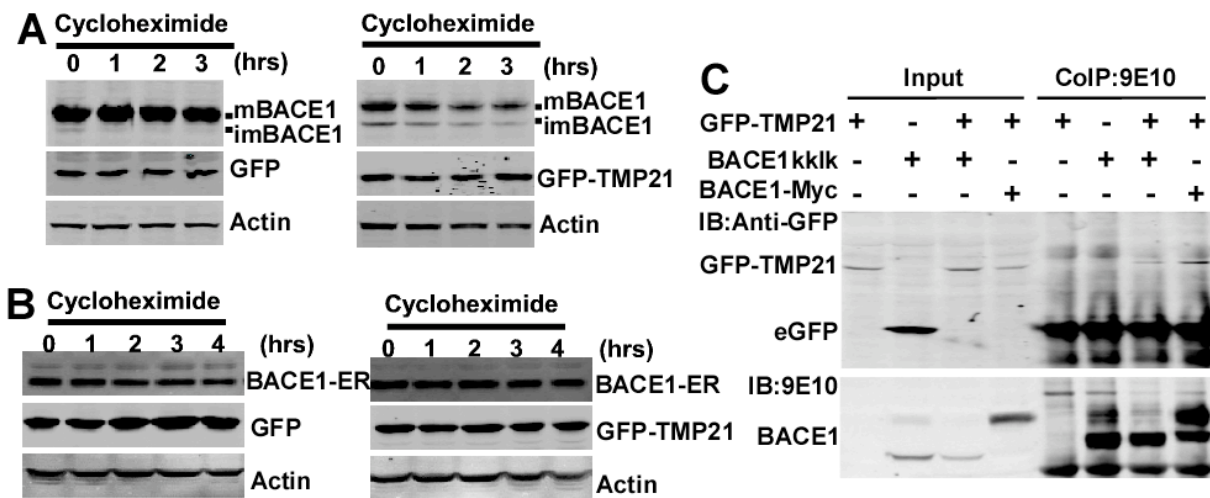


Figure 4.4 TMP21 delayed the ER export of immature BACE1 without affecting its ER degradation.

(A) Cells cotransfected with BACE1-myc plasmid and GFP-TMP21 or eGFP vector, then treated by the protein synthesis inhibitor, cycloheximide (CHX), chasing at different time points, we harvest the cells and equal amount of total proteins from each sample were loaded on the 8% glycine gel. The pattern of mature and immature BACE1 was detected by 9E10 antibody. The TMP21 and eGFP control were visualized by anti-GFP antibody. (B) HEK cells transfected BACE1-ER with or without TMP21 were treated by 100ug/ml CHX and collected at different time points, then the western blot analyzed the BACE1kklk by 9E10 and BACE1 pro-peptide antibody. The TMP21 and eGFP control were detected by anti-GFP antibody. (C). HEK cells were transfected with myc-tagged expression plasmid of BACE1-ER and GFP tagged-TMP21, eGFP or pcDNA4 vectors as negative controls. BACE1-myc and GFP-TMP21 cotransfected cells were positive control. Lysates were immunoprecipitated with anti-myc antibody 9E10 and analyzed by immunoblot using anti-GFP antibody. The GFP-TMP21 can be coimmunoprecipitated with BACE1-ER.

4.3.4 TMP21 contributed to BACE1 trafficking between ER and Golgi.

To further investigate that how the function of TMP21 in ER/Golgi transport contributes to BACE1 maturation, we constructed two mutant TMP21 plasmids. TMP21K/S plasmid has the mutation in its C-terminal KKLE motif to SSLE and this mutant TMP21 abolished its binding with COPI subunits which mediated the retrograde transport from Golgi to ER (Blum & Lepier, 2008; P. Cosson & Letourneur, 1994a; Sohn, et al., 1996a). TMP21F/A plasmid changed its C-terminal diphenylalanines motif mutant to AA, and this mutation interrupt the TMP21/Sec23 interaction that is essential for vesicles budding from ER (Barlowe, 1998; Dominguez, Dejgaard,

Chapter 4: TMP21 Affects APP and BACE1 Trafficking

Fullekrug, et al., 1998). When we cotransfected TMP21K/S or TMP21 F/A with BACE1, these two mutants TMP21 also interacted with BACE1. As expected, TMP21F/A, rather than TMP21K/S, led to a significant higher ratio of BACE1 immature/mature form, comparing to TMP21 wild type. A previous study indicates that the luminal domain of TMP21 contributed to its plasma membrane transport, while the transmembrane domain and cytoplasmic domain with KKLE motif are mainly responsible for the protein ER/Golgi transport (Blum & Lepier, 2008). We also constructed the GFP-tagged TMP21 transmembrane domain and cytoplasmic domain with wild type and mutant C-terminal, named TMPTDCD, TMPTDCDK/S, TMPTDCDF/A, respectively. Consistent with the previous results, we found that the TMP21TDCDF/A led to a higher ratio of BACE1 immature/mature form than TMP21 wild type. Taken together, our results showed that TMP21 interacted with immature form of BACE1 and prevented this immature BACE1 exiting from ER, which caused the accumulation of immature BACE1. Fig 4.5.

Chapter 4: TMP21 Affects APP and BACE1 Trafficking

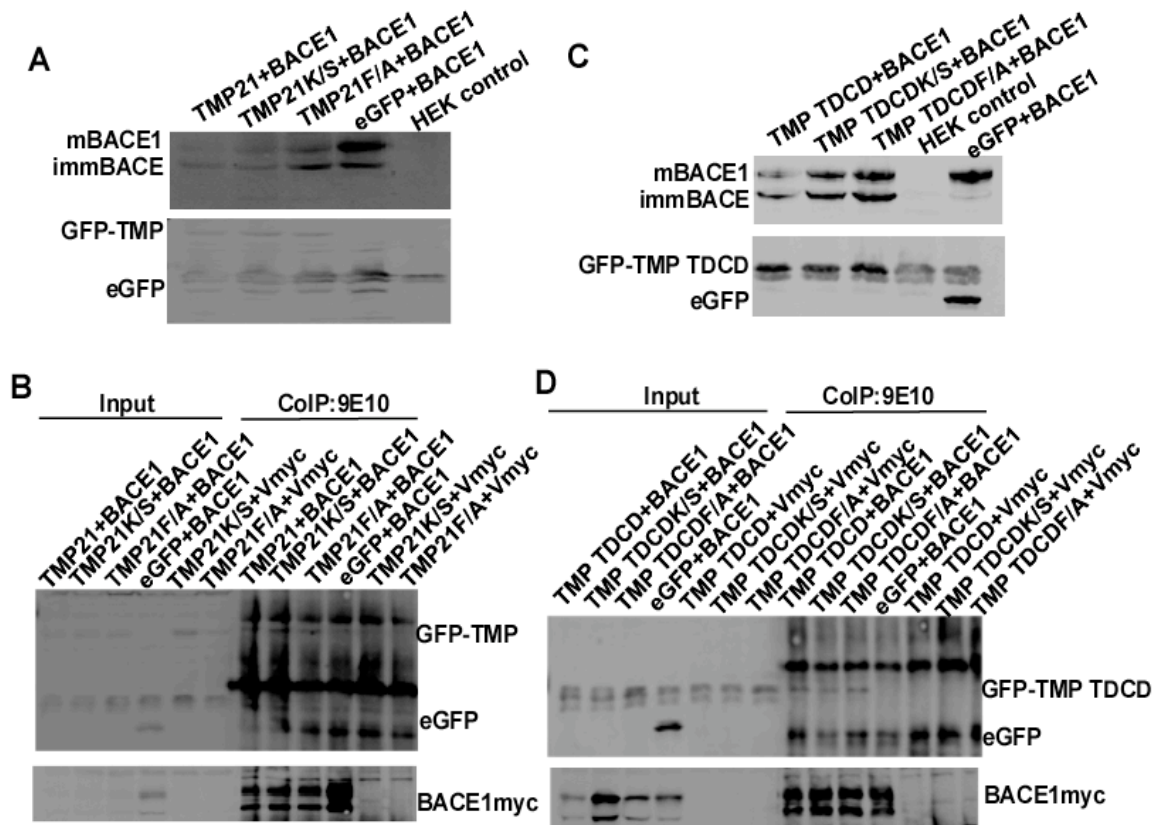


Figure 4.5 TMP21 contributed to BACE1 trafficking between ER and Golgi.

(A) Two mutant TMP21 plasmids, the one with mutation of its C-terminal KKLE motif to SSLE, named TMP21K/S and the other one with its C-terminal diphenylalanines motif mutant to AA, named TMP21F/A. These two plasmids were transfected into the HEK cells expressed BACE1, the TMP21 wild type was positive control, the eGFP vector and blank HEK cells were negative control. The pattern of mature and immature BACE1 was detected by 9E10 antibody. The TMP21 was visualized by anti-GFP. (B) TMP21 wild type, TMP21K/S and TMP21 F/A cotransfected with BACE1, eGFP and pcDNA4 were negative control. The interaction of BACE1 and TMP21 can be accessed by coimmunoprecipitated with anti-myc antibody 9E10 and analyzed by immunoblot using anti-GFP antibody. (C) GFP-tagged TMP21 transmembrane domain and cytoplasmic domain with wild type and mutant C-terminal plasmids, named TMPTDCD, TMPTDCDK/S, TMPTDCDF/A, respectively, were transfected into BACE1 expressed cells, the pattern of mature and immature BACE1 was detected by 9E10 antibody. The TMP21 was visualized by anti-GFP. (D) The interaction of BACE1 and TMP21-TDCD can be accessed by coimmunoprecipitated with anti-myc antibody 9E10 and analyzed by immunoblot using anti-GFP antibody.

4.3.5 P24a interacted with APP and BACE1

p24a, always forms hetero-oligomer with TMP21. The TMP21/p24a complex mediates the budding of COPI and COPII vesicles, and the protein ER/Golgi trafficking. It is possible that p24a might have the similar effect on trafficking of BACE1. As expected, p24a interacted with immature BACE1 and APP (Fig 4.6 B C). And both overexpression and knockdown of p24a, as TMP21, significantly increased the immature/mature BACE1 ratio (Fig 4.6 A). However, neither knockdown of p24a did not affect the interaction between TMP21 and BACE1, nor knockdown of TMP21 did not affect BACE1/p24a interaction (Fig 4.6 D). However, knockdown of p24a, caused 50% reduce of TMP21, also showed specifically increase of C99. It is possible that TMP21 and p24a might interact with BACE1 independently, but led to the same consequence; this evidence also suggested that TMP21 and p24a, probably TMP21/p24a heteromeric complex, played an essential role in APP and BACE1 trafficking, thus affected the BACE1 cleavage on APP.

Chapter 4: TMP21 Affects APP and BACE1 Trafficking

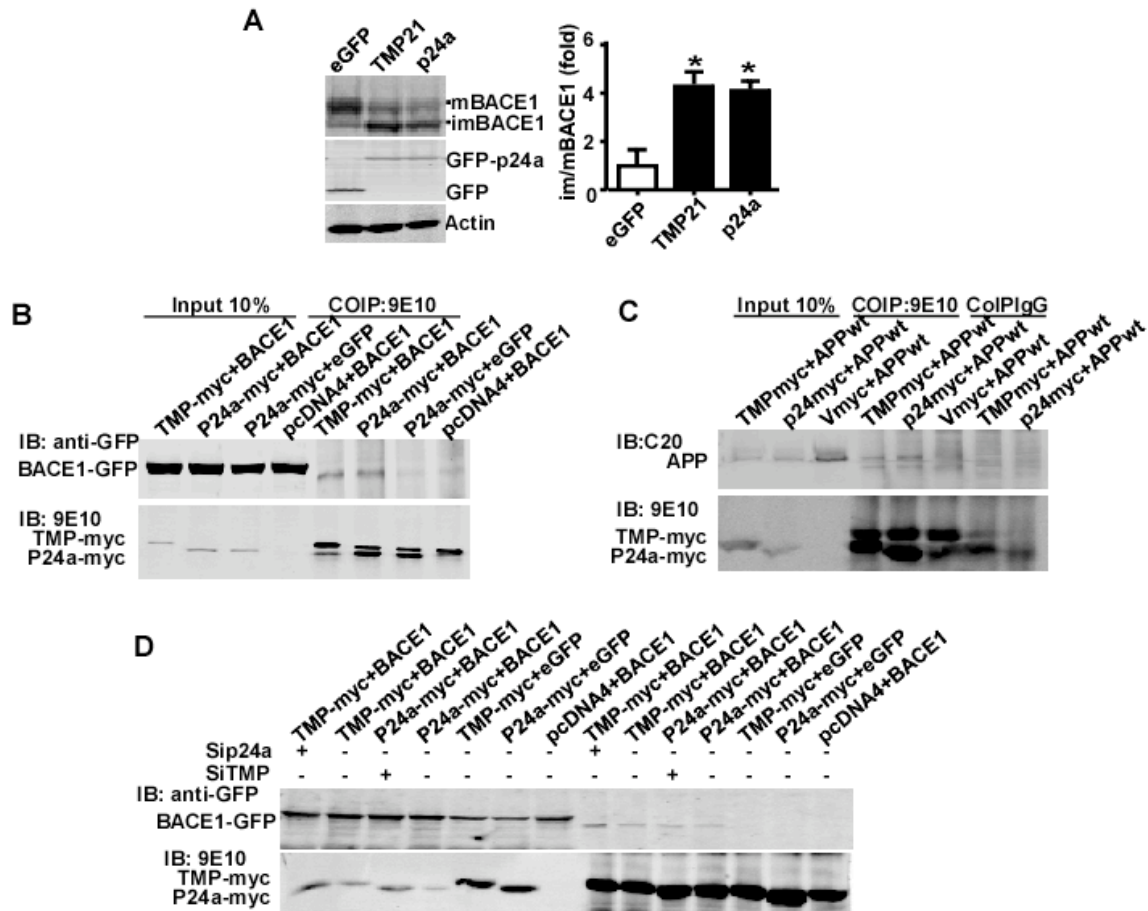


Figure 4.6 P24 interacted with APP and BACE1.

(A) GFP-p24a, GFP-TMP21 and eGFP control were transfected into HEK cells with BACE1-myc expression, the same amounts of total proteins were loaded on 8% glycine gel and the pattern of mature and immature of BACE1 was detected by 9E10 antibody. (A) p24a-myc and BACE1-GFP were cotransfected into HEK cells, the TMP21-myc/BACE1-GFP cotransfection was considered as positive control, the p24a-myc/eGFP and BACE1-GFP/pcDNA4 cotransfection were negative controls. The p24a/BACE1 interaction was detected by coimmunoprecipitated with anti-myc antibody 9E10 and analyzed by immunoblot using anti-GFP. (C) p24a-myc, TMP21-myc and pcDNA4 vector control were transfected into HEK cells with APPwt expression. The p24a/APP interaction was detected by coimmunoprecipitated with anti-myc antibody 9E10 and analyzed by immunoblot using anti-APP antibody C20. (D). The p24a/BACE1 coimmunoprecipitation experiment was performed with or without TMP21siRNA treatment; the TMP21/BACE1 coimmunoprecipitation experiment was performed with or without p24a siRNA treatment. Anti-myc antibody 9E10 was used in coimmunoprecipitation and anti-GFP antibody was used in immunoblotting.

4.3.6 TMP21 increased the co-residency of APP and BACE1

To investigate how this immature BACE1 contributes to APP processing, we first examined whether TMP21 affects the spatial coexistence of APP and BACE1. The distribution of APPwt and BACE1 in HTM cells and HEK cells was determined by immunocytochemistry. BACE1 was tagged by GFP at the C-terminal and APP was stained by C20 antibody. The results showed that overexpression TMP21 significantly increased the co-residency of APP and BACE1 (Fig .4.7. A.). Furthermore, we found that the interaction between APP and immature BACE1 (Fig .4.7. B), and the interaction between APP and TMP21 as well (Fig .4.7. C). More importantly, we found that the APP and immature BACE1 interaction can be enhanced by TMP21 (Fig .4.7. D). Here, we used inactive mutant BACE1D93A and BACE1D93/289A to abolish the BACE1 cleavage on APP (Bennett, et al., 2000), thus the amount of mutant BACE1 immunoprecipitated by APP could represent the actual amount of BACE1 that bind with APP. Our results showed that TMP21 increased spatial co-residency of APP and BACE1, specifically increased the immature BACE1 and APP interaction, which probably increased the chance that immature BACE1 cleavage on APP; therefore, TMP21 affected APP processing via increasing the cleavage of immature BACE1 on APP. It has known that the immature form of BACE1 cleaved APP at Asp-1 site, and produce C99 (Huse, et al., 2002; Vetrivel, et al., 2011). Here we observed that the subcellular localization of APP was altered in HTM cells, indicating that TMP21 also affected the trafficking of APP. This result is consistent with the previous published studies showing the effect of TMP21 on APP cell surface trafficking and maturation (Vetrivel, et al., 2007). Overall, our studies demonstrated that TMP21 facilitated APP amyloidogenic processing by affecting both APP and BACE1 trafficking. Overexpression of TMP21 delayed immature BACE1 ER export and enhanced the co-residency of APP/BACE1, as a result, there were more APP being cleaved by immature BACE1 at Asp-1 site to generate C99.

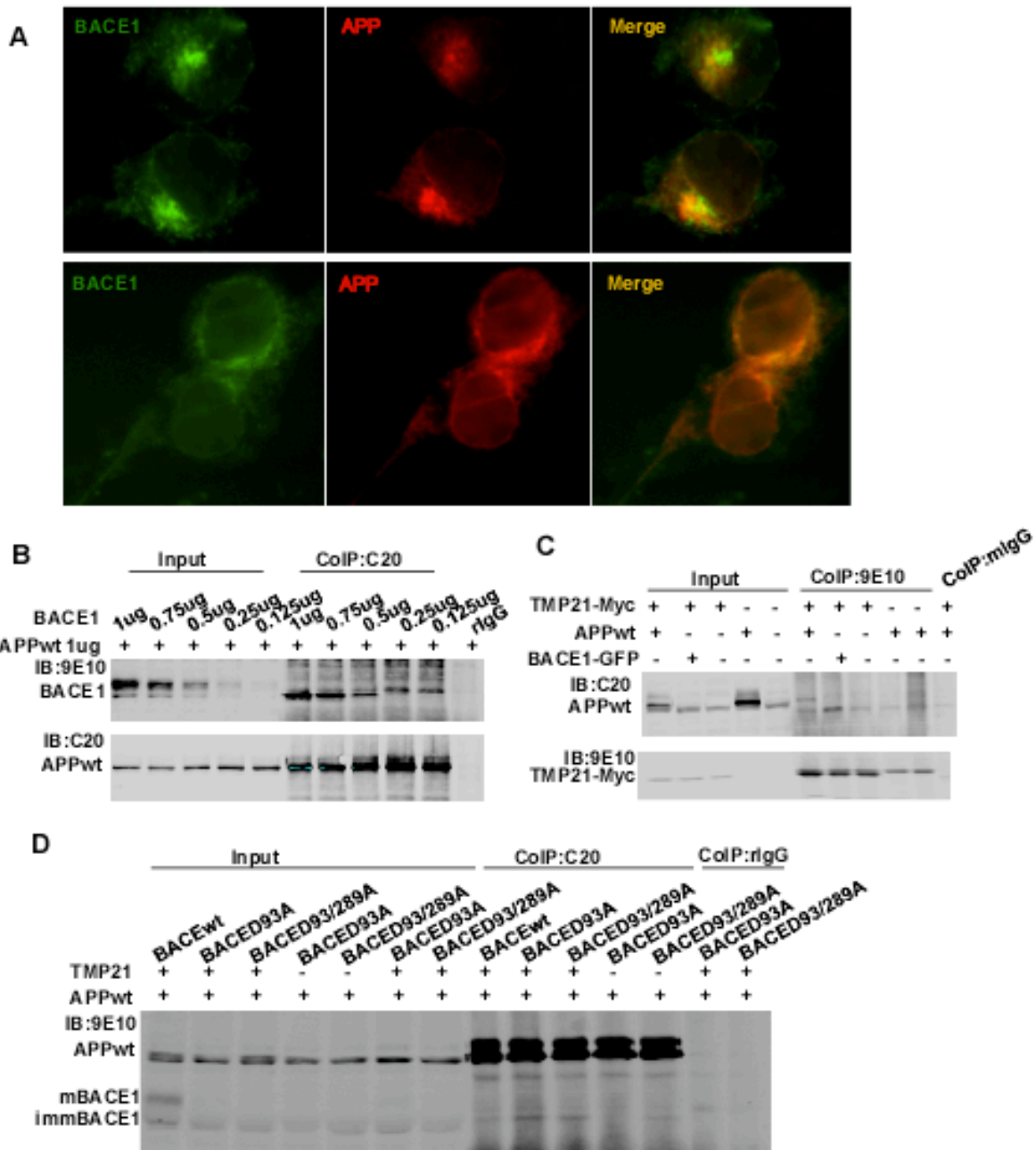


Figure 4.7 TMP21 enhanced the co-residency of APP/BACE1 and the interaction APP/immature BACE1.

(A) APPwt and BACE1-GFP were cotransfected in the TMP21 stable cells HTM and HEK cells, then APP was stained by immunocytochemistry using C20 antibody and then anti-rabbit Alexa Fluor 568 (red). Green and red fluorescents were imaged with a 100x oil objective lens on a Carl Zeiss Axiovert-200 epi fluorescent microscope.

Chapter 4: TMP21 Affects APP and BACE1 Trafficking

Images were merged using ImagJ 10.2. (B) Different amount of BACE1myc plasmids were transfected into APPwt expressed cells, the APP/BACE1 interaction was detected by coimmunoprecipitated with anti-APP antibody C20 and analyzed by immunoblot using anti-myc antibody 9E10. (C) TMP-myc and APPwt were cotransfected into HEK cells, the TMP21-myc/BACE1-GFP cotransfection was considered as positive control, the TMP21/pcDNA4 and APPwt/pcDNA4 cotransfection were negative controls. The APP/TMP21 interaction was detected by coimmunoprecipitated with anti-myc antibody 9E10 and analyzed by immunoblot using anti-APP antibody C20. Lysate coimmunoprecipitated with mouse normal IgG was negative control. (D) BACE1myc wild type, BACE1myc D93A mutant, BACE1myc D93/289A with or without TMP21 were transfected into the APPwt expressed cells. The APP/BACE1 interaction was detected by coimmunoprecipitated with anti-APP antibody C20 and analyzed by immunoblot using anti-myc antibody 9E10. Lysate coimmunoprecipitated with rabbit normal IgG was negative control.

4.3.7 TMP21 guided both the immature BACE1 and APP in detergent-resistant structures

Sequence analysis showed that BACE1 was not a GPI-anchored protein and the immature BACE1 was soluble (Tun, et al., 2002). Interestingly, we found that a significant amount of TMP21 existed in TritonX-100-insoluble pellet (Figure 4.8). Moreover, only the immature BACE1 was present in this pellet when cotransfected with TMP21. In the soluble part of BACE1, which can be detected in lysis, the ratio of immature to mature BACE1 showed no significant change between the TMP21 cotransfected cells and eGFP cotransfected cells (Figure 4.7 A). When the TMP21/BACE1 interaction was disrupted by TMP21-GFP, there was no immature BACE1 can be detected in the pellet (Fig. 4.3 C). These results indicated that TMP21 might cluster the immature form of BACE1 in the membrane structures that are insoluble in Triton X-100, probably lipid raft-like structures. Since the TMP21 enhanced interaction between APP and immature BACE1 and increased their co-localization, we further investigated that whether TMP21 also affected APP solubility. We found that when cotransfected with TMP21, both the APP and immature form of BACE1 were detected in the detergent resistant membrane structures. The soluble protein marker calnexin did not show in the pellet while the lipid raft marker flotillin2 mainly presented in pellet (Fig 4.8 B). Previously published papers showed that the lipid raft provided platform for APP and BACE1 interaction and preferentially generated

Chapter 4: TMP21 Affects APP and BACE1 Trafficking

C99(Cordy, et al., 2003; Vetrivel, et al., 2011). To investigate whether the pellet are enriched lipid raft-like structure and TMP21 enhances the APP/BACE1 interaction in lipid raft, to prove this hypothesis, we used 1% TritonX-100, and 0.5% Lubrol WX, respectively, to isolate the lipid raft from APP/BACE1 cotransfected HTM cells and HEK cells (Vetrivel, et al., 2004). However, we did not detect the significantly difference of APP/BACE1 distribution in lipid raft fractions, in which showed more flotillin2 while less calnexin (Fig. 4.9). It is possible that lipid rafts are highly dynamic entities and the interaction between APP and BACE1 in lipid raft is transient so that cannot be easily detected. More sensitive or efficiency methods for lipid raft isolation are required to be explored for the next step. Meanwhile, we used BACE1-GFP transfected HEK cells and HTM cells to do the immunostaining and using flotillin 2 to show the lipid raft structures. Here we observed that the co-localization of BACE1-GFP and flotillin 2 is increased in HTM cells 1.00 ± 0.03 vs. 1.97 ± 0.18 (Fig 4.8. C). Here our study showed that the TMP21 might cluster both APP and immature form of BACE1 in the lipid raft-like structures, and it might be one of the mechanisms that TMP21 affected BACE1 cleavage on APP and preferentially generated more C99.

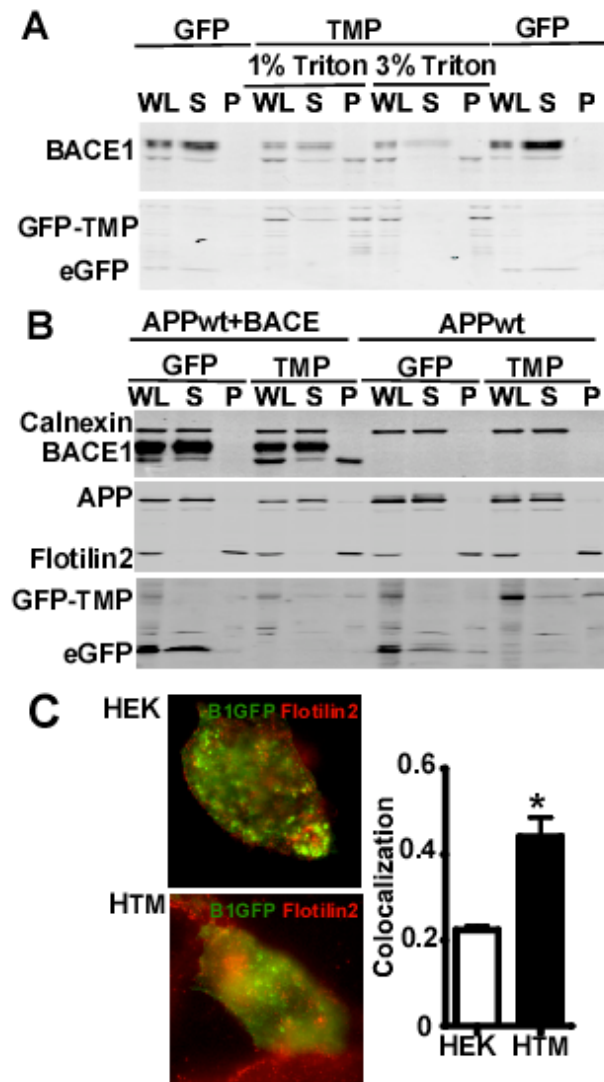


Figure 4.8 TMP21 guided both the immature BACE1 and APP in detergent-resistant structures.

(A) BACE1-myc expressed cells, (B) BACE1-myc/APP coexpressed cells and APP expressed cells were transfected with eGFP and TMP-GFP. Cells were lysed in 1% or 3% Triton X-100 lysis buffer; the insoluble pellet was isolated by centrifugation. The 10% proteins from whole lysate (WL), 5% soluble proteins (S) and 10% proteins from pellet (P) were collected and loaded on 8% glycine gel. The pattern of mature and immature of BACE1 was detected by 9E10 antibody. The soluble proteins marker, calnexin only showed in WL and S fractions and the lipid raft associated protein flotillin2 only presented in WL and P fractions. (C) HEK and HTM cells were transfected by BACE1-GFP and were fixed 24 hours after transfection. Then the flotillin2 was stained by immunocytochemistry using anti-flotillin2 antibody and then anti-rabbit Alexa Fluor 568 (red). Green and red fluorescents were captured

Chapter 4: TMP21 Affects APP and BACE1 Trafficking

by a 100x oil objective lens on a Carl Zeiss Axiovert-200 epi fluorescent microscope. Images were merged and the co-localization areas were analyzed using ImagJ 10.2.

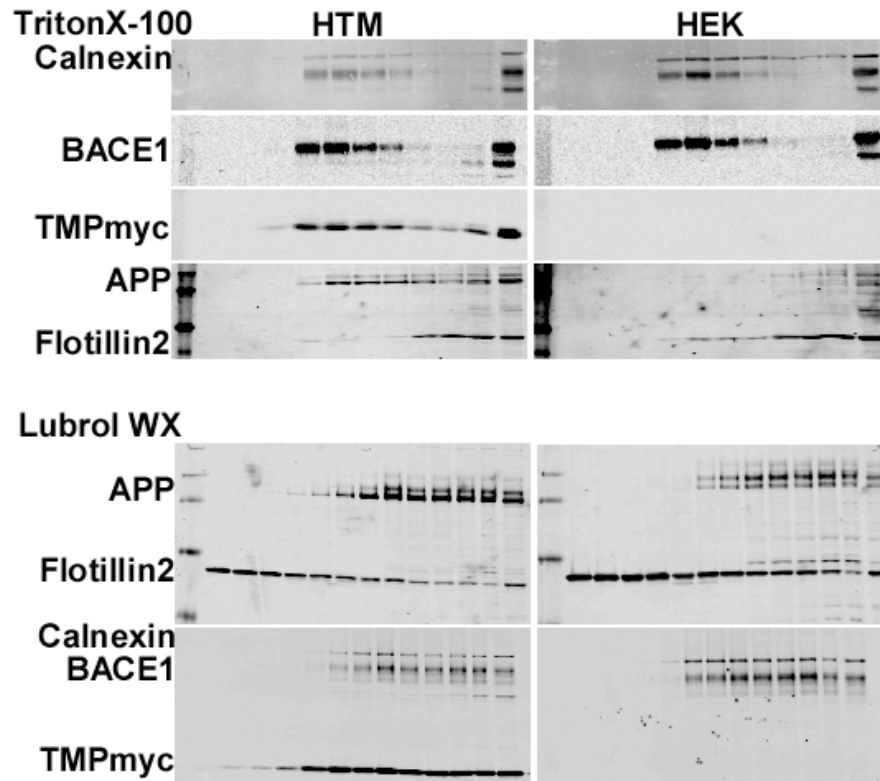


Figure 4.9 Lipid raft isolation of HEK and HTM cells with coexpression of APP and BACE1.

(A) Expression plasmid of APPwt and BACE1 were cotransfected into the HEK and HTM cells. After 48 hours, cells were washed in PBS and scraped into 0.5 ml of lysis buffer containing different detergents: (A) 1% Triton X-100 (Sigma) in 25mM Tris-HCl (pH 8) and 140mM NaCl or (B) 0.5% Lubrol WX (Lubrol 17A17; Serva) in 25mM Tris-HCl (pH 7.4), 150mM NaCl, and 5mMEDTA. All the lysis buffers were supplemented with a protease inhibitor mixture (Roche). Cells were homogenized by five passages through a 25-gauge needle. The lysates were adjusted to 45% final concentration of sucrose and transferred to the ultracentrifuge tube. A discontinuous sucrose gradient is then formed by sequentially layering 35% sucrose and 5% sucrose, and the tubes were subject to ultracentrifugation at 39,000 rpm for 19 h in Beckman MLS50 rotor at 4 °C. Twelve to sixteen fractions were collected from the top of the gradient and equal volume of each fraction was analyzed by Western blotting. APP was detected by C20 antibody, BACE1 was detected by 9E10 antibody, antibody against the lipid raft associated protein flotillin2 was used to indicate the lipid rafts fraction and calnexin the indicated soluble proteins.

4.3.8 TMP21 didn't affect the trafficking of C99.

Previous studies suggested that C99 can be further transport out of ER and cleaved by BACE1 on its Glu-11 site in TGN to produce C89 (K. Liu, et al., 2002). To exclude the possibility that TMP21 prevents the further cleavage of C99 into C89, the coimmunoprecipitation was performed. The results showed the very weak interaction between C99 and TMP21 (Fig 4.10). However, when we cotransfected APP and BACE1 into HEK cells and treated with γ -secretase inhibitor (GSI), compared to those non-treated cells, we found that the C89 was significantly accumulated by more than 10 folds accumulated while C99 did not show significant change. It suggested that most of the C99 could be cleaved into C89. The same phenomenon was observed in TMP21 overexpression cells. Most of the C99 was further processed into C89, and C89 was significantly accumulated after treatment of γ -secretase inhibitor (Fig 4.10 A). Additionally, when we cotransfected C99 and BACE1 into HTM and HEK cells, after the treatment of γ -secretase inhibitor, the C89 was detected, and the same amount of C99 was cleaved into C89 in both HTM and HEK cells (Fig 4.10 B). The above evidence suggested that C99 can be further cleaved by BACE1 in both HEK and HTM cells, and the overexpression of TMP21 did not affect the trafficking of C99 from ER to TGN.

Chapter 4: TMP21 Affects APP and BACE1 Trafficking

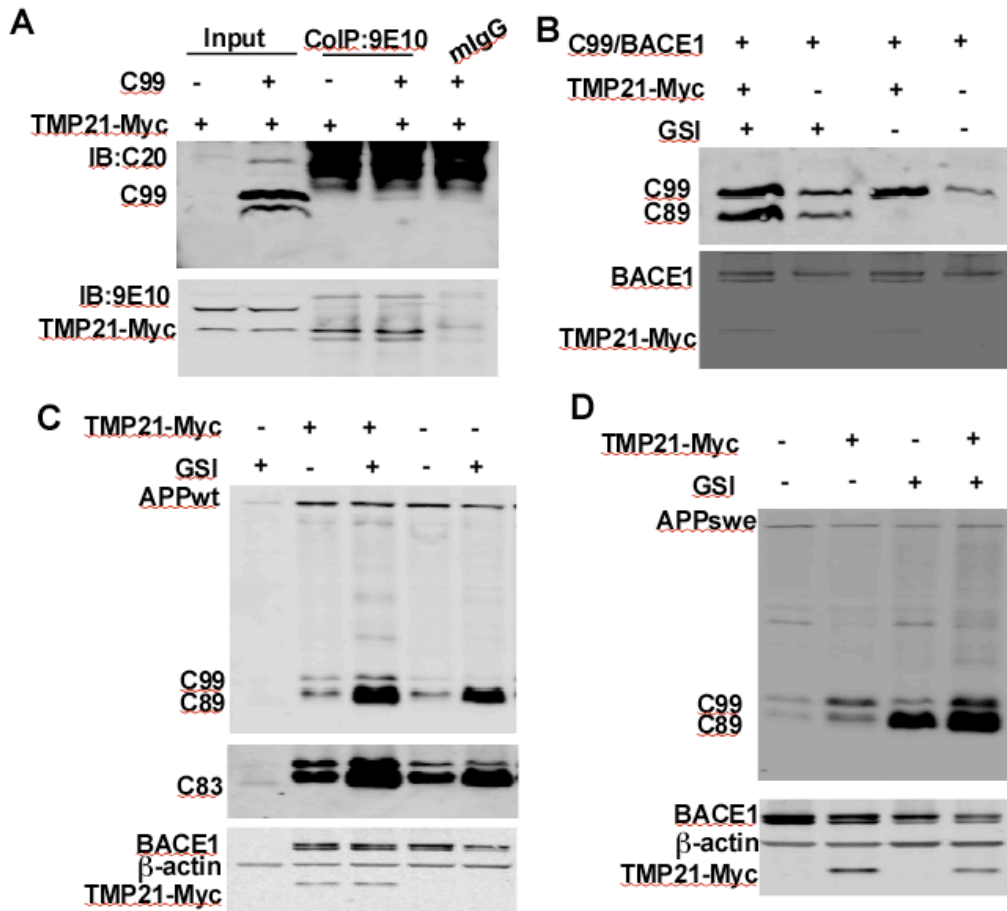


Figure 4.10 TMP21 did not affect the trafficking of C99.

(A) pAPP-C99 plasmid and vector control were transfected into TMP21-myc overexpressed HTM cells. The C99/TMP21 interaction was detected by coimmunoprecipitated with anti-myc antibody 9E10 and analyzed by immunoblot using anti-APP antibody C20, using 16% Tris-Tricine gel. Coimmunoprecipitated with mouse normal IgG was negative control. (B) pAPP-C99 plasmid and BACE1 was transfected into HEK or HTM cells with or without γ -secretase inhibitor (GSI). The equal amounts of total proteins were loaded on 16% Tris-Tricine gel and the pattern of C99 and C89 was detected by C20 antibody. (C, D) We cotransfected APPwt or APPswe and BACE1 into HTM and HEK cells then treated with or without γ -secretase inhibitor, the same amounts of total proteins were loaded on 16% Tris-Tricine gel and the pattern of C99 and C89 was detected by C20 antibody.

4.4 Discussion

BACE1 is the β -secretase *in vivo*. Knockout of BACE1 abolishes the generation of CTF β and A β (H. Cai, et al., 2001), and rescue the memory deficit in mice (H. Cai, et al., 2001; Ohno, et al., 2004; Roberds, et al., 2001). Interestingly, BACE1 knockout mice are developmentally normal and show no discernable phenotype compared with wild type mice (Y. Luo, et al., 2001). These studies suggest that BACE1 inhibition could be an attractive therapeutic strategy that may be free of mechanism-based toxicity. Cleavage of APP by BACE1 at either Asp-1 or Glu-11 site is strongly dependent on BACE1 maturation and subcellular trafficking, especially trafficking between ER/Golgi and lipid rafts translocation (Cordy, et al., 2003; Huse, et al., 2002; Vetrivel, et al., 2011). However, very few studies have investigated the molecular mechanisms of BACE1 trafficking between ER and Golgi. Here, we showed that TMP21 interacts with immature BACE1 and facilitates its ER export and further maturation. However, TMP21-mediated BACE1 ER/Golgi transport might be quick and transient, as the majority BACE1 exits as its mature form and the interaction between endogenous TMP21 and immature BACE1 cannot be easily detected. However, when TMP21 overexpressed, the TMP21 clusters in the ER and expands the ER membrane, where the significant interaction between TMP21 and immature BACE1 occur, resulting in accumulation of the immature BACE1.

Chapter 4: TMP21 Affects APP and BACE1 Trafficking

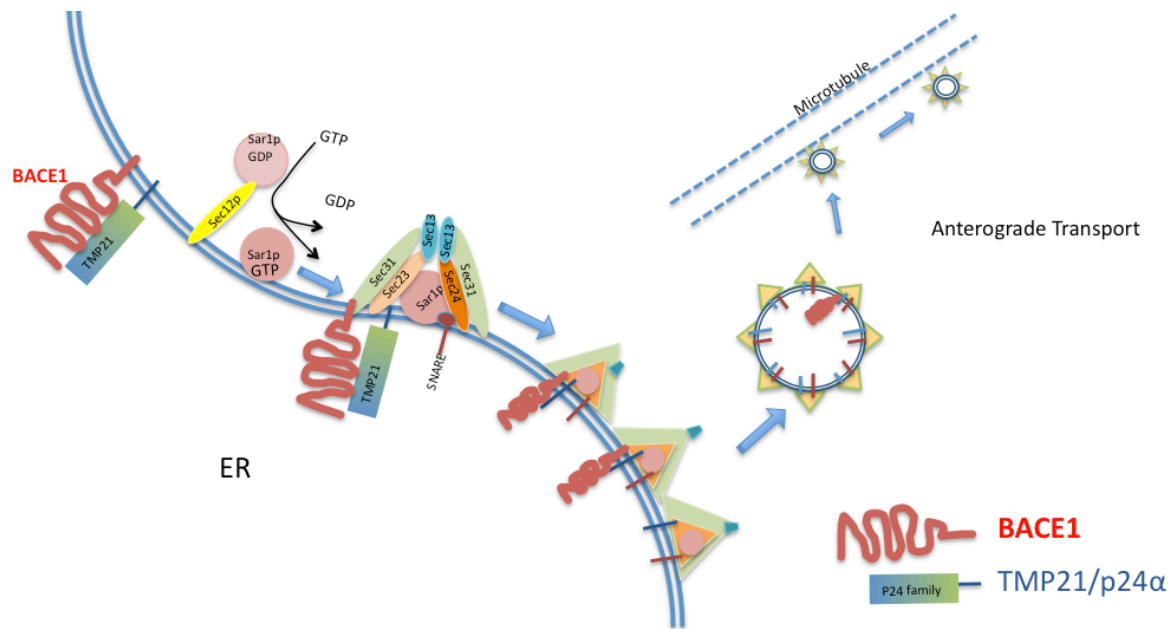


Figure 4.11 Suggested model for the essential role of TMP21 in BACE1 trafficking and maturation-----

TMP21/BACE1 interaction might be the initial step.

The TMP21/BACE1 Interaction might be the initial step that TMP21 delays the BACE1 maturation. The conformation of TMP21 or BACE1 is essential for their interaction. This process also requires lots of other trafficking proteins, such as p24a, other than TMP21 alone. When both TMP21 and p24a express at endogenous level, BACE1 ER/Golgi transport might be quick and transient, as the majority BACE1 exits as its mature form. Knockdown of TMP21 or p24a lead to the accumulation of immature BACE1 because lacking of receptor. However, when TMP21 overexpressed, the TMP21 clusters in the ER and expands the ER membrane; at the same time, the significant interaction between TMP21 and immature BACE1 appears; this interaction clusters immature BACE1 and delays the immature BACE1 exits out of ER.

TMP21 prevents immature BACE1 exits out of early biosynthetic compartment, thereby increasing its residence time for encountering APP. Our results also find that TMP21 enhances the APP/immature BACE1 interaction and the co-residency of APP and BACE1. The co-residency of APP and immature BACE1 occurs in lipid rafts-like structures. The lipid raft is known to contribute to the APP amyloidogenic pathway (Ehehalt, et al., 2003; Tun, et al., 2002; Vetrivel, et al., 2011; Yoon, et al., 2007). Additional GPI localized BACE1 in lipid raft and up-regulated β -site cleavage on APP and produced more C99 and intact A β (Cordy, et al., 2003;

Chapter 4: TMP21 Affects APP and BACE1 Trafficking

Vetrivel, et al., 2011). The early lipid-raft-like structures can be observed in the ER (Browman, et al., 2006; Sevlever, et al., 1999) and the active γ -secretase complex, are located predominantly in a specialized subcompartment called ER-MAM, which is the extended ER compartment that is physically and biochemically connected to mitochondria, and it is an intracellular lipid raft-like structure (Estela Area-Gomez, et al., 2009). It suggests that the early form of lipid raft in ER could also contribute to the APP amyloidogenic pathway.

Sequence analysis shows that BACE1 is not GPI anchored. However, the localization of BACE1 in lipid rafts depends on the palmitoylation on its three cysteine residues (Benjannet, et al., 2001). It has been suggested that BACE1 is stabilized and regulated in lipid raft via its association with unknown GPI-anchored proteins (Hattori, et al., 2006; Marlow, Cain, Pappolla, & Sambamurti, 2003; Tun, et al., 2002). TMP21 interacts with the newly synthesized GPI-anchored proteins and guides them into lipid raft in the ER, resulting in facilitating ER export of these GPI-anchored proteins (Bonnon, Wendeler, Paccaud, & Hauri). As TMP21 acts as a cargo receptor for GPI-anchored proteins, it might also accumulate these proteins together. It is possible that all of these GPI-anchored proteins/TMP21/BACE1 are guided into this premature lipid raft-like structure. Indeed, in our study, when TMP21 and BACE1 cotransfected, some immature form of BACE1 and APP became insoluble at 4°C in the non-ionic detergent Triton X-100, and so does lipid raft (Brown & London, 2000; London & Brown, 2000). It is possible that when newly synthesized BACE1 trafficking from ER to Golgi, the immature form of BACE1 interacts with TMP21 and is guided into lipid raft-like domains in ER or ERGIC, at the same time, the interaction between TMP21 and APP also trapped APP into lipid raft-like domains when APP traffic through ER and ERGIC. Such effect leads to the increased the interaction between immature BACE1 and APP, and the co-residency of APP and BACE1 in lipid raft-like structures, resulting in preferentially cleavage of APP at its Asp-1 site and more generation of C99 level and A β .

Chapter 4: TMP21 Affects APP and BACE1 Trafficking

The increase of C99 in TMP21 overexpressing cells could be due to the stronger C99 generation by BACE1, or weaker γ -cleavage of C99, or both. Here, we found that the C99 level was significantly higher in HTM cells than HEK cells (Fig 3.1), the same result was observed in HTM and HEK cells after GSI treatment (Fig. 4.10). These results implicate that C99 elevation in TMP21 overexpressing cells is not because of a weaker γ -cleavage but very likely due to stronger β -cleavage, and TMP21 overexpression potentiates the γ -cleavage of C99. Additionally, we observed that the C99 could be further cleaved into C89 in both HTM and HEK cells, indicating the further trafficking of C99 is not affected by overexpression of TMP21.

4.5 Conclusion

In this chapter, we found that the TMP21/immBACE1 interaction delayed the maturation of BACE1 and the conformation of TMP21 was important for this TMP21/BACE1 interaction; TMP21 delayed the maturation of BACE1 by affecting its ER/Golgi trafficking but not the ER degradation of immature BACE1. Prevention of immature BACE1 exiting out of early biosynthetic compartment increases its interaction and co-residency with APP. Furthermore, TMP21 guides both the immature BACE1 and APP into lipid raft-like structures. Our studies demonstrate that TMP21 affects BACE1 trafficking and maturation. The study provides further evidence that TMP21 facilitates APP amyloidogenic process. It is the first time the BACE1 ER/Golgi trafficking has been revealed. Interrupting TMP21/BACE1 interaction and facilitating immature BACE1 ER export will be new therapeutic targets for future research.

Chapter 5: Conclusion and Future Directions

5.1 Overall conclusions

Although concerns arise in many aspects, the A β hypothesis offers a board framework to explain AD pathogenesis. Shifting the APP processing away from amyloidogenic pathway remains a rational therapeutic target for AD. Knockdown of TMP21 selectively enhances A β generation without affecting Notch cleavage, indicating the upregulated TMP21 might be a protector. However, the precise role of TMP21 in AD pathogenesis is still unknown. The overall goal of this thesis is to examine in detail the roles of TMP21 in AD pathogenesis. The first, we examine the genetic linkage between *Tmp21* and AD and identify a novel AD-associated SNP. We find that this SNP significantly increases TMP21 expression at both mRNA and protein level by potentiating the splicing efficiency. This discovery suggested the upregulated TMP21 might contribute to AD pathogenesis. Then we observe the enhanced APP amyloidogenic processing and specifically increased C99 generation by attenuating TMP21 expression in cell model. Also the deficit TMP21 facilitates APP amyloidogenic processing via preferentially increases C99 generation both in cells model and in AD mice model. These facts supported that the TMP21 plays important role in APP amyloidogenic processing and the dysregulation TMP21 facilitates C99 production and A β generation. C99 is generated by BACE1 cleaving APP at Asp-1 site. Our data also indicates the impact of TMP21 on BACE1 cleavage at APP Asp-1 site. The preferential cleavage of BACE1 depends on the subcellular trafficking and localization of BACE1. Targeting BACE1 into ER or lipid rafts specifically enhances its cleavage at APP Asp-1 site. Further, we find the interaction between TMP21 and immature BACE1 and the accumulation of immature BACE1 upon TMP21 dysregulation, suggesting the role of TMP21 on BACE1 maturation and trafficking. Finally, we investigate the mechanism through which TMP21 affects BACE1 trafficking and maturation. We find the multiple binding sites between TMP21/BACE1 and the conformation of TMP21 is essential for the TMP21/BACE1 interaction. The TMP21/BACE1 interaction contributes to the immature BACE1 accumulation by delaying immature BACE1 ER export. Furthermore, TMP21 enhances the interaction and co-residency of APP and BACE1,

Chapter 5: Conclusion and Future Directions

which might occur in lipid raft-like membrane structures. Taken together, these studies demonstrate that TMP21 facilitates APP amyloidogenic process and preferentially enhances the production of C99 by affecting maturation and trafficking of BACE1. Interrupting TMP21/BACE1 interaction and facilitating immature BACE1 ER export could be novel therapeutic targets for AD.

5.1.1 Chapter 2: A novel AD-associated SNP in *Tmp21* increases TMP21 expression by potentiating the splicing efficiency

In chapter 2, we first identify that rs12435391 (IVS4-28T>C) located in intron 4 of *Tmp21* is an AD-associated SNP by screening 261 AD patients and 236 controls. A novel cloning strategy is used to investigate the role of this AD-associated SNP in TMP21 pre-mRNA processing and mRNA protein expression *in vitro*. Although rs12435391 (IVS4-28T>C) does not affect the splicing site recognition, it significantly increases TMP21 expression at both mRNA and protein levels. Furthermore, we find that this SNP significantly increases the splicing efficiency of *Tmp21* pre-mRNA, leading to the elevation of mature mRNA. However, the stability of *Tmp21* pre-mRNA and transcription activity of *Tmp21* is not affected. Taken together, our study identifies an AD-associated *Tmp21* SNP and indicates that the upregulation of TMP21 may contribute to AD pathogenesis.

5.1.2 Chapter 3: The dysregulated TMP21 facilitates APP amyloidogenic processing

In chapter 3, we further examine whether the dysregulation of TMP21 expression levels contributes to AD pathogenesis. We discover that the dysregulation of TMP21 facilitates APP amyloidogenic processing. Overexpression of TMP21 shifts APP process from the α -cleavage to β -cleavage. Disruption of TMP21 generates more C99 and increases A β level in AD mice model. These results suggest that the proper expression level of TMP21 is essential in APP processing. Moreover, rather than altering overall CTFs levels, the dysregulated TMP21 preferentially increases C99. It indicates that the BACE1, rather than γ -secretase, may be the major player. Here, our study suggests the impact of TMP21 on BACE1 and its preferential cleavage at Asp-1

Chapter 5: Conclusion and Future Directions

site of APP. We discover the interaction between TMP21 and immature BACE1 and the alteration of BACE1 transport. Also the immature BACE1 accumulates upon TMP21 dysregulation suggests the potential role of TMP21 on BACE1 maturation and trafficking. Overall, our study shows that dysregulation of TMP21 facilitates APP amyloidogenic processing by preferentially increasing C99 generation, indicating the impact of TMP21 on BACE1; further evidence suggests that the TMP21 might affect BACE1 maturation and trafficking.

5.1.3 Chapter 4: TMP21 affects BACE1 maturation and trafficking

Finally, we illustrate the mechanism through which the TMP21 affects BACE1 trafficking and maturation. We find the multiple binding sites between TMP21/BACE1 and the conformation of TMP21 is essential for the TMP21/BACE1 interaction. The TMP21/BACE1 interaction contributes to the immature BACE1 accumulation. TMP21 delays the maturation and increased immature BACE1 level by affecting its ER/Golgi trafficking. Moreover, TMP21 increases the co-residency of APP and BACE1 which might enhance the chance of APP encountering and being cleaved by immature BACE1. Interestingly, we find that TMP21 guides both the APP and immature BACE1 into lipid rafts-like structure, which might provide platform for APP/immature BACE1 interaction. To sum up, our studies show that TMP21 delays maturation process and trafficking of BACE1 and APP, as a result, APP is more accessible for immature BACE1 and preferentially cleaved at Asp-1 site to generate more C99.

5.2 Significance and novelty of the research

This thesis presents several novel findings on genetic and bimolecular mechanisms of AD pathogenesis. These findings could significantly advance the understanding of genetic polymorphism associated to AD risk, and greatly emphasize the importance of subcellular trafficking and maturation of BACE1 in APP processing. It also provides evidence to further explore the therapeutic target on TMP21.

1. The first study on the genetic linkage between *Tmp21* SNPs and AD pathogenesis and identification of the novel SNP in *Tmp21* in AD patients.

Chapter 5: Conclusion and Future Directions

2. Investigate the role of intronic SNP on pre-mRNA processing, mRNA and protein expression *in vitro*.
3. Evidence that dysregulation of TMP21 expression, both upregulation and downregulation, facilitates APP amyloidogenic processing.
4. Demonstration that TMP21 interacts with immature BACE1 and accumulates immature form of BACE1, which cleaves APP on Asp-1 site and produces intact A β .
5. Investigation of the mechanisms that TMP21 affects BACE1 trafficking and maturation, and modulating the BACE1 trafficking and maturation by TMP21 will be a new therapeutic target for future research.

5.3 Strengths and weaknesses

5.3.1 Elucidate the clinical relevance of TMP21 expression levels and gene polymorphisms in AD patients

This chapter first elucidates the genetic impact of TMP21 on the risk of AD and the clinical relevance of TMP21 expression levels in AD pathogenesis. The previous studies suggest that TMP21 levels are significantly altered in disease state and that TMP21 may play an integral, clinically relevant role in AD pathogenesis. However, there is still no genetic association study between *Tmp21* and AD. Using gDNA bank from AD patients and controls (Zhou, et al.), we screen *Tmp21* SNPs in exonic regions excluding the 5' UTR and 3' UTR, and find that *rs12435391* (IVS4-28T>C) in intron 4 shows significant difference of allele and genotype frequency in AD patients and controls. This is the first time to elucidate the *Tmp21* gene polymorphisms in AD patients. It greatly emphasizes the genetic impact of TMP21 on the risk of AD and also indicates that upregulation of TMP21 may also contribute to AD pathogenesis.

To further exam the role of this intronic SNP on pre-mRNA processing and TMP21 expression levels, in this chapter, we propose a novel cloning strategy and construct an expression plasmid consist of all coding exons and the intron of interest, driven by the endogenous promoter. After transfected into cells, TMP21 protein with correct size was readily detected in the cell lysis,

Chapter 5: Conclusion and Future Directions

indicating that the pre-mRNA from this construct could be recognized by endogenous splicing machinery and properly processed into mRNA, subsequently, transcript into protein of the proper size. This in vitro approach is further used to study how rs12435391 affects TMP21 pre-mRNA processing. One of the traditional approaches analyzing RNA splicing relies on hybrid minigene plasmid, which is a “simplified” version of the gene. A typical hybrid minigene plasmid contains sequences of transcriptional enhancer (e.g. CMV, cytomegalovirus promoter, for ubiquitous expression and polymerase II transcription), upstream and downstream exons from the report gene (e.g. α -globin). The genomic DNA region of interest that contains alternatively splicing region and flanking regions is introduced between exons of report gene (F. Pagani, Baralle, FE, 2010; F. Pagani, et al., 2002). This minigene assay involves the sequences from multiple genes. However, our expression construct consists of all coding exons and the intron of interest, driven by its endogenous promoter, and it removes many of the confounding variables. More importantly, our novel construct can be recognized by endogenous splicing machinery, expressed mRNA and protein at proper size. It provides an effective approach to assess the intronic SNPs, which may interfere with RNA splicing in future research.

5.3.2 Evidence the role of TMP21 in APP processing and indicates its impact on BACE1

In this chapter, one of the strengths is the comprehensive examination of CTFs levels, not only $A\beta$ levels. It provides general information about the APP processing and the α -, β -, β' - and γ -cleavage. In non-amyloidogenic pathway, APP is cleaved within the $A\beta$ domain to preclude $A\beta$ generation. α -secretase cleaves APP to produce a secreted form of APP (sAPP α) and membrane-bound C83. Also, BACE1 mainly cleaves APP within the $A\beta$ region (Glu-11 site) to produce C89 (Deng, et al., 2013; Huse, et al., 2002). All the CTFs can be further cleaved by γ -secretase complex. In amyloidogenic pathway, APP is first cleaved by BACE1 at the amino terminus of $A\beta$ (Asp-1 site), producing C99. C99 is subsequently cleaved by γ -secretase to generate $A\beta$. Most of the previously published papers only focus on the downregulation of TMP21 on $A\beta$ production (F. S. Chen, et al., 2006; Dolcini, et al., 2008; Pardossi-Piquard, et al., 2009; Vetrivel, et al., 2007). However, both the inhibition of the γ -secretase activity and the increased β -site

Chapter 5: Conclusion and Future Directions

cleavage lead to the increased A β level. Therefore, without thoroughly examination of all CTFs, one could not figure out how TMP21 affects A β production. It is possible that TMP21 alters APP processing not only by its negative regulation on γ -secretase, but also by effects on BACE1. In examining CTFs, we find that the upregulation of TMP21, instead of increasing overall CTFs levels, preferentially increases C99 but decreases C83 levels. This result indicates that overexpression of TMP21 specific enhances BACE1 cleavage on APP Asp-1 site. To illustrate this effect, we test the BACE1 expression and the accumulation of immature form of BACE1 upon the dysregulation of TMP21 is observed. Subsequently, we identify the interaction between TMP21 and immature BACE1 and further, overexpression of TMP21 delays BACE1 trafficking. These results confirm the impact of TMP21 on BACE1. Consistently, the TMP21 deficit also accumulated more immature BACE1, which contributed to the increased C99 level; it suggested that the TMP21 deficit might also alters the trafficking and maturation process of BACE1.

One of the weaknesses in this chapter is that we still cannot totally distinguish the effect of TMP21 on γ -cleavage and BACE1 based on the present data. Dysregulated TMP21 results in an increased C99 level, which provides much more substrates for A β generation. However, it is possible that the dysregulated TMP21 might interfere the secretion of A β . The A β here we measured by ELISA is the secreted A β from medium, which cannot represent the total A β level. Thus, an overall analysis of A β level, both secreted and intercellular, is required in the next step. Additionally, all the CTFs and A β generations rely on the activities of all these secretases and the dynamic interactions between secretases and their substrates. It reported that TMP21 inhibited γ -cleavage of C99 in cells and also *in vitro* using cell-free γ -secretase assay (F. Chen, et al., 2006). However, another group found that TMP21 did not exist in mature and active γ -secretase complex. Meanwhile, they assigned additive and independent effect of TMP21 on APP trafficking (Vetrivel, et al., 2007). These evidences show the dual role of TMP21 in enzymes activities modulation and trafficking. Therefore, TMP21 might play an integral and comprehensive role in APP processing. It will be very interesting to further investigate the role of TMP21 on assembling and trafficking of all the γ -secretase complex members.

5.3.3 Examine the fundamental role of TMP21 in mice models

In addition to the roles of TMP21 in AD pathogenesis, a more striking function, the fundamental function of TMP21 in early stage of development demands further attention. In this thesis, we took advantage of mice models to determine the causal linkage between the expression level of TMP21 and AD pathogenesis. The *Tmp21* hemizygous knockout (S2P23) mouse strain was established by Micheal Owen's lab (Denzel, et al., 2000b). Dr. Kelley Bromley-Brits, graduated from our lab, characterized the general behaviors of these mice using a range of comprehensive behavioral tests. Consistently with previous study by Denzel, et al., the S2P23 mice are viable and fertile, they appear grossly normal and grow as well as control mice. No significant differences is observed in many behavior tests, such as hanging wire test for measuring hang strength, Y-maze task and Morris water maze task for testing hippocampal-dependent learning and memory. The S2P23 mice perform better in motor coordination test---rotarod test, and show heightened anxiety in open field test and decreased contextually conditioned response in fear conditioning test. Our lab also bred APP23 mice, which strongly express APP751 isoform harboring the APP^{swe} mutation and displays plaque deposition mainly in the cortex and in hippocampus (Andra, et al., 1996; Reaume, et al., 1996; Sturchler-Pierrat, et al., 1997). The APP23 mice are viable even though there are large number of plaques occupying substantial areas of cortex, hippocampus, thalamus and olfactory at the age of 24 months. However, the APP23XS2P23 double crossed mice appeared smaller than their littermate controls. Much less APPXS2P23 double crossed offspring (9% instead of expected 25% according to Mendel's Law of Inheritance) could be produced and few of them can survive after 6 months. The fatality of the APP23XS2P23 mice is detrimental. More significantly, the *Tmp21* homozygous knockouts are embryonic lethal, no *Tmp21*^{-/-} homozygous embryos at 7.5 days post coitus (dpc) or blastocysts at 3.5dpc could be detected (Denzel, et al., 2000b). It indicates the fundamental functions of TMP21 in the early stage of development. A more satisfying mouse model, in which the *Tmp21* gene is ablated in a conditional manner, is necessary to fully clarify this issue. We will discuss this in future research section 5.4.2.

Chapter 5: Conclusion and Future Directions

Moreover, there is still no practicable TMP21 transgenic mice model. Transgenic mice harbored human *Tmp21* at various expression levels in neurons established by Dr. Gopal group, they found that even a 50% increase of TMP21 overexpression in central nervous system leads to post-natal growth retardation, sever neurologic problems and early death. The newborn human *Tmp21* transgenic mice are normal and show no symptom in the first two weeks after birth, pathologic symptoms reveals when endogenous TMP21 begins to decline and the onset and severity of the symptoms are highly correlated with the TMP21 expression levels (Gong, et al., 2011). Additionally, no *Tmp21* homozygous knockout embryo survives (Denzel, et al., 2000b). As we discussed previously, the endogenous TMP21 expression levels are precisely controlled. The robust expression level of TMP21 is higher demanded and more essential for the development of embryonic and early post-natal stage but it begins to decline with age after birth. However, in human *Tmp21* transgenic mice, the sustained high-level TMP21 expressed during post-natal development, especially when endogenous TMP21 declines, the mice begin to show complex neurological problems. Therefore, to test the role of TMP21 with greater precision requires a more practicable method *in vivo*, for instant, using the tetracycline-inducible system or the Cre/loxP recombinase system to spatiotemporal control the gene expression.

5.3.4 Characterize the TMP21/BACE1 interaction

BACE1, considered as the major, or probably the only, β -secretase that cleavage APP at Asp-1 site in the brain. BACE1 knockout neurons and mice completely fail to generate CTF β and A β , and knockout BACE1 rescues the memory deficit in AD mice (H. Cai, et al., 2001; Ohno, et al., 2004; Roberds, et al., 2001). Interestingly, BACE1 knockout mice are healthy and show no discernible phenotype comparing with wild type mice (Y. Luo, et al., 2001). These studies suggest that BACE1 inhibition could be an attractive therapeutic strategy that may be free of mechanism-based toxicity. Here, our studies at the beginning of chapter 4 suggested the multiple binding sites between TMP21 and BACE1. As the fundamental function of TMP21, it will be more prospective to identify the TMP21 binding sites on BACE1; thus we could further develop small peptides, or a dominate negative BACE1 lacking TMP21 binding motifs that are

Chapter 5: Conclusion and Future Directions

introduced enter cells and specifically interfere the TMP21/BACE1 interaction under TMP21 overexpression condition; these will be great protectors in TMP21 overexpression-mediated APP amyloidogenic processing. The works in TMP21 binding motifs on BACE1 are continuing by Dr Zhe Wang, who is an expert in protein-protein interaction and proteins intracellular trafficking.

5.3.5 Explore the role of TMP21 in APP/BACE1 lipid raft-like domains translocation

At the end of chapter 4, our results suggested that when newly synthesized BACE1 trafficking from ER to Golgi, the immature form of BACE1 interacted with TMP21/p24a complex and was guided into lipid raft-like domains in ER or ERGIC, at the same time, the interaction between TMP21/p24a and APP also trapped APP into lipid raft-like structures when APP traffic through ER and ERGIC, thus increased the interaction of immature BACE1 and APP, and probably increased the chance of APP and BACE1 co-residency in lipid raft-like domains, finally led to the preferentially cleavage on Asp-1 site of APP and produced more C99, the significantly augment of C99 level provided more substrate for γ -secretase hence to generate more A β . To isolate lipid raft, here we used floating lipid raft isolation method with 1% TritonX-100, 1% NP-40 or 0.5% Lubrol WX as previously described (Vetrivel, et al., 2004). However, we did not detect the significantly difference of APP/BACE1 distribution in lipid raft fractions in which the lipid raft marker flotillin2 was enriched and the soluble protein calnexin is limited. The possible reasons might be that only a small percentage of APP and BACE1 cofractionate in lipid raft under normal physical condition (Riddell, Christie, Hussain, & Dingwall, 2001). The immature BACE1 is a minor proportion of total cellular BACE1. The synthesis of lipid raft begins in ER (Browman, et al., 2006; Sevlever, et al., 1999), where the levels of sterol and sphingolipid are still low (van Meer & Lisman, 2002). Thus, the interaction between APP and immature BACE1 in lipid raft so that cannot be easily detected by traditional approach because of its relatively weak and transient state. Additionally, BACE1 interacts with GPI proteins (Hattori, et al., 2006; Marlow, et al., 2003; Tun, et al., 2002) while TMP21 acts as a receptor for GPI-anchored proteins and guide them into the early lipid rafts in ER (Bonnon, et al., 2010; M. Fujita, et al.,

2011; Takida, et al., 2008), it is also possible that TMP21 translocates immature BACE1 into the early lipid raft indirectly via GPI-anchored protein(s).

5.4 Future directions

5.4.1 The effect of TMP21 on γ -secretase complex

Rationale The assembly of the γ -secretase complex starts at the ER (Capell, et al., 2005; Kim, et al., 2004). Aph-1 contributed to the trafficking and maturation of the γ -secretase complex. First, Aph-1 polypeptides formed a subcomplex with immature NCT in ER, dependent on its GXXXG motif, which is the initial step for the formation of the whole complex (Hu & Fortini, 2003; LaVoie, et al., 2003; Niimura, et al., 2005). This subcomplex further recruited and stabilized nascent PS through the hydrophobic interface formed by the transmembrane domains of Aph-1 and Nct. PS1, only a small fraction locates on the cell surface, most of them are mainly localized at ER, Golgi/TGN and endosome (J. H. Chyung, Raper, & Selkoe, 2005; Bart De Strooper, et al., 1997; J. Zhang, et al., 1998). This holo PS/Aph-1/immature NCT complex form in ER is a stabilized but γ -secretase-inactive intermediate (Takasugi, et al., 2003). Then PS is subjected to endoproteolysis to generate its amino- and carboxyl-terminal fragments in Golgi (PS-CTF and PS-NTF, respectively) (Capell, et al., 1998; Thinakaran, et al., 1996). The heterodimer of PS-NTF/PS-CTF is the active center that harboring two critical aspartyl residues for physiological activity of γ -secretase (Fukumori, Fluhrer, Steiner, & Haass, 2010; Shirotani, et al., 2003). PS fragments preferentially binds to the mature and fully glycosylated NCT (Edbauer, Winkler, Haass, & Steiner, 2002); Pen-2 is required for the proteolytic processing of PS (Takasugi, et al., 2003) and it interacted with PS-NTF (Fraering, et al., 2004). Therefore after passing through the Golgi, a fully matured glycosylated NCT, a heterodimeric form of PS-NTF/PS-CTF, Pen-2 and Aph-1 exist as a mature and active γ -secretase complex (Kimberly, et al., 2003). (Fig 5.1) This complex can be isolated and cleave its substrates, C99 and Notch, in the *in vitro* activity assays (J. H. Chyung, et al., 2005). PS1 could also play a role in modulation the trafficking of membrane and secretory proteins (Naruse, et al., 1998). Significant amounts of full-length PS1 are found cycling between ER and Golgi, regulated by COPI-mediated retrograde transport

Chapter 5: Conclusion and Future Directions

(Rechards, Xia, Oorschot, Selkoe, & Klumperman, 2003). It has been reported that the overexpression of PS1 results in an increase of A β -containing CTFs and/or A β in COPI-coated membranes of the vesicular tubular clusters between ER and Golgi, while increasing the mutant PS-1 or PS-knockout, which is mainly present in post-Golgi, shows the opposite effect that retains these APP derivatives in ER (Rechards, et al., 2006). This data suggests the potential role of PS1 in the trafficking of APP and its derivatives.

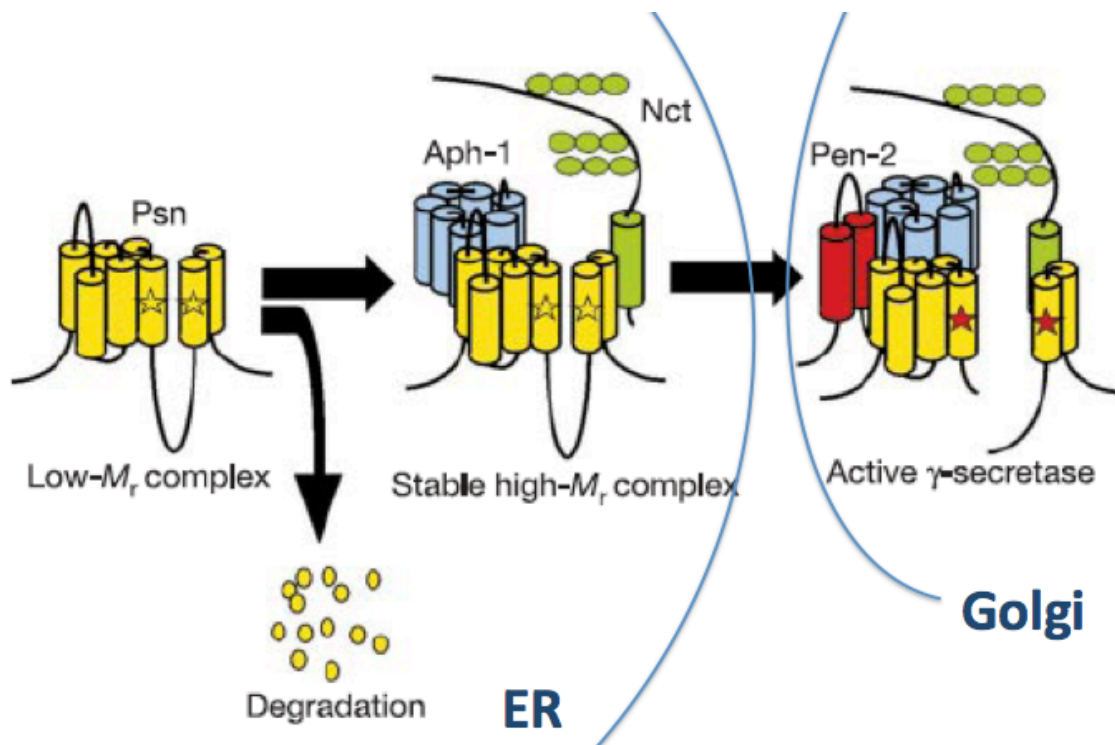


Figure 5.1 The assembly, trafficking and maturation of γ -secretase complex.

Assembly of the γ -secretase complex starts within the ER where Aph-1 (blue cylinders) forms a subcomplex with immature Nct (green cylinder). This subcomplex also interacts with nascent presenillin (Psn, yellow cylinders). This Aph-1/immature NCT trimetric subcomplex includes nascent PS and forms stabilized but γ -secretase-inactive intermediate. PS has to be endoproteolyzed to generate PS-CTF and PS-NTF in Golgi and the heterodimer of PS-NTF/PS-CTF that harbors the two critical aspartyl residues refers to the physiological activity of γ -secretase. PS-CTF preferentially binds to the mature and fully glycosylated NCT and Pen-2 (red cylinders) is required for the proteolytic processing of PS and interacts with PS-NTF. Finally, after passing through the Golgi, a fully matured

Chapter 5: Conclusion and Future Directions

glycosylated NCT, a heterodimeric form of PS-NTF/PS-CTF, Pen-2 and Aph-1 exist as a mature and active γ -secretase complex. Modified from (Takasugi, et al., 2003) and (Niimura, et al., 2005)

Here, we detected the increased A β levels when TMP21 expressions were dysregulated. The increased β -cleavage and/or γ -cleavage can lead to increased A β levels. Based on the present data in this thesis, we cannot totally distinguish the effect of TMP21 on γ -cleavage from BACE1 here. It reported that TMP21 inhibited γ -secretase activity *in vitro* (F. Chen, et al., 2006). However, another group found that TMP21 was not exist in mature and active γ -secretase complex, they assigned additive and independent effect of TMP21 on APP trafficking (Vetrivel, et al., 2007). In their study, they also noted the increased immature NCT when 80% knockdown of TMP21. These evidences showed the dual role of TMP21 in enzymes activities modulation and trafficking. As thus, it is very interesting to further investigate the actual role of TMP21 on the γ -secretase complex, especially the assembling and trafficking of its all members.

Preliminary data Firstly, we detected the interactions between all of the γ -secretase complex members and TMP21 individually. The PS1 expression plasmid was cotransfected with myc-tagged TMP21. Cells were harvest after 48 hours and lysed in NP-40 lysis buffer. The lysates were immunoprecipitated with anti-myc antibody 9E10 and analyzed by immunoblot using anti-PS1 NTF antibody. Interestingly, we found that the full-length of PS1, rather than NTF of PS1, can be coimmunoprecipitated with TMP21 (Fig 5.2 A). Also, the myc-tagged NCT, Aph-1, Pen2 were cotransfected with GFP-TMP21, respectively. Cells were harvest after 48 hours and lysed in NP-40 lysis buffer. The lysates were immunoprecipitated with anti-myc antibody 9E10 and analyzed by immunoblot using anti-GFP antibody. While the TMP21 can coimmunoprecipitate with Aph-1 (Fig 5.2 C D), but not NCT (Fig 5.2 B) or Pen-2 (Fig 5.2 D).

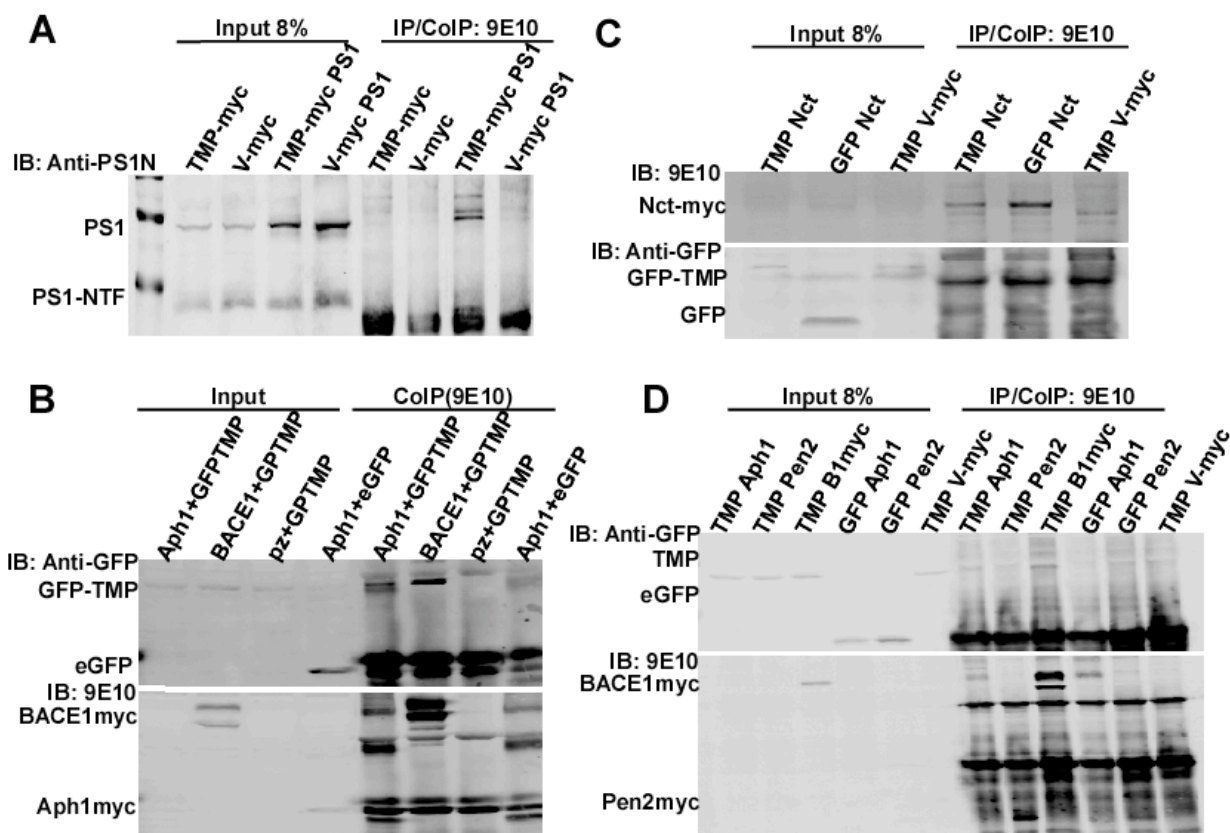


Figure 5.2 TMP21/ γ -secretase interaction.

(A). The PS1 expression plasmid was cotransfected with myc-tagged TMP21. Cells were harvest after 48 hours and lysed in NP-40 lysis buffer. The lysates were immunoprecipitated with anti-myc antibody 9E10 and analyzed by immunoblot using anti-PS1 NTF antibody. (B) The myc-tagged NCT, (C) Aph-1, (D) Pen-2 was cotransfected with GFP-TMP21, respectively. TMP21/BACE1 coimmunoprecipitation was used as positive control. eGFP or myc-Vector were used as negative controls. Cells were harvest after 48 hours and lysed in NP-40 lysis buffer. The lysates were immunoprecipitated with anti-myc antibody 9E10 and analyzed by immunoblot using anti-GFP antibody.

Discussion Assembling of the γ -secretase complex starts at the ER (Capell, et al., 2005; Kim, et al., 2004), where Aph-1 interacts with immature NCT (Hu & Fortini, 2003; LaVoie, et al., 2003; Niimura, et al., 2005). This Aph-1/immNCT subcomplex includes nascent PS and forms stabilized but γ -secretase-inactive intermediate (Takasugi, et al., 2003). After being endoproteolyzed, PS-CTF and PS-NTF form heterodimer which refers to the physiological activity of γ -secretase (Fukumori, et al., 2010) (Fig 1.4). Significant amounts of full-length PS1

Chapter 5: Conclusion and Future Directions

were found cycling between ER and Golgi, regulated by COPI-mediated retrograde transport (Rechards, et al., 2003). TMP21 plays essential role in proteins ER/Golgi trafficking (Belden & Barlowe, 1996; Blum, et al., 1996b, 1996c; Schimmoller, et al., 1995; Stannnes, et al., 1995). When the whole matured γ -secretase complex is isolated using an active-site γ -secretase inhibitor, there is no TMP21 presents. It is consistent with our preliminary data that TMP21 only interacts with full length PS1 and Aph-1 but not all the members of γ -secretase complex (Vetrivel, et al., 2007). Therefore, it is probably that TMP21 associates with the early assembly or the early secretory pathway trafficking of γ -secretase complex via Aph-1/nascent PS1 interaction in ER. However, to demonstrate this statement and explore the exact role of TMP21 in assembling and trafficking of γ -secretase complex, further studies are required using similar techniques in Chapter 4.

5.4.2 Establish the inducible TMP21 knockout mice

The *Tmp21* homozygous knockouts are embryonic lethal and expression of human *Tmp21* in mice central nervous system leads to post-natal growth retardation, sever neurologic problems shortly after birth, and early death. These facts indicate the fundamental functions of TMP21 in early stage of development and meanwhile, the expression level of TMP21 are strictly controlled during pre- and post-natal developments. An ideal mice model is necessary for further application. The site-specific recombination system, Cre-LoxP system, has now made it possible that the genes deletions, insertions, inversions and exchanges can be induced in a spatially and temporally restricted fashion in cells and animal models (Araki, Araki, Miyazaki, & Vassalli, 1995; Branda & Dymecki, 2004). Taking advantage of Cre-LoxP system, we would like to firstly establish a conditional TMP21 knockout mice strain. Then the mice carrying LoxP-flanked TMP21 will be further bred with a neuron-specific Cre expressing mouse to achieve an inducible neuronal-TMP21 knockout offspring. For further usage in the study of TMP21 suppression in AD pathogenesis, these mice could be crossbred with AD mice and the offspring mice will provide a powerful tool.

Chapter 5: Conclusion and Future Directions

Preliminary data The full construct of the *Tmp21* targeted vector was completed (Fig. 5.3, A). There are three loxP sites respectively flanking positive selection marker, neomycin resistant gene and essential gene segment of mouse *Tmp21* consists of Exon 2 and the flanking intronic region; the deletion of this segment can abolish TMP21 expression. Mouse embryonic stem (ES) cells were electroporated with this targeting vector and neomycin was used to select the positive transfected cells. The neomycin-resistant ES colonies were screened by PCR. The correctly targeted colony was confirmed by sequencing (Fig. 5.3). There were three LoxP sites flanking the neomycin-resistant gene and the gene segment from TMP21. Currently, I am attempting to produce chimeric ES cells expressing LoxP-targeted TMP21 by transient transfection of Cre-GFP. Ideally, the cre-recombinase will cut off the selection marker and achieve the type II deletion in cells. The positive ES cells carrying LoxP-flanked TMP21 could be screened by neomycin selection and PCR (Fig. 5.4). Then these ES cells would be ready for microinjection in mouse blastocyst. If these cells can growth up to be a sperm or an egg (germline transmission) and it can breed the LoxP-flanked TMP21 mice. These mice, with normal TMP21 expression, are supposed to show the similar phenotype as wild type mice in life span, birth rate, biomolecular and behavioral tests results. However, the TMP21 expression and general behaviors characterization will be preformed. Then these mice will be crossed with spatial or temporal controlled Cre-recombinase (e.g. Thy1-Cre or tamoxifen-inducible Cre) (Araki, et al., 1995; Branda & Dymecki, 2004; Feil, et al., 1996) mice to generate inducible TMP21 knockout offspring (indTMP21^{-/-}) mice. Firstly, the biomedical and behaviors phenotypes of these indTMP21^{-/-} mice will be fully characterized. The results will reveal the consequences caused by TMP21 deficit in neurons. Further, the indTMP21^{-/-} mice were crossbred with APP23 mice to produce indTMP21^{-/-}/APP23. The LoxP-TMP21 mice, indTMP21^{-/-} mice, LoxP-TMP21/APP23 double-crossed mice and indTMP21^{-/-}/APP23 mice will be examined from biomolecular levels to behavioral levels by serials of comprehensive tests.

Chapter 5: Conclusion and Future Directions

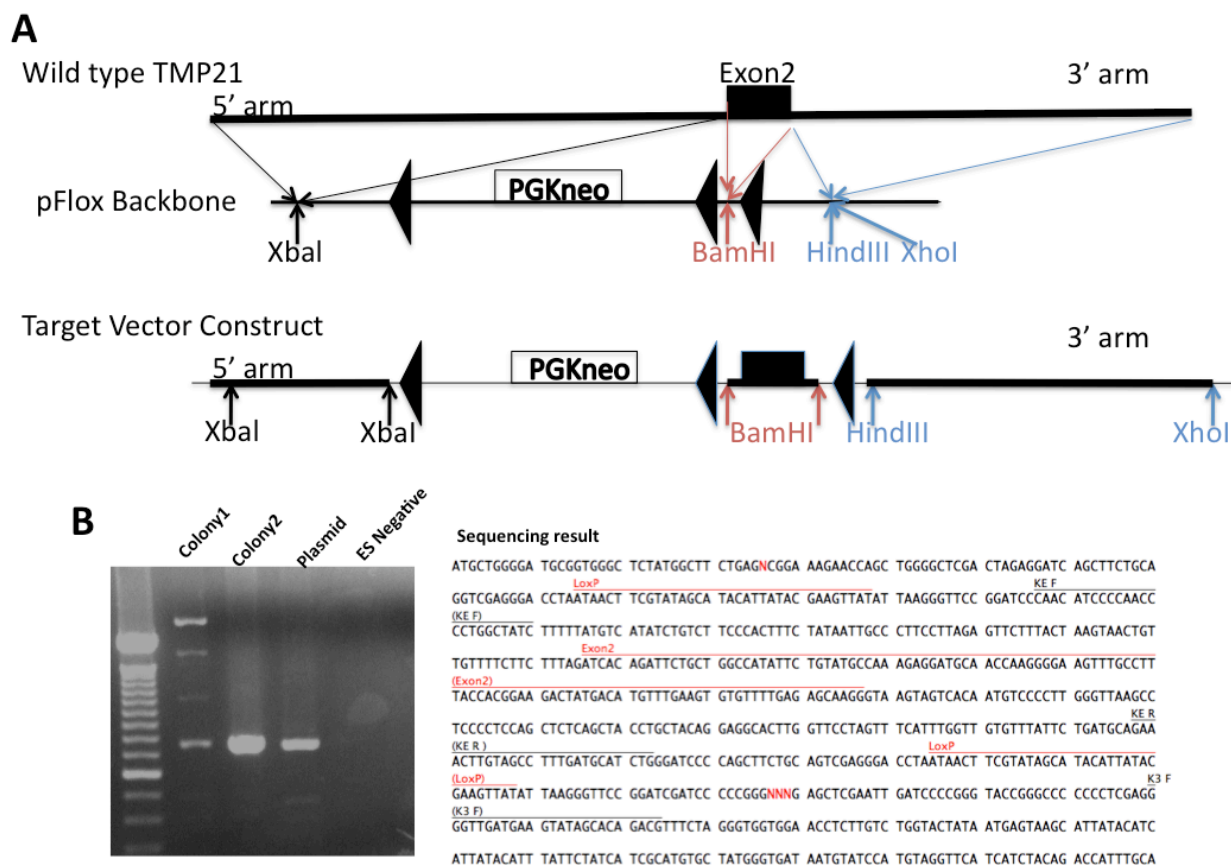


Figure 5.3 LoxP-flanked *TMP21* vector construct.

(A) Schematic diagram of the *Tmp21* locus, the targeting vector and the structure of the targeted allele. (B) ES cells were electroporated with the targeting vector and correctly targeted, G418-resistant colonies were identified by PCR then confirmed by sequencing.

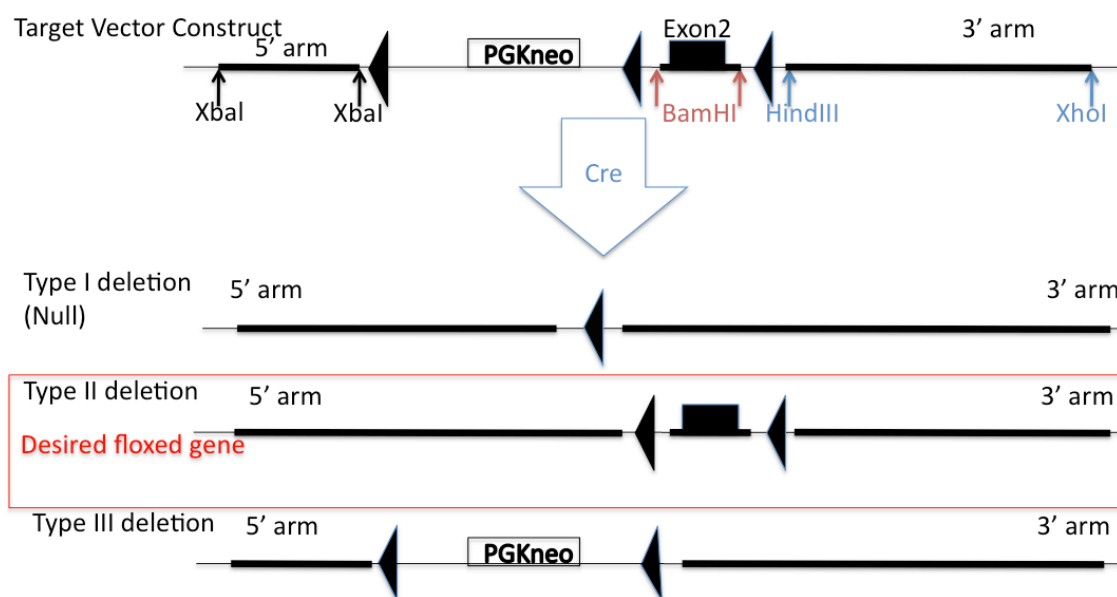


Figure 5.4 Strategies for generating a loxP-flanked gene for conditional gene targeting.

Three different types of ES cell subclones are generated: one harboring the desired floxed gene (Type II deletion), one a null allele (Type I deletion), and the other, a floxed selection marker (Type III deletion). Type I and Type II subclones can be distinguished from Type III by sib-sensitivity to G418; Type I subclones can be distinguished from Type II by PCR.

Discussion The $\text{indTMP21}^{-/-}$ mice model is an excellent tool in examining the fundamental roles of TMP21. Further, the $\text{indTMP21}^{-/-}/\text{APP23}$ mice model could be used in confirming the roles of TMP21 in AD pathogenesis *in vivo*. The $\text{indTMP21}^{-/-}/\text{APP23}$ mice might survive longer and with a better health condition than $\text{APP23}/\text{S2P23}$ double-crossed mice. More importantly, this mice model bypasses the embryonic lethality associated with TMP21 knockout.

5.4.3 Examine TMP21/GPI-anchored proteins/BACE1/APP interaction

Sequence analysis shows that BACE1 is not a GPI-anchored protein, while its localization and stability in lipid raft depend on the interaction with GPI-anchored proteins (Hattori, et al., 2006; Marlow, et al., 2003; Tun, et al., 2002), even though the identification of these GPI-anchored proteins is yet to be exclusive. As TMP21 acts as a cargo receptor for GPI-anchored proteins and targets the ER export and lipid raft translocation. A small percentage of APP and BACE1 cofractionate in lipid raft under normal physical condition (Riddell, et al., 2001). Here, we observed the co-existence of immature BACE1 and ubiquitous lipid raft marker, flotillin2, as well as partial TMP21 in Triton X-100 resistant pellet; it is reasonable as the early lipid-raft-like domains can be observed in the ER (Browman, et al., 2006; Sevlever, et al., 1999). Further, the co-localization between BACE1 and flotillin2 increased when TMP21 upregulated. Overexpression of TMP21 enhanced the co-localization and interaction between APP and immature BACE1. However, we did not detect the significantly difference of APP/BACE1 distribution in lipid raft fractions using common methods, it might be the relatively weak and transient interaction between APP and immature BACE1 in lipid raft. Alternatively, APP and BACE1 might directly interact with TMP21, and the BACE1-associated GPI-anchored protein might mediate this TMP21/BACE1 interaction. Thus, it is possible that all of these GPI-anchored proteins/TMP21/BACE1/APP cluster into this premature lipid raft-like structure. It will be interesting to identify the GPI-anchored protein(s) that can associate with BACE1, and to determine whether this GPI-anchored protein mediate the TMP21/BACE1 interaction and BACE1 translocation to lipid raft.

References

- Abad-Rodriguez, J., Ledesma, M. D., Craessaerts, K., Perga, S., Medina, M., Delacourte, A., et al. (2004). Neuronal membrane cholesterol loss enhances amyloid peptide generation. *The Journal of cell biology*, 167(5), 953-960.
- Abad-Rodriguez, J., Ledesma, M. D., Craessaerts, K., Perga, S., Medina, M., Delacourte, A., et al. (2004). Neuronal membrane cholesterol loss enhances amyloid peptide generation. *J Cell Biol*, 167(5), 953-960.
- Abbott, A. (2011). Dementia: a problem for our age. *Nature*, 475(7355), S2-S4.
- Abdul, H. M., Sama, M. A., Furman, J. L., Mathis, D. M., Beckett, T. L., Weidner, A. M., et al. (2009). Cognitive decline in Alzheimer's disease is associated with selective changes in calcineurin/NFAT signaling. *J Neurosci*, 29(41), 12957-12969.
- ADI (2010). World Alzheimer report 2010: the global economic impact of dementia. *Alzheimer Disease International, London*.
- ADI (2013). World Alzheimer Report 2013: An analysis of long-term care for dementia. *Alzheimer Disease International, London*.
- Allinson, T. M., Parkin, E. T., Condon, T. P., Schwager, S. L., Sturrock, E. D., Turner, A. J., et al. (2004). The role of ADAM10 and ADAM17 in the ectodomain shedding of angiotensin converting enzyme and the amyloid precursor protein. *Eur J Biochem*, 271(12), 2539-2547.
- Anantharaman, V., & Aravind, L. (2002). The GOLD domain, a novel protein module involved in Golgi function and secretion. *Genome Biol*, 3(5), research0023.
- Andra, K., Abramowski, D., Duke, M., Probst, A., Wiederhold, K. H., Burki, K., et al. (1996). Expression of APP in transgenic mice: a comparison of neuron-specific promoters. *Neurobiol Aging*, 17(2), 183-190.
- Arai, H., Lee, V. M., Messinger, M. L., Greenberg, B. D., Lowery, D. E., & Trojanowski, J. Q. (1991). Expression patterns of beta-amyloid precursor protein (beta-APP) in neural and nonneural human tissues from Alzheimer's disease and control subjects. *Ann Neurol*, 30(5), 686-693.
- Araki, K., Araki, M., Miyazaki, J.-i., & Vassalli, P. (1995). Site-specific recombination of a transgene in fertilized eggs by transient expression of Cre recombinase. *Proceedings of the National Academy of Sciences*, 92(1), 160-164.
- Area-Gomez, E., de Groof, A. J., Boldogh, I., Bird, T. D., Gibson, G. E., Koehler, C. M., et al. (2009). Presenilins are enriched in endoplasmic reticulum membranes associated with mitochondria. *The American journal of pathology*, 175(5), 1810-1816.
- Area-Gomez, E., Del Carmen Lara Castillo, M., Tambini, M. D., Guardia-Laguarta, C., de Groof, A. J., Madra, M., et al. Upregulated function of mitochondria-associated ER membranes in Alzheimer disease. *EMBO J*, 31(21), 4106-4123.
- Artavanis-Tsakonas, S., Rand, M. D., & Lake, R. J. (1999). Notch signaling: cell fate control and signal integration in development. *Science*, 284(5415), 770-776.

References

- Asai, M., Hattori, C., Szabo, B., Sasagawa, N., Maruyama, K., Tanuma, S., et al. (2003). Putative function of ADAM9, ADAM10, and ADAM17 as APP alpha-secretase. *Biochem Biophys Res Commun*, 301(1), 231-235.
- Barlowe, C. (1998). COPII and selective export from the endoplasmic reticulum. *Biochim Biophys Acta*, 1404(1-2), 67-76.
- Barlowe, C., Orci, L., Yeung, T., Hosobuchi, M., Hamamoto, S., Salama, N., et al. (1994). COPII: a membrane coat formed by Sec proteins that drive vesicle budding from the endoplasmic reticulum. *Cell*, 77(6), 895-907.
- Belden, W. J., & Barlowe, C. (1996). Erv25p, a component of COPII-coated vesicles, forms a complex with Emp24p that is required for efficient endoplasmic reticulum to Golgi transport. *J Biol Chem*, 271(43), 26939-26946.
- Belden, W. J., & Barlowe, C. (2001). Deletion of yeast p24 genes activates the unfolded protein response. *Mol Biol Cell*, 12(4), 957-969.
- Belden, W. J., & Barlowe, C. (2001). Distinct roles for the cytoplasmic tail sequences of Emp24p and Erv25p in transport between the endoplasmic reticulum and Golgi complex. *Journal of Biological Chemistry*, 276(46), 43040-43048.
- Benjannet, S., Elagoz, A., Wickham, L., Mamarbachi, M., Munzer, J. S., Basak, A., et al. (2001). Post-translational processing of beta-secretase (beta-amyloid-converting enzyme) and its ectodomain shedding. The pro- and transmembrane/cytosolic domains affect its cellular activity and amyloid-beta production. *J Biol Chem*, 276(14), 10879-10887.
- Bennett, B. D., Denis, P., Haniu, M., Teplow, D. B., Kahn, S., Louis, J. C., et al. (2000). A furin-like convertase mediates propeptide cleavage of BACE, the Alzheimer's beta -secretase. *J Biol Chem*, 275(48), 37712-37717.
- Bergmans, B. A., & De Strooper, B. Gamma-secretases: from cell biology to therapeutic strategies. *The Lancet Neurology*, 9(2), 215-226.
- Bethune, J., Wieland, F., & Moelleken, J. (2006). COPI-mediated transport. *The Journal of membrane biology*, 211(2), 65-79.
- Blum, R. (2007). Cell surface trafficking of the COPI receptor p23 (Tnp21) in the presence of an ER retrieval signal is mediated by its luminal domain. *European Journal of Cell Biology*, 86, 60-60.
- Blum, R., Feick, P., Puype, M., Vandekerckhove, J., Klengel, R., Nastainczyk, W., et al. (1996a). Tnp21 and p24A, two type I proteins enriched in pancreatic microsomal membranes, are members of a protein family involved in vesicular trafficking. *J Biol Chem*, 271(29), 17183--17189.
- Blum, R., Feick, P., Puype, M., Vandekerckhove, J., Klengel, R., Nastainczyk, W., et al. (1996b). Tnp21 and p24A, two type I proteins enriched in pancreatic microsomal membranes, are members of a protein family involved in vesicular trafficking. *Journal of Biological Chemistry*, 271(29), 17183-17189.
- Blum, R., Feick, P., Puype, M., Vandekerckhove, J., Klengel, R., Nastainczyk, W., et al. (1996c). Tnp21 and p24A, two type I proteins enriched in pancreatic microsomal membranes, are members of a protein family involved in vesicular trafficking. *J Biol Chem*, 271(29), 17183-17189.

References

- Blum, R., & Lepier, A. (2008). The luminal domain of p23 (Timp21) plays a critical role in p23 cell surface trafficking. *Traffic*, *9*(9), 1530-1550.
- Blum, R., Pfeiffer, F., Feick, P., Nastainczyk, W., Kohler, B., Schafer, K. H., et al. (1999). Intracellular localization and in vivo trafficking of p24A and p23. *Journal of Cell Science*, *112*(4), 537-548.
- Bonnon, C., Wendeler, M. W., Paccaud, J. P., & Hauri, H. P. Selective export of human GPI-anchored proteins from the endoplasmic reticulum. *J Cell Sci*, *123*(Pt 10), 1705-1715.
- Bonnon, C., Wendeler, M. W., Paccaud, J. P., & Hauri, H. P. (2010). Selective export of human GPI-anchored proteins from the endoplasmic reticulum. *J Cell Sci*, *123*(Pt 10), 1705-1715.
- Borchelt, D. R., Thinakaran, G., Eckman, C. B., Lee, M. K., Davenport, F., Ratovitsky, T., et al. (1996). Familial Alzheimer's disease-linked presenilin 1 variants elevate Abeta1-42/1-40 ratio in vitro and in vivo. *Neuron*, *17*(5), 1005-1013.
- Braak, H., & Braak, E. (1991). Neuropathological staging of Alzheimer-related changes. *Acta Neuropathol*, *82*(4), 239-259.
- Braak, H., Braak, E., & Bohl, J. (1993). Staging of Alzheimer-related cortical destruction. *Eur Neurol*, *33*(6), 403-408.
- Branda, C. S., & Dymecki, S. M. (2004). Talking about a revolution: The impact of site-specific recombinases on genetic analyses in mice. *Developmental cell*, *6*(1), 7-28.
- Bray, S. J. (2006). Notch signalling: a simple pathway becomes complex. *Nat Rev Mol Cell Biol*, *7*(9), 678-689.
- Browman, D. T., Resek, M. E., Zajchowski, L. D., & Robbins, S. M. (2006). Erlin-1 and erlin-2 are novel members of the prohibitin family of proteins that define lipid-raft-like domains of the ER. *J Cell Sci*, *119*(Pt 15), 3149-3160.
- Brown, D. A., & London, E. (2000). Structure and function of sphingolipid- and cholesterol-rich membrane rafts. *J Biol Chem*, *275*(23), 17221-17224.
- Bu, G. (2009). Apolipoprotein E and its receptors in Alzheimer's disease: pathways, pathogenesis and therapy. *Nat Rev Neurosci*, *10*(5), 333-344.
- Burgos, P. V., Mardones, G. A., Rojas, A. L., daSilva, L. L., Prabhu, Y., Hurley, J. H., et al. (2010). Sorting of the Alzheimer's disease amyloid precursor protein mediated by the AP-4 complex. *Dev Cell*, *18*(3), 425-436.
- Cai, H., Wang, Y., McCarthy, D., Wen, H., Borchelt, D. R., Price, D. L., et al. (2001). BACE1 is the major beta-secretase for generation of Abeta peptides by neurons. *Nat Neurosci*, *4*(3), 233-234.
- Cai, X. D., Golde, T. E., & Younkin, S. G. (1993). Release of excess amyloid beta protein from a mutant amyloid beta protein precursor. *Science*, *259*(5094), 514-516.
- Capell, A., Behr, D., Prokop, S., Steiner, H., Kaether, C., Shearman, M. S., et al. (2005). Gamma-secretase complex assembly within the early secretory pathway. *J Biol Chem*, *280*(8), 6471-6478.
- Capell, A., Grunberg, J., Pesold, B., Diehlmann, A., Citron, M., Nixon, R., et al. (1998). The proteolytic fragments of the Alzheimer's disease-associated presenilin-1 form

References

- heterodimers and occur as a 100-150-kDa molecular mass complex. *J Biol Chem*, 273(6), 3205--3211.
- Capell, A., Steiner, H., Willem, M., Kaiser, H., Meyer, C., Walter, J., et al. (2000). Maturation and pro-peptide cleavage of beta-secretase. *J Biol Chem*, 275(40), 30849-30854.
- Caporaso, G. L., Takei, K., Gandy, S. E., Matteoli, M., Mundigl, O., Greengard, P., et al. (1994). Morphologic and biochemical analysis of the intracellular trafficking of the Alzheimer beta/A4 amyloid precursor protein. *J Neurosci*, 14(5 Pt 2), 3122-3138.
- Cataldo, A. M., Barnett, J. L., Pieroni, C., & Nixon, R. A. (1997). Increased neuronal endocytosis and protease delivery to early endosomes in sporadic Alzheimer's disease: neuropathologic evidence for a mechanism of increased beta-amyloidogenesis. *J Neurosci*, 17(16), 6142-6151.
- Chang, W. J., Ying, Y. S., Rothberg, K. G., Hooper, N. M., Turner, A. J., Gambliel, H. A., et al. (1994). Purification and characterization of smooth muscle cell caveolae. *J Cell Biol*, 126(1), 127-138.
- Chartier-Harlin, M. C., Parfitt, M., Legrain, S., Perez-Tur, J., Brousseau, T., Evans, A., et al. (1994). Apolipoprotein E, epsilon 4 allele as a major risk factor for sporadic early and late-onset forms of Alzheimer's disease: analysis of the 19q13.2 chromosomal region. *Hum Mol Genet*, 3(4), 569-574.
- Chen, F., Hasegawa, H., Schmitt-Ulms, G., Kawarai, T., Bohm, C., Katayama, T., et al. (2006). TMP21 is a presenilin complex component that modulates gamma-secretase but not epsilon-secretase activity. *Nature*, 440(7088), 1208-1212.
- Chen, F., Yang, D. S., Petanceska, S., Yang, A., Tandon, A., Yu, G., et al. (2000). Carboxyl-terminal fragments of Alzheimer beta-amyloid precursor protein accumulate in restricted and unpredicted intracellular compartments in presenilin 1-deficient cells. *J Biol Chem*, 275(47), 36794-36802.
- Chen, F. S., Hasegawa, H., Schmitt-Ulms, G., Kawarai, T., Bohm, C., Katayama, T., et al. (2006). TMP21 is a presenilin complex component that modulates gamma-secretase but not epsilon-secretase activity. *Nature*, 440(7088), 1208-1212.
- Cheng, S. V., Nadeau, J. H., Tanzi, R. E., Watkins, P. C., Jagadesh, J., Taylor, B. A., et al. (1988). Comparative mapping of DNA markers from the familial Alzheimer disease and Down syndrome regions of human chromosome 21 to mouse chromosomes 16 and 17. *Proc Natl Acad Sci U S A*, 85(16), 6032-6036.
- Christensen, M. A., Zhou, W., Qing, H., Lehman, A., Philipsen, S., & Song, W. (2004). Transcriptional regulation of BACE1, the beta-amyloid precursor protein beta-secretase, by Sp1. *Mol Cell Biol*, 24(2), 865-874.
- Chyung, A. S., Greenberg, B. D., Cook, D. G., Doms, R. W., & Lee, V. M. (1997). Novel beta-secretase cleavage of beta-amyloid precursor protein in the endoplasmic reticulum/intermediate compartment of NT2N cells. *J Cell Biol*, 138(3), 671-680.
- Chyung, J. H., Raper, D. M., & Selkoe, D. J. (2005). Gamma-secretase exists on the plasma membrane as an intact complex that accepts substrates and effects intramembrane cleavage. *J Biol Chem*, 280(6), 4383-4392.

References

- Cirrito, J. R., Kang, J. E., Lee, J., Stewart, F. R., Verges, D. K., Silverio, L. M., et al. (2008). Endocytosis is required for synaptic activity-dependent release of amyloid-beta in vivo. *Neuron*, 58(1), 42-51.
- Citron, M., Oltersdorf, T., Haass, C., McConlogue, L., Hung, A. Y., Seubert, P., et al. (1992). Mutation of the beta-amyloid precursor protein in familial Alzheimer's disease increases beta-protein production. *Nature*, 360(6405), 672-674.
- Citron, M., Westaway, D., Xia, W., Carlson, G., Diehl, T., Levesque, G., et al. (1997). Mutant presenilins of Alzheimer's disease increase production of 42-residue amyloid beta-protein in both transfected cells and transgenic mice. *Nat Med*, 3(1), 67-72.
- Cook, D. G., Forman, M. S., Sung, J. C., Leight, S., Kolson, D. L., Iwatsubo, T., et al. (1997). Alzheimer's A beta(1-42) is generated in the endoplasmic reticulum/intermediate compartment of NT2N cells. *Nat Med*, 3(9), 1021--1023.
- Corder, E. H., Saunders, A. M., Strittmatter, W. J., Schmechel, D. E., Gaskell, P. C., Small, G. W., et al. (1993). Gene dose of apolipoprotein E type 4 allele and the risk of Alzheimer's disease in late onset families. *Science*, 261(5123), 921-923.
- Cordy, J. M., Hussain, I., Dingwall, C., Hooper, N. M., & Turner, A. J. (2003). Exclusively targeting beta-secretase to lipid rafts by GPI-anchor addition up-regulates beta-site processing of the amyloid precursor protein. *Proc Natl Acad Sci U S A*, 100(20), 11735-11740.
- Cosson, P., & Letourneur, F. (1994a). Coatamer interaction with di-lysine endoplasmic reticulum retention motifs. *Science*, 263(5153), 1629-1631.
- Cosson, P., & Letourneur, F. (1994b). Coatamer interaction with di-lysine endoplasmic reticulum retention motifs. *Science*, 263(5153), 1629--1631.
- Cosson, P., & Letourneur, F. (1997). Coatamer (COPI)-coated vesicles: role in intracellular transport and protein sorting. *Current opinion in cell biology*, 9(4), 484-487.
- Creemers, J. W., Ines Dominguez, D., Plets, E., Serneels, L., Taylor, N. A., Multhaup, G., et al. (2001). Processing of beta-secretase by furin and other members of the proprotein convertase family. *J Biol Chem*, 276(6), 4211-4217.
- Cupers, P., Bentahir, M., Craessaerts, K., Orleans, I., Vanderstichele, H., Saftig, P., et al. (2001). The discrepancy between presenilin subcellular localization and gamma-secretase processing of amyloid precursor protein. *J Cell Biol*, 154(4), 731-740.
- de Sauvage, F., & Octave, J. N. (1989). A novel mRNA of the A4 amyloid precursor gene coding for a possibly secreted protein. *Science*, 245(4918), 651-653.
- De Strooper, B. (2003). Aph-1, Pen-2, and nicastrin with presenilin generate an active gamma-secretase complex. *Neuron*, 38(1), 9-12.
- De Strooper, B., Annaert, W., Cupers, P., Saftig, P., Craessaerts, K., Mumm, J. S., et al. (1999). A presenilin-1-dependent gamma-secretase-like protease mediates release of Notch intracellular domain. *Nature*, 398(6727), 518-522.
- De Strooper, B., Beullens, M., Contreras, B., Levesque, L., Craessaerts, K., Cordell, B., et al. (1997). Phosphorylation, subcellular localization, and membrane orientation of the Alzheimer's disease-associated presenilins. *Journal of Biological Chemistry*, 272(6), 3590-3598.

References

- De Strooper, B., Saftig, P., Craessaerts, K., Vanderstichele, H., Guhde, G., Annaert, W., et al. (1998). Deficiency of presenilin-1 inhibits the normal cleavage of amyloid precursor protein. *Nature*, *391*(6665), 387-390.
- De Strooper, B., Saftig, P., Craessaerts, K., Vanderstichele, H., Guhde, G., Annaert, W., et al. (1998). Deficiency of presenilin-1 inhibits the normal cleavage of amyloid precursor protein. *Nature*, *391*(6665), 387-390.
- Deng, Y., Wang, Z., Wang, R., Zhang, X., Zhang, S., Wu, Y., et al. (2013). Amyloid-beta protein (A β) Glu11 is the major beta-secretase site of beta-site amyloid-beta precursor protein-cleaving enzyme 1(BACE1), and shifting the cleavage site to A β Asp1 contributes to Alzheimer pathogenesis. *Eur J Neurosci*, *37*(12), 1962-1969.
- Denzel, A., Otto, F., Girod, A., Pepperkok, R., Watson, R., Rosewell, I., et al. (2000a). The p24 family member p23 is required for early embryonic development. *Curr Biol*, *10*(1), 55--58.
- Denzel, A., Otto, F., Girod, A., Pepperkok, R., Watson, R., Rosewell, I., et al. (2000b). The p24 family member p23 is required for early embryonic development. *Curr Biol*, *10*(1), 55-58.
- Dolcini, V., Dunys, J., Sevalle, J., Chen, F., Guillot-Sestier, M. V., George-Hyslop, P. S., et al. (2008). TMP21 regulates A β production but does not affect caspase-3, p53, and neprilysin. *Biochemical and Biophysical Research Communications*, *371*(1), 69-74.
- Dominguez, M., Dejgaard, K., Fullekrug, J., Dahan, S., Fazel, A., Paccaud, J. P., et al. (1998). gp25L/emp24/p24 protein family members of the cis-Golgi network bind both COP I and II coatomer. *J Cell Biol*, *140*(4), 751-765.
- Dominguez, M., Dejgaard, K., Füllekrug, J., Dahan, S., Fazel, A., Paccaud, J. P., et al. (1998). gp25L/emp24/p24 protein family members of the cis-Golgi network bind both COP I and II coatomer. *J Cell Biol*, *140*(4), 751--765.
- Edbauer, D., Winkler, E., Haass, C., & Steiner, H. (2002). Presenilin and nicastrin regulate each other and determine amyloid beta-peptide production via complex formation. *Proc Natl Acad Sci U S A*, *99*(13), 8666-8671.
- Eehalt, R., Keller, P., Haass, C., Thiele, C., & Simons, K. (2003). Amyloidogenic processing of the Alzheimer beta-amyloid precursor protein depends on lipid rafts. *J Cell Biol*, *160*(1), 113-123.
- Ellgaard, L., & Helenius, A. (2001). ER quality control: towards an understanding at the molecular level. *Curr Opin Cell Biol*, *13*(4), 431-437.
- Ellgaard, L., & Helenius, A. (2003). Quality control in the endoplasmic reticulum. *Nat Rev Mol Cell Biol*, *4*(3), 181-191.
- Elortza, F., Nuhse, T. S., Foster, L. J., Stensballe, A., Peck, S. C., & Jensen, O. N. (2003). Proteomic analysis of glycosylphosphatidylinositol-anchored membrane proteins. *Mol Cell Proteomics*, *2*(12), 1261-1270.
- Emery, G., Gruenberg, J., & Rojo, M. (1999). The p24 family of transmembrane proteins at the interface between endoplasmic reticulum and Golgi apparatus. *Protoplasma*, *207*(1-2), 24-30.

References

- Emery, G., Rojo, M., & Gruenberg, J. (2000). Coupled transport of p24 family members. *J Cell Sci*, *113* (Pt 13), 2507-2516.
- Ennis, H. L., & Lubin, M. (1964). Cycloheximide: Aspects of Inhibition of Protein Synthesis in Mammalian Cells. *Science*, *146*(3650), 1474-1476.
- Esch, F. S., Keim, P. S., Beattie, E. C., Blacher, R. W., Culwell, A. R., Oltersdorf, T., et al. (1990). Cleavage of amyloid beta peptide during constitutive processing of its precursor. *Science*, *248*(4959), 1122-1124.
- Feil, R., Brocard, J., Mascrez, B., LeMeur, M., Metzger, D., & Chambon, P. (1996). Ligand-activated site-specific recombination in mice. *Proc Natl Acad Sci U S A*, *93*(20), 10887-10890.
- Foster, L. J., De Hoog, C. L., & Mann, M. (2003). Unbiased quantitative proteomics of lipid rafts reveals high specificity for signaling factors. *Proc Natl Acad Sci U S A*, *100*(10), 5813-5818.
- Fraering, P. C., LaVoie, M. J., Ye, W., Ostaszewski, B. L., Kimberly, W. T., Selkoe, D. J., et al. (2004). Detergent-dependent dissociation of active gamma-secretase reveals an interaction between Pen-2 and PS1-NTF and offers a model for subunit organization within the complex. *Biochemistry*, *43*(2), 323-333.
- Freund, M., Asang, C., Kammler, S., Konermann, C., Krummheuer, J., Hipp, M., et al. (2003). A novel approach to describe a U1 snRNA binding site. *Nucleic Acids Res*, *31*(23), 6963-6975.
- Fujita, M., & Jigami, Y. (2008). Lipid remodeling of GPI-anchored proteins and its function. *Biochimica et Biophysica Acta (BBA)-General Subjects*, *1780*(3), 410-420.
- Fujita, M., & Kinoshita, T. (2008). Structural remodeling of GPI anchors during biosynthesis and after attachment to proteins. *FEBS letters*, *584*(9), 1670-1677.
- Fujita, M., Watanabe, R., Jaensch, N., Romanova-Michaelides, M., Satoh, T., Kato, M., et al. (2011). Sorting of GPI-anchored proteins into ER exit sites by p24 proteins is dependent on remodeled GPI. *J Cell Biol*, *194*(1), 61-75.
- Fukumori, A., Fluhrer, R., Steiner, H., & Haass, C. (2010). Three-amino acid spacing of presenilin endoproteolysis suggests a general stepwise cleavage of gamma-secretase-mediated intramembrane proteolysis. *J Neurosci*, *30*(23), 7853-7862.
- Fullekrug, J., Suganuma, T., Tang, B. L., Hong, W., Storrie, B., & Nilsson, T. (1999). Localization and recycling of gp27 (hp24gamma3): complex formation with other p24 family members. *Mol Biol Cell*, *10*(6), 1939-1955.
- Gahmberg, N., Pettersson, R. F., & Kaanainen, L. (1986). Efficient transport of Semliki Forest virus glycoproteins through a Golgi complex morphologically altered by Uukuniemi virus glycoproteins. *The EMBO journal*, *5*(12), 3111.
- Glenner, G. G., & Wong, C. W. (1984). Alzheimer's disease: initial report of the purification and characterization of a novel cerebrovascular amyloid protein. *Biochem Biophys Res Commun*, *120*(3), 885-890.
- Goate, A., Chartier-Harlin, M. C., Mullan, M., Brown, J., Crawford, F., Fidani, L., et al. (1991). Segregation of a missense mutation in the amyloid precursor protein gene with familial Alzheimer's disease. *Nature*, *349*(6311), 704-706.

References

- Golde, T. E., Estus, S., Younkin, L. H., Selkoe, D. J., & Younkin, S. G. (1992). Processing of the amyloid protein precursor to potentially amyloidogenic derivatives. *Science*, *255*(5045), 728--730.
- Goldgaber, D., Lerman, M. I., McBride, O. W., Saffiotti, U., & Gajdusek, D. C. (1987). Characterization and chromosomal localization of a cDNA encoding brain amyloid of Alzheimer's disease. *Science*, *235*(4791), 877-880.
- Gommel, D., Orci, L., Emig, E. M., Hannah, M. J., Ravazzola, M., Nickel, W., et al. (1999). p24 and p23, the major transmembrane proteins of COPI-coated transport vesicles, form hetero-oligomeric complexes and cycle between the organelles of the early secretory pathway. *FEBS Lett*, *447*(2-3), 179-185.
- Gommel, D. U., Memon, A. R., Heiss, A., Lottspeich, F., Pfannstiel, J., Lechner, J., et al. (2001). Recruitment to Golgi membranes of ADP-ribosylation factor 1 is mediated by the cytoplasmic domain of p23. *EMBO J*, *20*(23), 6751-6760.
- Gong, P., Roseman, J., Fernandez, C. G., Vetrivel, K. S., Bindokas, V. P., Zitzow, L. A., et al. (2011). Transgenic neuronal overexpression reveals that stringently regulated p23 expression is critical for coordinated movement in mice. *Mol Neurodegener*, *6*, 87.
- Gong, P., Roseman, J., Vetrivel, K. S., Bindokas, V. P., Zitzow, L. A., Kar, S., et al. (2012). Stringently regulated p23 expression is critical for coordinated movement in mice: implications for Alzheimer's disease. *Mol Neurodegener*, *7 Suppl 1*, L2.
- Gooding, C., Clark, F., Wollerton, M. C., Grellscheid, S. N., Groom, H., & Smith, C. W. (2006). A class of human exons with predicted distant branch points revealed by analysis of AG dinucleotide exclusion zones. *Genome Biol*, *7*(1), R1.
- Gouras, G. K., Xu, H., Jovanovic, J. N., Buxbaum, J. D., Wang, R., Greengard, P., et al. (1998). Generation and regulation of beta-amyloid peptide variants by neurons. *J Neurochem*, *71*(5), 1920-1925.
- Haass, C., Hung, A. Y., Schlossmacher, M. G., Oltersdorf, T., Teplow, D. B., & Selkoe, D. J. (1993). Normal cellular processing of the beta-amyloid precursor protein results in the secretion of the amyloid beta peptide and related molecules. *Ann N Y Acad Sci*, *695*, 109-116.
- Haass, C., Koo, E. H., Capell, A., Teplow, D. B., & Selkoe, D. J. (1995). Polarized sorting of beta-amyloid precursor protein and its proteolytic products in MDCK cells is regulated by two independent signals. *J Cell Biol*, *128*(4), 537-547.
- Haass, C., Koo, E. H., Mellon, A., Hung, A. Y., & Selkoe, D. J. (1992). Targeting of cell-surface beta-amyloid precursor protein to lysosomes: alternative processing into amyloid-bearing fragments. *Nature*, *357*(6378), 500--503.
- Haass, C., Lemere, C. A., Capell, A., Citron, M., Seubert, P., Schenk, D., et al. (1995). The Swedish mutation causes early-onset Alzheimer's disease by beta-secretase cleavage within the secretory pathway. *Nat Med*, *1*(12), 1291-1296.
- Hansen, G. H., Niels-Christiansen, L. L., Thorsen, E., Immerdal, L., & Danielsen, E. M. (2000). Cholesterol depletion of enterocytes. Effect on the Golgi complex and apical membrane trafficking. *J Biol Chem*, *275*(7), 5136-5142.

References

- Harold, D., Abraham, R., Hollingworth, P., Sims, R., Gerrish, A., Hamshere, M. L., et al. (2009). Genome-wide association study identifies variants at *CLU* and *PICALM* associated with Alzheimer's disease. *Nature genetics*, *41*(10), 1088-1093.
- Harris, B., Pereira, I., & Parkin, E. (2009). Targeting ADAM10 to lipid rafts in neuroblastoma SH-SY5Y cells impairs amyloidogenic processing of the amyloid precursor protein. *Brain Res*, *1296*, 203-215.
- Harter, C., & Wieland, F. T. (1998). A single binding site for dilysine retrieval motifs and p23 within the $\text{C}\epsilon\geq$ subunit of coatamer. *Proceedings of the National Academy of Sciences*, *95*(20), 11649-11654.
- Hartmann, L., Theiss, S., Niederacher, D., & Schaal, H. (2008). Diagnostics of pathogenic splicing mutations: does bioinformatics cover all bases? *Front Biosci*, *13*, 3252-3272.
- Hasegawa, H., Liu, L., & Nishimura, M. (2010). Dilysine retrieval signal-containing p24 proteins collaborate in inhibiting gamma-cleavage of amyloid precursor protein. *J Neurochem*.
- Hattori, C., Asai, M., Onishi, H., Sasagawa, N., Hashimoto, Y., Saido, T. C., et al. (2006). BACE1 interacts with lipid raft proteins. *J Neurosci Res*, *84*(4), 912-917.
- He, X., Chang, W. P., Koelsch, G., & Tang, J. (2002). Memapsin 2 (beta-secretase) cytosolic domain binds to the VHS domains of GGA1 and GGA2: implications on the endocytosis mechanism of memapsin 2. *FEBS Lett*, *524*(1-3), 183-187.
- He, X., Li, F., Chang, W. P., & Tang, J. (2005). GGA proteins mediate the recycling pathway of memapsin 2 (BACE). *J Biol Chem*, *280*(12), 11696-11703.
- He, X., Zhu, G., Koelsch, G., Rodgers, K. K., Zhang, X. C., & Tang, J. (2003). Biochemical and structural characterization of the interaction of memapsin 2 (beta-secretase) cytosolic domain with the VHS domain of GGA proteins. *Biochemistry*, *42*(42), 12174-12180.
- Helfman, D. M., & Ricci, W. M. (1989). Branch point selection in alternative splicing of tropomyosin pre-mRNAs. *Nucleic Acids Res*, *17*(14), 5633-5650.
- Hilioti, Z., Gallagher, D. A., Low-Nam, S. T., Ramaswamy, P., Gajer, P., Kingsbury, T. J., et al. (2004). GSK-3 kinases enhance calcineurin signaling by phosphorylation of RCNs. *Genes Dev*, *18*(1), 35-47.
- Hollingworth, P., Harold, D., Sims, R., Gerrish, A., Lambert, J.-C., Carrasquillo, M. M., et al. (2011). Common variants at *ABCA7*, *MS4A6A/MS4A4E*, *EPHA1*, *CD33* and *CD2AP* are associated with Alzheimer's disease. *Nature genetics*, *43*(5), 429-435.
- Hook, V. Y., Toneff, T., Aaron, W., Yasothornsrikul, S., Bunday, R., & Reisine, T. (2002). Beta-amyloid peptide in regulated secretory vesicles of chromaffin cells: evidence for multiple cysteine proteolytic activities in distinct pathways for beta-secretase activity in chromaffin vesicles. *J Neurochem*, *81*(2), 237-256.
- Hsia, A. Y., Masliah, E., McConlogue, L., Yu, G. Q., Tatsuno, G., Hu, K., et al. (1999). Plaque-independent disruption of neural circuits in Alzheimer's disease mouse models. *Proc Natl Acad Sci U S A*, *96*(6), 3228-3233.
- Hu, Y., & Fortini, M. E. (2003). Different cofactor activities in gamma-secretase assembly: evidence for a nicastrin-Aph-1 subcomplex. *J Cell Biol*, *161*(4), 685-690.

References

- Hur, J. Y., Teranishi, Y., Kihara, T., Yamamoto, N. G., Inoue, M., Hosia, W., et al. (2012). Identification of novel gamma-secretase-associated proteins in detergent-resistant membranes from brain. *J Biol Chem*, 287(15), 11991-12005.
- Huse, J. T., Liu, K., Pijak, D. S., Carlin, D., Lee, V. M., & Doms, R. W. (2002). Beta-secretase processing in the trans-Golgi network preferentially generates truncated amyloid species that accumulate in Alzheimer's disease brain. *J Biol Chem*, 277(18), 16278-16284.
- Huse, J. T., Pijak, D. S., Leslie, G. J., Lee, V. M., & Doms, R. W. (2000). Maturation and endosomal targeting of beta-site amyloid precursor protein-cleaving enzyme. The Alzheimer's disease beta-secretase. *J Biol Chem*, 275(43), 33729-33737.
- Hussain, I., Powell, D., Howlett, D. R., Tew, D. G., Meek, T. D., Chapman, C., et al. (1999). Identification of a novel aspartic protease (Asp 2) as beta-secretase. *Mol Cell Neurosci*, 14(6), 419-427.
- Hutton, M., Lendon, C. L., Rizzu, P., Baker, M., Froelich, S., Houlden, H., et al. (1998). Association of missense and 5'-splice-site mutations in tau with the inherited dementia FTDP-17. *Nature*, 393(6686), 702-705.
- Ikezawa, H. (2002). Glycosylphosphatidylinositol (GPI)-anchored proteins. *Biol Pharm Bull*, 25(4), 409-417.
- Jackson, M. R., Nilsson, T., & Peterson, P. A. (1990). Identification of a consensus motif for retention of transmembrane proteins in the endoplasmic reticulum. *Embo J*, 9(10), 3153--3162.
- Jenne, N., Frey, K., Brugger, B., & Wieland, F. T. (2002). Oligomeric state and stoichiometry of p24 proteins in the early secretory pathway. *J Biol Chem*, 277(48), 46504-46511.
- Kaether, C., Schmitt, S., Willem, M., & Haass, C. (2006). Amyloid precursor protein and Notch intracellular domains are generated after transport of their precursors to the cell surface. *Traffic*, 7(4), 408-415.
- Kang, J., Lemaire, H. G., Unterbeck, A., Salbaum, J. M., Masters, C. L., Grzeschik, K. H., et al. (1987). The precursor of Alzheimer's disease amyloid A4 protein resembles a cell-surface receptor. *Nature*, 325(6106), 733-736.
- Kim, S. H., Yin, Y. I., Li, Y. M., & Sisodia, S. S. (2004). Evidence that assembly of an active gamma-secretase complex occurs in the early compartments of the secretory pathway. *J Biol Chem*, 279(47), 48615-48619.
- Kimberly, W. T., LaVoie, M. J., Ostaszewski, B. L., Ye, W., Wolfe, M. S., & Selkoe, D. J. (2003). Gamma-secretase is a membrane protein complex comprised of presenilin, nicastrin, Aph-1, and Pen-2. *Proc Natl Acad Sci U S A*, 100(11), 6382-6387.
- King, G. D., & Scott Turner, R. (2004). Adaptor protein interactions: modulators of amyloid precursor protein metabolism and Alzheimer's disease risk? *Exp Neurol*, 185(2), 208-219.
- Kingsbury, T. J., & Cunningham, K. W. (2000). A conserved family of calcineurin regulators. *Genes Dev*, 14(13), 1595-1604.
- Kinoshita, A., Fukumoto, H., Shah, T., Whelan, C. M., Irizarry, M. C., & Hyman, B. T. (2003). Demonstration by FRET of BACE interaction with the amyloid precursor protein at the cell surface and in early endosomes. *J Cell Sci*, 116(Pt 16), 3339-3346.

References

- Kinoshita, T., Fujita, M., & Maeda, Y. (2008). Biosynthesis, remodelling and functions of mammalian GPI-anchored proteins: recent progress. *Journal of biochemistry*, *144*(3), 287-294.
- Kinoshita, T., & Inoue, N. (2000). Dissecting and manipulating the pathway for glycosylphosphatidylinositol-anchor biosynthesis. *Curr Opin Chem Biol*, *4*(6), 632-638.
- Kitaguchi, N., Takahashi, Y., Tokushima, Y., Shiojiri, S., & Ito, H. (1988). Novel precursor of Alzheimer's disease amyloid protein shows protease inhibitory activity. *Nature*, *331*(6156), 530-532.
- Konig, G., Beyreuther, K., Masters, C. L., Schmitt, H. P., & Salbaum, J. M. (1989). PreA4 mRNA distribution in brain areas. *Prog Clin Biol Res*, *317*, 1027-1036.
- Koo, E. H., & Squazzo, S. L. (1994). Evidence that production and release of amyloid beta-protein involves the endocytic pathway. *J Biol Chem*, *269*(26), 17386--17389.
- Koo, E. H., Squazzo, S. L., Selkoe, D. J., & Koo, C. H. (1996). Trafficking of cell-surface amyloid beta-protein precursor. I. Secretion, endocytosis and recycling as detected by labeled monoclonal antibody. *J Cell Sci*, *109* (Pt 5), 991--998.
- Kozutsumi, Y., Segal, M., Normington, K., Gething, M.-J., & Sambrook, J. (1988). The presence of malfolded proteins in the endoplasmic reticulum signals the induction of glucose-regulated proteins.
- Kuehn, M. J., & Schekman, R. (1997). COPII and secretory cargo capture into transport vesicles. *Current opinion in cell biology*, *9*(4), 477-483.
- Lai, A., Sisodia, S. S., & Trowbridge, I. S. (1995). Characterization of sorting signals in the beta-amyloid precursor protein cytoplasmic domain. *J Biol Chem*, *270*(8), 3565-3573.
- Lambert, J. C., Heath, S., Even, G., Champion, D., Slegers, K., Hiltunen, M., et al. (2009). Genome-wide association study identifies variants at CLU and CR1 associated with Alzheimer's disease. *Nat Genet*, *41*(10), 1094-1099.
- Lambert, M. P., Barlow, A. K., Chromy, B. A., Edwards, C., Freed, R., Liosatos, M., et al. (1998). Diffusible, nonfibrillar ligands derived from Abeta1-42 are potent central nervous system neurotoxins. *Proc Natl Acad Sci U S A*, *95*(11), 6448-6453.
- Langhans, M., Marcote, M. J., Pimpl, P., Virgili-Lopez, G., Robinson, D. G., & Aniento, F. (2008). In vivo trafficking and localization of p24 proteins in plant cells. *Traffic*, *9*(5), 770-785.
- LaVoie, M. J., Fraering, P. C., Ostaszewski, B. L., Ye, W., Kimberly, W. T., Wolfe, M. S., et al. (2003). Assembly of the gamma-secretase complex involves early formation of an intermediate subcomplex of Aph-1 and nicastrin. *J Biol Chem*, *278*(39), 37213-37222.
- Lee, J., Retamal, C., Cuitino, L., Caruano-Yzermans, A., Shin, J. E., van Kerkhof, P., et al. (2008). Adaptor protein sorting nexin 17 regulates amyloid precursor protein trafficking and processing in the early endosomes. *J Biol Chem*, *283*(17), 11501-11508.
- Lee, M. C., Miller, E. A., Goldberg, J., Orci, L., & Schekman, R. (2004). Bi-directional protein transport between the ER and Golgi. *Annu Rev Cell Dev Biol*, *20*, 87-123.
- Letourneur, F., Gaynor, E. C., Hennecke, S., Demolliere, C., Duden, R., Emr, S. D., et al. (1994). Coatamer is essential for retrieval of dilysine-tagged proteins to the endoplasmic reticulum. *Cell*, *79*(7), 1199-1207.

References

- Letourneur, F., Gaynor, E. C., Hennecke, S., Démollière, C., Duden, R., Emr, S. D., et al. (1994). Coatamer is essential for retrieval of dilysine-tagged proteins to the endoplasmic reticulum. *Cell*, 79(7), 1199--1207.
- Li, K.-C., Liu, C.-T., Sun, W., Yuan, S., & Yu, T. (2004). A system for enhancing genome-wide coexpression dynamics study. *Proceedings of the National Academy of Sciences of the United States of America*, 101(44), 15561-15566.
- Li, Y., Zhou, W., Tong, Y., He, G., & Song, W. (2006). Control of APP processing and Abeta generation level by BACE1 enzymatic activity and transcription. *FASEB J*, 20(2), 285-292.
- Liao, P.-Y., Lee, Kelvin H. (2010). From SNPs to functional polymorphism: The insight into biotechnology applications. [JOUR]. *Biochemical Engineering Journal*, 49(2), 9.
- Lin, X., Koelsch, G., Wu, S., Downs, D., Dashti, A., & Tang, J. (2000). Human aspartic protease memapsin 2 cleaves the beta-secretase site of beta-amyloid precursor protein. *Proc Natl Acad Sci U S A*, 97(4), 1456-1460.
- Lindholm, D., Wootz, H., & Korhonen, L. (2006). ER stress and neurodegenerative diseases. *Cell Death & Differentiation*, 13(3), 385-392.
- Liu, K., Doms, R. W., & Lee, V. M. (2002). Glu11 site cleavage and N-terminally truncated A beta production upon BACE overexpression. *Biochemistry*, 41(9), 3128-3136.
- Liu, S., Zhang, S., Bromley-Brits, K., Cai, F., Zhou, W., Xia, K., et al. (2011). Transcriptional Regulation of TMP21 by NFAT. *Mol Neurodegener*, 6, 21.
- Liu, S. C., Bromley-Brits, K., Xia, K., Mittelholtz, J., Wang, R. T., & Song, W. (2008). TMP21 degradation is mediated by the ubiquitin-proteasome pathway. *European Journal of Neuroscience*, 28(10), 1980-1988.
- London, E., & Brown, D. A. (2000). Insolubility of lipids in triton X-100: physical origin and relationship to sphingolipid/cholesterol membrane domains (rafts). *Biochim Biophys Acta*, 1508(1-2), 182-195.
- Lord, J. M., Davey, J., Frigerio, L., & Roberts, L. M. (2000). Endoplasmic reticulum-associated protein degradation. *Semin Cell Dev Biol*, 11(3), 159-164.
- Lowe, M., & Kreis, T. E. (1998). Regulation of membrane traffic in animal cells by COPI. *Biochimica et Biophysica Acta (BBA)-Molecular Cell Research*, 1404(1), 53-66.
- Luo, W., Wang, Y., & Reiser, G. (2007). p24A, a type I transmembrane protein, controls ARF1-dependent resensitization of protease-activated receptor-2 by influence on receptor trafficking. *J Biol Chem*, 282(41), 30246-30255.
- Luo, Y., Bolon, B., Kahn, S., Bennett, B. D., Babu-Khan, S., Denis, P., et al. (2001). Mice deficient in BACE1, the Alzheimer's beta-secretase, have normal phenotype and abolished beta-amyloid generation. *Nat Neurosci*, 4(3), 231-232.
- Ly, P. T., Cai, F., & Song, W. (2011). Detection of neuritic plaques in Alzheimer's disease mouse model. *J Vis Exp*(53).
- Ly, P. T., Wu, Y., Zou, H., Wang, R., Zhou, W., Kinoshita, A., et al. (2012). Inhibition of GSK3beta-mediated BACE1 expression reduces Alzheimer-associated phenotypes. *J Clin Invest*, 123(1), 224-235.

References

- Maltese, W. A., Wilson, S., Tan, Y., Suomensaaari, S., Sinha, S., Barbour, R., et al. (2001). Retention of the Alzheimer's amyloid precursor fragment C99 in the endoplasmic reticulum prevents formation of amyloid beta-peptide. *J Biol Chem*, 276(23), 20267-20279.
- Marlow, L., Cain, M., Pappolla, M. A., & Sambamurti, K. (2003). Beta-secretase processing of the Alzheimer's amyloid protein precursor (APP). *J Mol Neurosci*, 20(3), 233-239.
- Martone, R. L., Zhou, H., Atchison, K., Comery, T., Xu, J. Z., Huang, X., et al. (2009). Begacestat (GSI-953): a novel, selective thiophene sulfonamide inhibitor of amyloid precursor protein gamma-secretase for the treatment of Alzheimer's disease. *J Pharmacol Exp Ther*, 331(2), 598-608.
- Marzioch, M., Henthorn, D. C., Herrmann, J. M., Wilson, R., Thomas, D. Y., Bergeron, J. J., et al. (1999). Erp1p and Erp2p, partners for Emp24p and Erv25p in a yeast p24 complex. *Mol Biol Cell*, 10(6), 1923-1938.
- Masters, C. L., Simms, G., Weinman, N. A., Multhaup, G., McDonald, B. L., & Beyreuther, K. (1985). Amyloid plaque core protein in Alzheimer disease and Down syndrome. *Proc Natl Acad Sci U S A*, 82(12), 4245-4249.
- Moore, M. J. (2000). Intron recognition comes of AGE. *Nat Struct Biol*, 7(1), 14-16.
- Morsomme, P., Prescianotto-Baschong, C., & Riezman, H. (2003). The ER v-SNAREs are required for GPI-anchored protein sorting from other secretory proteins upon exit from the ER. *J Cell Biol*, 162(3), 403-412.
- Morsomme, P., & Riezman, H. (2002). The Rab GTPase Ypt1p and tethering factors couple protein sorting at the ER to vesicle targeting to the Golgi apparatus. *Dev Cell*, 2(3), 307-317.
- Mucke, L., Masliah, E., Yu, G. Q., Mallory, M., Rockenstein, E. M., Tatsuno, G., et al. (2000). High-level neuronal expression of abeta 1-42 in wild-type human amyloid protein precursor transgenic mice: synaptotoxicity without plaque formation. *J Neurosci*, 20(11), 4050-4058.
- Mullan, M., Crawford, F., Axelman, K., Houlden, H., Lilius, L., Winblad, B., et al. (1992). A pathogenic mutation for probable Alzheimer's disease in the APP gene at the N-terminus of beta-amyloid. *Nat Genet*, 1(5), 345-347.
- Mullan, M., Houlden, H., Windelspecht, M., Fidani, L., Lombardi, C., Diaz, P., et al. (1992). A locus for familial early-onset Alzheimer's disease on the long arm of chromosome 14, proximal to the alpha 1-antichymotrypsin gene. *Nat Genet*, 2(4), 340-342.
- Muniz, M., Nuoffer, C., Hauri, H. P., & Riezman, H. (2000). The Emp24 complex recruits a specific cargo molecule into endoplasmic reticulum-derived vesicles. *J Cell Biol*, 148(5), 925-930.
- Naj, A. C., Jun, G., Beecham, G. W., Wang, L.-S., Vardarajan, B. N., Buross, J., et al. (2011). Common variants at MS4A4/MS4A6E, CD2AP, CD33 and EPHA1 are associated with late-onset Alzheimer's disease. *Nature genetics*, 43(5), 436-441.
- Naruse, S., Thinakaran, G., Luo, J. J., Kusiak, J. W., Tomita, T., Iwatsubo, T., et al. (1998). Effects of PS1 deficiency on membrane protein trafficking in neurons. *Neuron*, 21(5), 1213--1221.

References

- Nickel, W., Sohn, K., Bunning, C., & Wieland, F. T. (1997). p23, a major COPI-vesicle membrane protein, constitutively cycles through the early secretory pathway. *Proc Natl Acad Sci U S A*, *94*(21), 11393-11398.
- Niimura, M., Isoo, N., Takasugi, N., Tsuruoka, M., Ui-Tei, K., Saigo, K., et al. (2005). Aph-1 contributes to the stabilization and trafficking of the gamma-secretase complex through mechanisms involving intermolecular and intramolecular interactions. *J Biol Chem*, *280*(13), 12967-12975.
- Nordstedt, C., Caporaso, G. L., Thyberg, J., Gandy, S. E., & Greengard, P. (1993). Identification of the Alzheimer beta/A4 amyloid precursor protein in clathrin-coated vesicles purified from PC12 cells. *J Biol Chem*, *268*(1), 608--612.
- Ohno, M., Sametsky, E. A., Younkin, L. H., Oakley, H., Younkin, S. G., Citron, M., et al. (2004). BACE1 deficiency rescues memory deficits and cholinergic dysfunction in a mouse model of Alzheimer's disease. *Neuron*, *41*(1), 27-33.
- Okamura, K., Kimata, Y., Higashio, H., Tsuru, A., & Kohno, K. (2000). Dissociation of Kar2p/BiP from an ER sensory molecule, Ire1p, triggers the unfolded protein response in yeast. *Biochem Biophys Res Commun*, *279*(2), 445-450.
- Orr, N., & Chanock, S. (2008). Common genetic variation and human disease. *Adv Genet*, *62*, 1-32.
- Pagani, F., & Baralle, F. E. (2004). Genomic variants in exons and introns: identifying the splicing spoilers. *Nat Rev Genet*, *5*(5), 389-396.
- Pagani, F., Baralle, FE (2010). Analysis of Human Splicing Defects Using Hybrid Minigenes. *Molecular Diagnostic*, 115-169.
- Pagani, F., Buratti, E., Stuani, C., Bendix, R., Dork, T., & Baralle, F. E. (2002). A new type of mutation causes a splicing defect in ATM. *Nat Genet*, *30*(4), 426-429.
- Palotas, A., & Kalman, J. (2006). Candidate susceptibility genes in Alzheimer's disease are at high risk for being forgotten-- they don't give peace of mind. *Curr Drug Metab*, *7*(3), 273-293.
- Pardossi-Piquard, R., Bohm, C., Chen, F. S., Kanemoto, S., Checler, F., Schmitt-Ulms, G., et al. (2009). TMP21 Transmembrane Domain Regulates gamma-Secretase Cleavage. *Journal of Biological Chemistry*, *284*(42), 28634-28641.
- Park, I. H., Hwang, E. M., Hong, H. S., Boo, J. H., Oh, S. S., Lee, J., et al. (2003). Lovastatin enhances Abeta production and senile plaque deposition in female Tg2576 mice. *Neurobiol Aging*, *24*(5), 637-643.
- Parvathy, S., Hussain, I., Karran, E. H., Turner, A. J., & Hooper, N. M. (1999). Cleavage of Alzheimer's amyloid precursor protein by alpha-secretase occurs at the surface of neuronal cells. *Biochemistry*, *38*(30), 9728-9734.
- Parvathy, S., Karran, E. H., Turner, A. J., & Hooper, N. M. (1998). The secretases that cleave angiotensin converting enzyme and the amyloid precursor protein are distinct from tumour necrosis factor-alpha convertase. *FEBS Lett*, *431*(1), 63-65.
- Pastorino, L., Ikin, A. F., Nairn, A. C., Pursnani, A., & Buxbaum, J. D. (2002). The carboxyl-terminus of BACE contains a sorting signal that regulates BACE trafficking but not the formation of total A(beta). *Mol Cell Neurosci*, *19*(2), 175-185.

References

- Pedersen, N. L., Gatz, M., Berg, S., & Johansson, B. (2004). How heritable is Alzheimer's disease late in life? Findings from Swedish twins. *Ann Neurol*, *55*(2), 180-185.
- Perez, R. G., Soriano, S., Hayes, J. D., Ostaszewski, B., Xia, W., Selkoe, D. J., et al. (1999). Mutagenesis identifies new signals for beta-amyloid precursor protein endocytosis, turnover, and the generation of secreted fragments, including Abeta42. *J Biol Chem*, *274*(27), 18851--18856.
- Pike, L. J. (2006). Rafts defined: a report on the Keystone Symposium on Lipid Rafts and Cell Function. *J Lipid Res*, *47*(7), 1597-1598.
- R.F. Clark, M. H. (1995). The structure of the presenilin 1 (S182) gene and identification of six novel mutations in early onset AD families. Alzheimer's Disease Collaborative Group. *Nat Genet*, *11*(2), 219-222.
- Rajendran, L., Honsho, M., Zahn, T. R., Keller, P., Geiger, K. D., Verkade, P., et al. (2006). Alzheimer's disease beta-amyloid peptides are released in association with exosomes. *Proc Natl Acad Sci U S A*, *103*(30), 11172-11177.
- Rajendran, L., Schneider, A., Schlechtingen, G., Weidlich, S., Ries, J., Braxmeier, T., et al. (2008). Efficient inhibition of the Alzheimer's disease beta-secretase by membrane targeting. *Science*, *320*(5875), 520-523.
- Reaume, A. G., Howland, D. S., Trusko, S. P., Savage, M. J., Lang, D. M., Greenberg, B. D., et al. (1996). Enhanced amyloidogenic processing of the beta-amyloid precursor protein in gene-targeted mice bearing the Swedish familial Alzheimer's disease mutations and a "humanized" Abeta sequence. *J Biol Chem*, *271*(38), 23380-23388.
- Rechards, M., Xia, W., Oorschot, V., van Dijk, S., Annaert, W., Selkoe, D. J., et al. (2006). Presenilin-1-mediated retention of APP derivatives in early biosynthetic compartments. *Traffic*, *7*(3), 354-364.
- Rechards, M., Xia, W., Oorschot, V. M., Selkoe, D. J., & Klumperman, J. (2003). Presenilin-1 exists in both pre- and post-Golgi compartments and recycles via COPI-coated membranes. *Traffic*, *4*(8), 553-565.
- Riddell, D. R., Christie, G., Hussain, I., & Dingwall, C. (2001). Compartmentalization of beta-secretase (Asp2) into low-buoyant density, noncaveolar lipid rafts. *Curr Biol*, *11*(16), 1288-1293.
- Robakis, N. K., Ramakrishna, N., Wolfe, G., & Wisniewski, H. M. (1987). Molecular cloning and characterization of a cDNA encoding the cerebrovascular and the neuritic plaque amyloid peptides. *Proc Natl Acad Sci U S A*, *84*(12), 4190-4194.
- Roberds, S. L., Anderson, J., Basi, G., Bienkowski, M. J., Branstetter, D. G., Chen, K. S., et al. (2001). BACE knockout mice are healthy despite lacking the primary beta-secretase activity in brain: implications for Alzheimer's disease therapeutics. *Hum Mol Genet*, *10*(12), 1317-1324.
- Rogaev, E. I., Sherrington, R., Rogaeva, E. A., Levesque, G., Ikeda, M., Liang, Y., et al. (1995). Familial Alzheimer's disease in kindreds with missense mutations in a gene on chromosome 1 related to the Alzheimer's disease type 3 gene. *Nature*, *376*(6543), 775-778.

References

- Rojo, M., Emery, G., Marjomaki, V., McDowall, A. W., Parton, R. G., & Gruenberg, J. (2000). The transmembrane protein p23 contributes to the organization of the Golgi apparatus. *J Cell Sci*, 113 (Pt 6), 1043-1057.
- Rojo, M., Emery, G., Marjomäki, V., McDowall, A. W., Parton, R. G., & Gruenberg, J. (2000). The transmembrane protein p23 contributes to the organization of the Golgi apparatus. *J Cell Sci*, 113 (Pt 6), 1043--1057.
- Rojo, M., Pepperkok, R., Emery, G., Kellner, R., Stang, E., Parton, R. G., et al. (1997a). Involvement of the transmembrane protein p23 in biosynthetic protein transport. *J Cell Biol*, 139(5), 1119--1135.
- Rojo, M., Pepperkok, R., Emery, G., Kellner, R., Stang, E., Parton, R. G., et al. (1997b). Involvement of the transmembrane protein p23 in biosynthetic protein transport. *J Cell Biol*, 139(5), 1119-1135.
- Sakurai, T., Kaneko, K., Okuno, M., Wada, K., Kashiwayama, T., Shimizu, H., et al. (2008). Membrane microdomain switching: a regulatory mechanism of amyloid precursor protein processing. *J Cell Biol*, 183(2), 339-352.
- Sambamurti, K., Sevlever, D., Koothan, T., Refolo, L. M., Pinnix, I., Gandhi, S., et al. (1999). Glycosylphosphatidylinositol-anchored proteins play an important role in the biogenesis of the Alzheimer's amyloid beta-protein. *J Biol Chem*, 274(38), 26810-26814.
- Sandoval, I. V., & Carrasco, L. (1997). Poliovirus infection and expression of the poliovirus protein 2B provoke the disassembly of the Golgi complex, the organelle target for the antipoliovirus drug Ro-090179. *Journal of virology*, 71(6), 4679-4693.
- Sanna, B., Brandt, E. B., Kaiser, R. A., Pfluger, P., Witt, S. A., Kimball, T. R., et al. (2006). Modulatory calcineurin-interacting proteins 1 and 2 function as calcineurin facilitators in vivo. *Proc Natl Acad Sci U S A*, 103(19), 7327-7332.
- Sannerud, R., Declerck, I., Peric, A., Raemaekers, T., Menendez, G., Zhou, L., et al. (2011). ADP ribosylation factor 6 (ARF6) controls amyloid precursor protein (APP) processing by mediating the endosomal sorting of BACE1. *Proc Natl Acad Sci U S A*, 108(34), E559-568.
- Sargiacomo, M., Sudol, M., Tang, Z., & Lisanti, M. P. (1993). Signal transducing molecules and glycosyl-phosphatidylinositol-linked proteins form a caveolin-rich insoluble complex in MDCK cells. *J Cell Biol*, 122(4), 789-807.
- Sastre, M., Steiner, H., Fuchs, K., Capell, A., Multhaup, G., Condrón, M. M., et al. (2001). Presenilin-dependent gamma-secretase processing of beta-amyloid precursor protein at a site corresponding to the S3 cleavage of Notch. *EMBO Rep*, 2(9), 835-841.
- Schellenberg, G. D., Bird, T. D., Wijsman, E. M., Orr, H. T., Anderson, L., Nemens, E., et al. (1992). Genetic linkage evidence for a familial Alzheimer's disease locus on chromosome 14. *Science*, 258(5082), 668-671.
- Schenk, H. C. S. M. H. A. V.-P. C. M. A. O. B. L. L. I. K. E. (1992). Amyloid beta-peptide is produced by cultured cells during normal metabolism. *Nature*, 359(6393), 322-325.
- Scheuner, D., Eckman, C., Jensen, M., Song, X., Citron, M., Suzuki, N., et al. (1996). Secreted amyloid beta-protein similar to that in the senile plaques of Alzheimer's disease is

References

- increased in vivo by the presenilin 1 and 2 and APP mutations linked to familial Alzheimer's disease. *Nat Med*, 2(8), 864-870.
- Schimmoller, F., Singer-Kruger, B., Schroder, S., Kruger, U., Barlowe, C., & Riezman, H. (1995). The absence of Emp24p, a component of ER-derived COPII-coated vesicles, causes a defect in transport of selected proteins to the Golgi. *EMBO J*, 14(7), 1329-1339.
- Schubert, U., Anton, L. C., Gibbs, J., Norbury, C. C., Yewdell, J. W., & Bennink, J. R. (2000). Rapid degradation of a large fraction of newly synthesized proteins by proteasomes. *Nature*, 404(6779), 770-774.
- Selkoe, D. J. (2008). Soluble oligomers of the amyloid beta-protein impair synaptic plasticity and behavior. *Behav Brain Res*, 192(1), 106-113.
- Selkoe, D. J., Yamazaki, T., Citron, M., Podlisny, M. B., Koo, E. H., Teplow, D. B., et al. (1996). The role of APP processing and trafficking pathways in the formation of amyloid beta-protein. *Ann N Y Acad Sci*, 777, 57-64.
- Seshadri, S., Fitzpatrick, A. L., Ikram, M. A., DeStefano, A. L., Gudnason, V., Boada, M., et al. (2010). Genome-wide analysis of genetic loci associated with Alzheimer disease. *JAMA*, 303(18), 1832-1840.
- Seubert, P., Vigo-Pelfrey, C., Esch, F., Lee, M., Dovey, H., Davis, D., et al. (1992). Isolation and quantification of soluble Alzheimer's beta-peptide from biological fluids. *Nature*, 359(6393), 325-327.
- Sevlever, D., Pickett, S., Mann, K. J., Sambamurti, K., Medof, M. E., & Rosenberry, T. L. (1999). Glycosylphosphatidylinositol-anchor intermediates associate with triton-insoluble membranes in subcellular compartments that include the endoplasmic reticulum. *Biochem J*, 343 Pt 3, 627-635.
- Sherrington, R., Rogaev, E. I., Liang, Y., Rogaeva, E. A., Levesque, G., Ikeda, M., et al. (1995). Cloning of a gene bearing missense mutations in early-onset familial Alzheimer's disease. *Nature*, 375(6534), 754-760.
- Shiba, T., Kametaka, S., Kawasaki, M., Shibata, M., Waguri, S., Uchiyama, Y., et al. (2004). Insights into the phosphoregulation of beta-secretase sorting signal by the VHS domain of GGA1. *Traffic*, 5(6), 437-448.
- Shin, S. Y., Yang, H. W., Kim, J. R., Do Heo, W., & Cho, K. H. (2011). A hidden incoherent switch regulates RCAN1 in the calcineurin-NFAT signaling network. *J Cell Sci*, 124(Pt 1), 82-90.
- Shirovani, K., Edbauer, D., Capell, A., Schmitz, J., Steiner, H., & Haass, C. (2003). Gamma-Secretase activity is associated with a conformational change of nicastrin. *Journal of Biological Chemistry*, 278(19), 16474-16477.
- Shrivastava-Ranjan, P., Faundez, V., Fang, G., Rees, H., Lah, J. J., Levey, A. I., et al. (2008). Mint3/X11 is an ADP-ribosylation factor-dependent adaptor that regulates the traffic of the Alzheimer's precursor protein from the trans-Golgi network. *Molecular biology of the cell*, 19(1), 51-64.
- Siemers, E. R., Quinn, J. F., Kaye, J., Farlow, M. R., Porsteinsson, A., Tariot, P., et al. (2006). Effects of a gamma-secretase inhibitor in a randomized study of patients with Alzheimer disease. *Neurology*, 66(4), 602-604.

References

- Sinha, S., Anderson, J. P., Barbour, R., Basi, G. S., Caccavello, R., Davis, D., et al. (1999). Purification and cloning of amyloid precursor protein beta-secretase from human brain. *Nature*, 402(6761), 537-540.
- Sisodia, S. S. (1992). Beta-amyloid precursor protein cleavage by a membrane-bound protease. *Proc Natl Acad Sci U S A*, 89(13), 6075-6079.
- Sisodia, S. S., Koo, E. H., Beyreuther, K., Unterbeck, A., & Price, D. L. (1990). Evidence that beta-amyloid protein in Alzheimer's disease is not derived by normal processing. *Science*, 248(4954), 492-495.
- Slack, B. E., Ma, L. K., & Seah, C. C. (2001). Constitutive shedding of the amyloid precursor protein ectodomain is up-regulated by tumour necrosis factor-alpha converting enzyme. *Biochem J*, 357(Pt 3), 787-794.
- Smart, E. J., Ying, Y. S., Mineo, C., & Anderson, R. G. (1995). A detergent-free method for purifying caveolae membrane from tissue culture cells. *Proc Natl Acad Sci U S A*, 92(22), 10104-10108.
- Sohn, K., Orci, L., Ravazzola, M., Amherdt, M., Bremser, M., Lottspeich, F., et al. (1996a). A major transmembrane protein of Golgi-derived COPI-coated vesicles involved in coatomer binding. *J Cell Biol*, 135(5), 1239-1248.
- Sohn, K., Orci, L., Ravazzola, M., Amherdt, M., Bremser, M., Lottspeich, F., et al. (1996b). A major transmembrane protein of Golgi-derived COPI-coated vesicles involved in coatomer binding. *J Cell Biol*, 135(5), 1239--1248.
- Song, W., Nadeau, P., Yuan, M., Yang, X., Shen, J., & Yankner, B. A. (1999). Proteolytic release and nuclear translocation of Notch-1 are induced by presenilin-1 and impaired by pathogenic presenilin-1 mutations. *Proc Natl Acad Sci U S A*, 96(12), 6959-6963.
- St George-Hyslop, P., Haines, J., Rogaev, E., Mortilla, M., Vaula, G., Pericak-Vance, M., et al. (1992). Genetic evidence for a novel familial Alzheimer's disease locus on chromosome 14. *Nat Genet*, 2(4), 330-334.
- Stamnes, M. A., Craighead, M. W., Hoe, M. H., Lampen, N., Geromanos, S., Tempst, P., et al. (1995). An integral membrane component of coatomer-coated transport vesicles defines a family of proteins involved in budding. *Proc Natl Acad Sci U S A*, 92(17), 8011-8015.
- Strating, J. R., & Martens, G. J. (2009). The p24 family and selective transport processes at the ER-Golgi interface. *Biology of the Cell*, 101(9), 495-509.
- Strating, J. R., van Bakel, N. H., Leunissen, J. A., & Martens, G. J. (2009). A comprehensive overview of the vertebrate p24 family: identification of a novel tissue-specifically expressed member. *Molecular biology and evolution*, 26(8), 1707-1714.
- Sturchler-Pierrat, C., Abramowski, D., Duke, M., Wiederhold, K. H., Mistl, C., Rothacher, S., et al. (1997). Two amyloid precursor protein transgenic mouse models with Alzheimer disease-like pathology. *Proc Natl Acad Sci U S A*, 94(24), 13287-13292.
- Sun, X., Bromley-Brits, K., & Song, W. (2012). Regulation of beta-site APP-cleaving enzyme 1 gene expression and its role in Alzheimer's disease. *J Neurochem*, 120 Suppl 1, 62-70.
- Sun, X., He, G., & Song, W. (2006). BACE2, as a novel APP theta-secretase, is not responsible for the pathogenesis of Alzheimer's disease in Down syndrome. *FASEB J*, 20(9), 1369-1376.

References

- Sun, X., Tong, Y., Qing, H., Chen, C. H., & Song, W. (2006). Increased BACE1 maturation contributes to the pathogenesis of Alzheimer's disease in Down syndrome. *FASEB J*, *20*(9), 1361-1368.
- Sun, X., Wang, Y., Qing, H., Christensen, M. A., Liu, Y., Zhou, W., et al. (2005). Distinct transcriptional regulation and function of the human BACE2 and BACE1 genes. *FASEB J*, *19*(7), 739-749.
- Sun, X., Wu, Y., Chen, B., Zhang, Z., Zhou, W., Tong, Y., et al. Regulator of calcineurin 1 (RCAN1) facilitates neuronal apoptosis through caspase-3 activation. *J Biol Chem*, *286*(11), 9049-9062.
- Takasugi, N., Tomita, T., Hayashi, I., Tsuruoka, M., Niimura, M., Takahashi, Y., et al. (2003). The role of presenilin cofactors in the gamma-secretase complex. *Nature*, *422*(6930), 438-441.
- Takida, S., Maeda, Y., & Kinoshita, T. (2008). Mammalian GPI-anchored proteins require p24 proteins for their efficient transport from the ER to the plasma membrane. *Biochem J*, *409*(2), 555-562.
- Tang, B. L. (2009). Neuronal protein trafficking associated with Alzheimer disease: from APP and BACE1 to glutamate receptors. *Cell Adh Migr*, *3*(1), 118-128.
- Tanzi, R. E., Gusella, J. F., Watkins, P. C., Bruns, G. A., St George-Hyslop, P., Van Keuren, M. L., et al. (1987). Amyloid beta protein gene: cDNA, mRNA distribution, and genetic linkage near the Alzheimer locus. *Science*, *235*(4791), 880-884.
- Teranishi, Y., Hur, J. Y., Welander, H., Franberg, J., Aoki, M., Winblad, B., et al. (2009). Affinity pulldown of gamma-secretase and associated proteins from human and rat brain. *J Cell Mol Med*.
- Thinakaran, G., Borchelt, D. R., Lee, M. K., Slunt, H. H., Spitzer, L., Kim, G., et al. (1996). Endoproteolysis of presenilin 1 and accumulation of processed derivatives in vivo. *Neuron*, *17*(1), 181-190.
- Tokuda, T., Tamaoka, A., Matsuno, S., Sakurai, S., Shimada, H., Morita, H., et al. (2001). Plasma levels of amyloid beta proteins did not differ between subjects taking statins and those not taking statins. *Ann Neurol*, *49*(4), 546-547.
- Tun, H., Marlow, L., Pinnix, I., Kinsey, R., & Sambamurti, K. (2002). Lipid rafts play an important role in A beta biogenesis by regulating the beta-secretase pathway. *J Mol Neurosci*, *19*(1-2), 31-35.
- Van Broeckhoven, C., Backhovens, H., Cruts, M., De Winter, G., Bruyland, M., Cras, P., et al. (1992). Mapping of a gene predisposing to early-onset Alzheimer's disease to chromosome 14q24.3. *Nat Genet*, *2*(4), 335-339.
- van der Sluijs, P., Hull, M., Webster, P., Male, P., Goud, B., & Mellman, I. (1992). The small GTP-binding protein rab4 controls an early sorting event on the endocytic pathway. *Cell*, *70*(5), 729-740.
- van Meer, G., & Lisman, Q. (2002). Sphingolipid transport: rafts and translocators. *J Biol Chem*, *277*(29), 25855-25858.

References

- Vassar, R., Bennett, B. D., Babu-Khan, S., Kahn, S., Mendiaz, E. A., Denis, P., et al. (1999). Beta-secretase cleavage of Alzheimer's amyloid precursor protein by the transmembrane aspartic protease BACE. *Science*, 286(5440), 735-741.
- Vega, R. B., Rothermel, B. A., Weinheimer, C. J., Kovacs, A., Naseem, R. H., Bassel-Duby, R., et al. (2003). Dual roles of modulatory calcineurin-interacting protein 1 in cardiac hypertrophy. *Proc Natl Acad Sci U S A*, 100(2), 669-674.
- Vetrivel, K. S., Barman, A., Chen, Y., Nguyen, P. D., Wagner, S. L., Prabhakar, R., et al. (2011). Loss of cleavage at beta'-site contributes to apparent increase in beta-amyloid peptide (A β) secretion by beta-secretase (BACE1)-glycosylphosphatidylinositol (GPI) processing of amyloid precursor protein. *J Biol Chem*, 286(29), 26166-26177.
- Vetrivel, K. S., Cheng, H., Kim, S. H., Chen, Y., Barnes, N. Y., Parent, A. T., et al. (2005). Spatial segregation of gamma-secretase and substrates in distinct membrane domains. *J Biol Chem*, 280(27), 25892-25900.
- Vetrivel, K. S., Cheng, H., Lin, W., Sakurai, T., Li, T., Nukina, N., et al. (2004). Association of gamma-secretase with lipid rafts in post-Golgi and endosome membranes. *J Biol Chem*, 279(43), 44945-44954.
- Vetrivel, K. S., Gong, P., Bowen, J. W., Cheng, H., Chen, Y., Carter, M., et al. (2007). Dual roles of the transmembrane protein p23/TMP21 in the modulation of amyloid precursor protein metabolism. *Molecular Neurodegeneration*, 2, -.
- Vetrivel, K. S., Kodam, A., Gong, P., Chen, Y., Parent, A. T., Kar, S., et al. (2008). Localization and regional distribution of p23/TMP21 in the brain. *Neurobiology of Disease*, 32(1), 37-49.
- Vetrivel, K. S., & Thinakaran, G. (2006). Amyloidogenic processing of beta-amyloid precursor protein in intracellular compartments. *Neurology*, 66(2 Suppl 1), S69-73.
- von Arnim, C. A., Tangredi, M. M., Peltan, I. D., Lee, B. M., Irizarry, M. C., Kinoshita, A., et al. (2004). Demonstration of BACE (beta-secretase) phosphorylation and its interaction with GGA1 in cells by fluorescence-lifetime imaging microscopy. *J Cell Sci*, 117(Pt 22), 5437-5445.
- Wahle, T., Prager, K., Raffler, N., Haass, C., Famulok, M., & Walter, J. (2005). GGA proteins regulate retrograde transport of BACE1 from endosomes to the trans-Golgi network. *Mol Cell Neurosci*, 29(3), 453-461.
- Walsh, D. M., Klyubin, I., Fadeeva, J. V., Cullen, W. K., Anwyl, R., Wolfe, M. S., et al. (2002). Naturally secreted oligomers of amyloid beta protein potently inhibit hippocampal long-term potentiation in vivo. *Nature*, 416(6880), 535-539.
- Weidler, M., Reinhard, C., Friedrich, G., Wieland, F. T., & Rosch, P. (2000). Structure of the cytoplasmic domain of p23 in solution: implications for the formation of COPI vesicles. *Biochem Biophys Res Commun*, 271(2), 401-408.
- Wen, C., & Greenwald, I. (1999). p24 proteins and quality control of LIN-12 and GLP-1 trafficking in *Caenorhabditis elegans*. *J Cell Biol*, 145(6), 1165-1175.
- Wettstein, F. O., Noll, H., & Penman, S. (1964). Effect of Cycloheximide on Ribosomal Aggregates Engaged in Protein Synthesis in Vitro. *Biochim Biophys Acta*, 87, 525-528.

References

- Wolfe, M. S., Xia, W., Moore, C. L., Leatherwood, D. D., Ostaszewski, B., Rahmati, T., et al. (1999). Peptidomimetic probes and molecular modeling suggest that Alzheimer's gamma-secretase is an intramembrane-cleaving aspartyl protease. *Biochemistry*, 38(15), 4720-4727.
- Wolozin, B., Kellman, W., Ruosseau, P., Celesia, G. G., & Siegel, G. (2000). Decreased prevalence of Alzheimer disease associated with 3-hydroxy-3-methylglutaryl coenzyme A reductase inhibitors. *Arch Neurol*, 57(10), 1439-1443.
- Wortmann, M. (2012). Dementia: a global health priority-highlights from an ADI and World Health Organization report. *Alzheimers Res Ther*, 4(5), 40.
- Xu, C., Bailly-Maitre, B., & Reed, J. C. (2005). Endoplasmic reticulum stress: cell life and death decisions. *Journal of Clinical Investigation*, 115(10), 2656-2664.
- Yamazaki, T., Koo, E. H., & Selkoe, D. J. (1996). Trafficking of cell-surface amyloid beta-protein precursor. II. Endocytosis, recycling and lysosomal targeting detected by immunolocalization. *J Cell Sci*, 109 (Pt 5), 999-1008.
- Yan, R., Bienkowski, M. J., Shuck, M. E., Miao, H., Tory, M. C., Pauley, A. M., et al. (1999). Membrane-anchored aspartyl protease with Alzheimer's disease beta-secretase activity. *Nature*, 402(6761), 533-537.
- Yan, R., Han, P., Miao, H., Greengard, P., & Xu, H. (2001). The transmembrane domain of the Alzheimer's beta-secretase (BACE1) determines its late Golgi localization and access to beta -amyloid precursor protein (APP) substrate. *J Biol Chem*, 276(39), 36788-36796.
- Yoon, I. S., Chen, E., Busse, T., Repetto, E., Lakshmana, M. K., Koo, E. H., et al. (2007). Low-density lipoprotein receptor-related protein promotes amyloid precursor protein trafficking to lipid rafts in the endocytic pathway. *FASEB J*, 21(11), 2742-2752.
- Yoshida, H. (2007). ER stress and diseases. *Febs Journal*, 274(3), 630-658.
- Zhang, J., Kang, D. E., Xia, W., Okochi, M., Mori, H., Selkoe, D. J., et al. (1998). Subcellular distribution and turnover of presenilins in transfected cells. *J Biol Chem*, 273(20), 12436-12442.
- Zhang, X., & Song, W. (2013). The role of APP and BACE1 trafficking in APP processing and amyloid-beta generation. *Alzheimers Res Ther*, 5(5), 46.
- Zhou, W., Cai, F., Li, Y., Yang, G. S., O'Connor, K. D., Holt, R. A., et al. BACE1 gene promoter single-nucleotide polymorphisms in Alzheimer's disease. *J Mol Neurosci*, 42(1), 127-133.
- Zhou, W., Qing, H., Tong, Y., & Song, W. (2004). BACE1 gene expression and protein degradation. *Ann N Y Acad Sci*, 1035, 49-67.
- Zhou, W., & Song, W. (2006). Leaky scanning and reinitiation regulate BACE1 gene expression. *Mol Cell Biol*, 26(9), 3353-3364.
- Zhuang, Y., & Weiner, A. M. (1986). A compensatory base change in U1 snRNA suppresses a 5' splice site mutation. *Cell*, 46(6), 827-835.